

ABSTRACT

Title of dissertation: HYBRID RESILIENCE FRAMEWORK
FOR SYSTEMS OF SYSTEMS
INCORPORATING STAKEHOLDER
PREFERENCES

Roy Nelson Emanuel II
Doctor of Philosophy, 2018

Dissertation directed by: Professor Bilal M. Ayyub
Department of Civil and Environmental Engineering

From Presidential Policy Directive 21, to professional societies national meetings, to major United Nations initiatives, stakeholders recognize the value of achieving resilient systems. The literature clamors with methods to assess resilience of systems quantitatively and qualitatively. Resilience models typically focus on system performance and the threat to the system. Few models consider the preferences of the stakeholders of the systems. This course of study identified three gaps in the literature: first, the focus on system performance without considering the preferences of stakeholders; second, lack of resilience model-to-model comparison; and third, lack of a common framework for applying resilience models across domains and systems of systems.

This course of study investigated the impact of incorporating stakeholder preferences into four existing resilience models: Resilience Factor, Quotient Resilience, Total Quotient Resilience, and Integral Resilience. The incorporated stakeholder

preferences were time horizon, endogenous performance preference, and intertemporal substitutability of system performance. An analysis of the resultant eight illustrative models showed the models' comparative sensitivity to changes in system performance and stakeholder preferences using four fundamental system performance and stakeholder preference models. A deterministic system dynamics model of a city's critical infrastructure provided inputs to the eight models for an initial case study. The first phase identifies three stakeholder preference profiles for the water delivery infrastructure. The second phase assesses the impact of electrical outages on seven other critical infrastructures.

The results of the sensitivity analysis and the initial case study led to selection of the Extended Integral Resilience model for additional demonstrations. Stochastic inputs for the system dynamics model showed a range of resilience outcomes for each stakeholders' infrastructure for five courses of action. The hybrid resilience model used Department of Energy reports on Puerto Rico's recovery from Hurricane Maria to generate a resilience value.

A discrete event simulation of a fleet of aircraft used to train aviators provided the basis for the second set of case studies. The study considered the points of view of the Squadron Commanders which were limited to three year increments, and the program manager which considered a thirty-five year time horizon. The functional outputs of the model were graduates per quarter, aircraft ready to fly each day, and satisfied graduates per quarter. The case study introduced and demonstrated an event and time dependent intertemporal substitutability algorithm to be defined by the stakeholder.

HYBRID RESILIENCE FRAMEWORK
FOR SYSTEMS OF SYSTEMS
INCORPORATING STAKEHOLDER PREFERENCES

by

Roy Nelson Emanuel II

Dissertation submitted to the Faculty of the Graduate School of the
University of Maryland, College Park in partial fulfillment
of the requirements for the degree of
Doctor of Philosophy
2018

Advisory Committee:
Professor Bilal Ayyub, Chair/Advisor
Professor Michel Cukier
Professor Jeffrey Herrmann
Professor Brian Phillips
Professor Peter Sandborn, Dean's Representative

© Copyright by
Roy Nelson Emanuel II
2018

Dedication

In loving memory of my Father, Roy

To Christy, Claire, Roy, and Lily

for all your love, support, and confidence.

“When you are a Bear of Very Little Brain, and you Think of Things, you find sometimes that a Thing which seemed very Thingish inside you is quite different when it gets out into the open and has other people looking at it.” A.A. Milne

Acknowledgments

I would like to express my deepest gratitude to my advisor, Dr. Bilal Ayyub. His patience, tireless support, and occasional, but necessary, prodding pushed me past my perceived limits.

A special thank you to Dr. Bill Kroshl who listened to my trials and tribulations with a sympathetic ear and helped me craft and scope this course of study.

Thank you to the Reliability Engineers I followed along this path: Dr. Obi Ndu, Dr. Clay Smith, and Dr. Saurabh Mishra.

Thank you to the leadership at the Johns Hopkins University Applied Physics Laboratory, especially Chris Ryder and Bruce Schneider, who supported my work and made the work/life/academic balance bearable. Thank you to Maggie Beecher, whose help with the defense materials at the eleventh hour made all the difference.

Thank you to my mother, Mary Lou, whose strength and sage advice put me in the position to complete this work.

My final thank-yous are for my wife, proofreader, and motivator, Christy, and my children Claire, Roy, and Lily who kept me smiling.

Table of Contents

Dedication	ii
Acknowledgements	iii
List of Tables	vii
List of Figures	viii
List of Abbreviations	x
1 Problem Statement and State of the Art	1
1.1 Resilience History	1
1.2 The Need for Resilience Models for Engineered Systems	3
1.3 Definitions	6
1.4 Resilience	8
1.4.1 Resistance phase	10
1.4.2 Robustness phase	11
1.4.3 Recovery Phase	11
1.5 Resilience Modeling State of the Art	12
1.5.1 Point-in-Time Resilience Models	12
1.5.2 Time Interval Resilience Models	16
1.5.3 Hybrid Resilience Models	21
1.5.4 Network Resilience Models	22
1.5.5 Resilience Model Comparisons	23
2 Gaps, Needs, and Research Objectives	25
2.1 Gap 1 - Stakeholder Preferences	25
2.1.1 Time Horizon	26
2.1.2 Endogenous Preferences	27
2.1.3 Intertemporal Substitutability	30
2.2 Gap 2 - Model Comparison	30
2.3 Gap 3 - Common Framework for Resilience Assessment	31
2.4 Research Objective 1 - Develop Hybrid Resilience Framework	31

2.5	Research Objective 2 - Conceptual Validation of the Resilience Models in the Context of the Hybrid Resilience Framework	32
2.6	Research Objective 3 - Apply Hybrid Resilience Framework to Case Studies	32
3	Methodology	34
3.1	Defining the Hybrid Modeling Framework	34
3.1.1	System Identification and Functional Output Measurement	40
3.1.2	Stakeholder Preference Profiles	41
3.2	Select Resilience Model Candidates	41
3.3	Extend the Models to Include Stakeholder Preferences	43
3.3.1	Incorporate Time Horizon	44
3.3.2	Stakeholder Endogenous Preference	45
3.3.3	Incorporate Intertemporal Substitutability	47
3.4	Case Studies	53
3.4.1	Infrastructure Resilience Case Study	53
3.4.2	Fleet Resilience Case Study	54
3.5	Methodology Review	57
4	Resilience Model Comparison	59
4.1	Fundamental performance and preference profiles	59
4.1.1	Time to Failure	62
4.1.2	Robustness	62
4.1.3	Recovery Time	65
4.1.4	Recovery Level	65
4.1.5	Time Horizon	65
4.1.6	Endogenous Preference	69
4.1.7	Intertemporal Substitutability	71
4.2	Results from Fundamental Performance and Preference Profiles	71
4.3	Conclusion	71
5	Infrastructure Resilience Case Study	75
5.1	City of Austin Infrastructure System Dynamics Model	76
5.2	Water System Stakeholder Perspective	80
5.2.1	Conclusions from Water Stakeholder Perspective	84
5.3	City Infrastructure Stakeholder Perspective	86
5.3.1	Conclusions from City Infrastructure Study	90
5.4	Hurricane Threat Case Study	90
5.4.1	Hybrid Resilience Framework Application	92
5.4.2	Projected Resilience Analysis	99
5.4.2.1	Stochastic Threat Model	99
5.4.3	Time-Dependent Stakeholder Models	101
5.4.4	Single Storm Experiment	103
5.4.5	Multiple Time Horizons Experiment	106
5.4.6	Hurricane Threat Case Study Discussion and Conclusion	111

6	Fleet Resilience Case Study	114
6.1	Department of Defense Sustainability Challenges	114
6.2	Case Study: Training Squadron of Aircraft	115
6.3	Training Squadron Simulation	119
6.3.1	Aircraft Model	121
6.3.2	Aircrew	122
6.3.3	SLEP Simulation	123
6.3.4	Flight Scheduling	124
6.4	Stakeholder Preference Profiles: Intertemporal Substitutability	125
6.5	Resilience Analytical Model	134
6.6	Hybrid Resilience Framework Demonstration	135
6.6.1	Stakeholder Profiles	135
6.6.2	Study Scenarios	137
6.6.3	Intertemporal Substitutability Investigation	139
6.7	Simulation Outputs	140
6.7.1	Resilience Results	140
6.8	Program Manager Perspective	143
6.9	Squadron Commander Perspective	147
6.10	Intertemporal Substitutability Investigation	151
6.11	Hybrid Resilience Framework Demonstration Discussion	159
6.12	Algorithm Demonstration Discussion	159
7	Conclusion, Contributions, and Future Work	161
7.1	Summary	161
7.2	Contributions	162
7.3	Future Work	163
7.3.1	Stakeholder Preferences	164
7.3.2	Case Studies	164
7.3.3	Benefit-Cost Analysis	165
7.4	Conclusion	165

List of Tables

1.1	System, Output, and Stakeholder Examples	8
1.2	Common Symbology	13
3.1	Model Criteria Assessment	43
3.2	Resilience models used in this study	44
3.3	Summary of the Eight Resilience Analytical Models	51
3.4	Scenarios for Deterministic Fundamental Profiles	52
4.1	Parameters for Fundamental Profiles	61
4.2	Resilience Model Sensitivity to Fundamental Profiles	73
5.1	Electrical System Courses of Action	81
5.2	Water System Stakeholder Preferences	81
5.3	Water Stakeholder Scenario Resilience	83
5.4	Stakeholder Preferences for All Critical Infrastructures	88
5.5	Infrastructure Stakeholder Scenario Resilience	89
5.6	Hurricane Properties and Effects on Electrical Infrastructure	100
5.7	Parameters for Electrical System Behavior	100
5.8	Endogenous Preference Profiles (% of current capacity)	102
5.9	Endogenous Preference Spikes Due to Storm	103
5.10	Storm Data for Each Time Horizon	109
5.11	Resilience Results	112
6.1	Simulation Parameter Starting Values	121
6.2	Aircraft Simulation Values	122
6.3	Model Parameter Values for Students and Instructors	123
6.4	Example of the χ matrix	126
6.5	Intertemporal Substitutability Terminology	127
6.6	SLEP Courses of Action	137
6.7	Student Class Sizes	137
6.8	Stakeholder Preference Profile	138
6.9	Values for χ Matrices	139
6.10	Program Manager Preferred Course of Action	147

List of Figures

1.1	F/A-18 undergoing repairs at the depot in NAS North Island, CA . . .	6
1.2	Performance trajectories	10
1.3	General performance and baseline profile for point-in-time models . . .	14
1.4	General performance and baseline profile for time interval models . . .	16
1.5	Resilience triangle	17
2.1	Moving time horizon	27
2.2	Constant performance and changing endogenous preference scenario . . .	29
3.1	Class III hybrid simulation analytic model	36
3.2	Class III model modified for the hybrid resilience framework	38
3.3	General methodology	39
3.4	Resilience model selection criteria	42
3.5	Extend resilience models to incorporate stakeholder preferences	45
3.6	Steps to conceptually validate the original and extended resilience models	50
3.7	Infrastructure resilience case study	55
3.8	Fleet resilience case study	56
3.9	Flow of the methodology from model selection to case studies	58
4.1	Fundamental performance and endogenous preference profiles	60
4.2	Resilience model responses varying failure time with no recovery	63
4.3	Resilience model responses to robustness	64
4.4	Resilience model responses to time to recover	66
4.5	Resilience model responses to recovery level	67
4.6	Resilience model response to time horizon	68
4.7	Step failure and recovery to endogenous preference	70
4.8	Resilience model responses to intertemporal substitutability	72
5.1	Map of electricity service for Travis County, Texas	77
5.2	City infrastructure case studies	79
5.3	Performance profiles from electrical system courses of action	82
5.4	Resilience model responses to water stakeholder case study	85

5.5	All infrastructures performance for a given course of action	87
5.6	Resilience model response to different courses of action	91
5.7	Hurricane Maria’s track across the Caribbean Sea	92
5.8	Powerline damage in Mayaguez, PR	93
5.9	Road and powerline damage in Canovanas, PR	94
5.10	Data flow through hybrid model	96
5.11	Map of Puerto Rico’s energy infrastructure	97
5.12	Peak load and customer services recovery after Hurrican Maria	98
5.13	Time-series example for a category 4 storm	105
5.14	Infrastructure resilience values for 1000 simulation runs	107
5.15	Infrastructure resilience values by hurricane category	108
5.16	Performance and endogenous preference for a ten year time horizon .	110
5.17	Resilience values for each time horizon and infrastructure pair	113
6.1	T-45 Goshawks on the flightline	116
6.2	T-38 Talon	117
6.3	Case study hybrid resilience framework	118
6.4	Squadron fleet operation flow of events	120
6.5	Intertemporal substitutability algorithm: define the χ matrix	128
6.6	Intertemporal substitutability algorithm: first transfer	129
6.7	Intertemporal substitutability algorithm: second transfer	130
6.8	Intertemporal substitutability algorithm: repeat for next shortfall . .	131
6.9	Intertemporal substitutability algorithm: final transfer	132
6.10	Intertemporal substitutability algorithm: transfers complete	133
6.11	Flightline size and quarterly graduates for a single run: no surge . .	141
6.12	Flightline size and quarterly graduates for a single run: surge	142
6.13	Program manager aircraft resilience results	144
6.14	Program manager graduate resilience results	145
6.15	Program manager satisfaction resilience results	146
6.16	Squadron commander student satisfaction resilience results	149
6.17	Squadron commander graduates resilience results	150
6.18	Program manager intertemporal substitutability, 15 year time horizon	152
6.19	Program manager intertemporal substitutability, 20 year time horizon.	153
6.20	Program manager intertemporal substitutability, 25 year time horizon	154
6.21	Program manager intertemporal substitutability, 30 year time horizon	155
6.22	Program manager intertemporal substitutability, 35 year time horizon	156
6.23	Commander Delta intertemporal substitutability	157
6.24	Commander Echo intertemporal substitutability	158

List of Abbreviations

χ	intertemporal substitutability
DoD	Department of Defense
DOE	Department of Energy
FOC	Full Operational Capability
INCOSE	International Council on Systems Engineering
IOC	Initial Operational Capability
$\varphi(t)$	system output
$\tilde{\varphi}_t$	modified system output
$\psi_{t,j}$	surplus system output j time steps from time t
$Q(t)$	endogenous preference
R_{QR}	Quotient Resilience
R_{EQR}	Extended Quotient Resilience
R_{TQR}	Total Quotient Resilience
R_{ETQR}	Extended Total Quotient Resilience
R_{IR}	Integral Resilience and
R_{EIR}	Extended Integral Resilience
ρ	Resilience Factor
ρ_E	Extended Resilience Factor
SLEP	System Life Extension Program
S_p	Speed Factor
t_d	failure completion time
t_f	failure completion time and recovery initiation time
t_h	time horizon
t_i	failure initiation time
t_r	recovery completion time

Chapter 1: Problem Statement and State of the Art

1.1 Resilience History

The term resilience applies to a broad range of subjects in the social sciences, natural sciences, and engineering. [Alexander \[2013\]](#) traced the etymological roots of resilience to ancient Rome where the terms *resilire* and *resilio* were found in the writings of such luminaries as Ovid, Cicero, and Pliny the Elder. Sir Francis Bacon described the loudness of echoes with the word resilience in an English translation of his Latin text *Sylva Sylvarum*. In the 19th century, Rankine used resilience as the term for the mathematical definition of “spring” in steel beams. The use of resilience to describe material properties such as ductility and stiffness spread to other industries such as textiles and watchmaking [[Alexander, 2013](#)]. In the 1950s psychology introduced resilience to describe the mindsets of traumatized youths [[Goldstein and Brooks, 2012](#)].

C. S. Holling’s [1973](#) seminal paper, “Resilience and the stability of ecological systems,” formed the basis for much of the current socio-ecological and socio-technical research in resilience. The paper established the concept of resilience in a dynamic system framework. Achieving ecological resilience departed from the traditional ecological management goal of establishing a stable equilibrium within the

environment to maximize resource extraction. Holling's resilience focused on the *persistence* of relationships, such as those among predator and prey, rather than stable populations. Holling proposed that relationships with large variability may persist through large disturbances in their environment while the low variability, stable relationships would not persist through large disturbances.

Ecology defined two types of resilience: engineering resilience and ecological resilience. In this paradigm, engineering resilience is focused upon steady-state equilibrium among the functions as measured by the outputs of a system of components. Holling's proposed measures of engineering resilience were total deviation from the steady-state after a disturbance and the time to return to steady-state [Holling, 1973].

Ecological resilience focused upon survival of the relationships, or *regimes of behavior* of the components in the system. Under ecological resilience, the systems may experience great variation over time, but the system operates under the same regime of behavior after disturbances. A proposed measure of resilience was the magnitude of disturbance required to move the system into a new regime of behavior [Holling, 2010, 1973].

The resilience concept in ecology led to development of the adaptive management decision framework. Under adaptive management, local managers based decisions upon accruing systemic knowledge, reducing uncertainties, increasing the ecological resilience of the system. Adaptive management achieved success for complex systems requiring urgent action in the presence of uncertainty [Garmestani et al., 2008].

1.2 The Need for Resilience Models for Engineered Systems

Multiple stakeholders of complex systems have identified resilience as a key concept to support decision-making among courses of action. Presidential Policy Directive 21 presented the case for resilience in critical infrastructure systems [[PPD \(Presidential Policy Directive\), 2013](#)]. The United Nations Office for Disaster Risk Reduction sponsored numerous documents and campaigns aimed to improve resilience around the world [[UNISDR, 2015](#), [United Nations Office for Disaster Risk Reduction, 2015](#)].

Academia, professional societies, and major organizations have recognized the demand for resilience quantification through panels, conferences, and published papers. [Hosseini et al. \[2015\]](#) showed an order of magnitude increase in the prevalence of papers covering resilience topics from 2000 to 2015. Society for Risk Analysis entitled its 2016 national symposium, “Risk and Resilience: Viva la Revolución!” [[Society for Risk Analysis, 2016](#)]. In 2015, the National Institute of Standards and Technology started the Community Resilience Level to address resilience concerns at a local level [[National Institute of Standards and Technology \(NIST\), 2016](#)]. IEEE has sponsored an annual resilience symposium since 2008 [[Idaho National Laboratories, 2017](#)]. The American Society of Civil Engineers established an infrastructure resilience division to, “. . . develop a unified approach in advancing the concepts of resiliency within lifeline and infrastructure systems” [[American Society of Civil Engineers, 2017](#)].

The U.S. Government, the DoD in particular, recognizes resilience as a key

aspect of the DoD’s strategy for assuring mission success[[Goerger et al., 2014](#), [Holland, 2014](#), [Neches, 2011, 2012](#)]. The current National Security Strategy of the U.S. places a priority on increasing the resilience of government functions [[Trump, 2017](#)] building upon earlier Presidential Policy Directives defining the future posture of critical infrastructure systems. [[PPD \(Presidential Policy Directive\), 2011, 2013](#)]. The DoD defined mission assurance as, “. . . a process to protect or ensure the continued function and resilience of capabilities and assets by refining, integrating and synchronizing all aspects of the DoD . . .” [[Department of Defense, 2016](#)]

The Department of Defense (DoD) in the United States manages an incredible number of complicated systems that must operate in austere and unforgiving environments while being sustained for long periods of time. Stakeholders expect new acquisitions to be more capable than predecessors. The difficulties surrounding DoD acquisition often lead to delays in the initial operational capability (IOC) and full operational capability (FOC) of the systems. Examples of delayed acquisitions include the F-35 [[Werner, 2018](#)], the Zumwalt class of destroyers [[Katz, 2018](#)], the KC-46 tanker aircraft [[Mehta, 2016](#)], and U.S. Army command and control systems [[Edwards, 2017](#)].

DoD program managers must make decisions under great uncertainty with long-term effects on the viability of the system over its life-span [[Burgess, 2015](#)]. The DoD acquires and operates many different complex systems, such as aircraft, ships, satellite constellations, and base infrastructure. These systems often have life-spans measured in decades. For example, three generations of pilots have flown the same B-52 bomber airframe [[W.J. Hennigan, 2013](#)]. Uncertainties affecting the system

over its lifecycle include changing operational demands, operational environments, training requirements, maintenance practices, budgetary constraints, and end of life activities.

Aging systems must operate past their planned lifetimes to compensate for these delays. This life extension has reliability, safety, and operational implications. One method to mitigate the challenges of aging systems is a System Life Extension Program (SLEP). A SLEP extends the lifetime and often adds capability to an aging system. Many government systems are undergoing SLEP including the Army Tactical Missile System [[The Office of the Director of Operational Test and Evaluation, 2017](#), [Zacks Equity Research, 2015](#)], Landing Craft-Air Cushioned [[Naval Sea Systems Command, 2018](#)], weather radars [[Radar Operations Center, 2018](#)], ships [[Eckstein, 2018](#)], and aircraft [[Garbarino, 2018](#), [Jennings, 2018](#), [Lockheed Martin Public Relations, 2017](#), [Tirpak, 2015](#)]. For example, the F/A-18 tactical strike-fighter aircraft faces a staggering backlog of maintenance resulting from years of unforeseen demand coupled with budget shortfalls and acquisition delays over the past fifteen years [[LaGrone, 2016](#)]. To meet demand, some variants have had their life extended from 6,000 to 10,000 flight hours. A service life extension program (SLEP) is a solution for a system nearing its operational limit when no replacement system is available [[Bartkus, 2002](#), [Broadstreet, 2007](#), [Tirpak, 2016](#), [Toussaint and Collery, 2012](#)]. Figure 1.1 shows an F/A-18 under repair at the Fleet Readiness Center in North Island, CA.



Figure 1.1: F/A-18 undergoing repairs at the depot in NAS North Island, CA [Staff Sgt. Gabriela Garcia, 2016]

1.3 Definitions

This study focused upon the performance of a *system*. The International Council on Systems Engineering (INCOSE) defines a system as, “. . . a construct or collection of different elements that together produce results not obtainable by the elements alone.” Elements of a system may include hardware, software, processes, people, infrastructure, or records. Law [Law, 2015] defines a system as “a collection of entities, e.g., people or machines, that act and interact together toward the accomplishment of some logical end.” A *system of systems* comprises, “. . . large-scale

integrated systems that are heterogeneous and independently operable on their own, but are networked together for a common goal” [Jamshidi, 2009]. A collection of variables defines the *state* of a system. *Metrics* quantify the values of the state variables. Metric examples include time, probability, length, resilience, robustness, and figure of merit. This study reserved the term metric as a value assigned to a concept [Ayyub and Klir, 2006].

The definitions emphasized a system’s purpose, desired output, or logical end. *Stakeholders* in the system define the system’s purpose. A stakeholder is an entity that has an interest in the existence, performance, outcome and future of some system [Aven, 2003, Ayyub, 2014c, Donaldson and Preston, 1995, Freeman, 1984, Mitroff, 1983]. The Stanford Research Institute first defined stakeholders as, “those groups without whose support the organization would cease to exist” (quoted in [Freeman, 1984]). Table 1.1 lists examples of systems, system outputs, and stakeholders.

Models represent a system’s internal relationships, inputs, and outputs with the intent to understand the system behavior and predict outcomes by reducing a system to characteristics of interest. A model may be physical, such as a scaled-down replica, or symbolic, such as a diagram or mathematical expression [INCOSE, 2017, Law, 2015]. *Analytic models* provide a closed-form solution represented as a mathematical expression. *Simulation models* solve problems through, “. . . numerically exercising the model for the inputs in question to see how they affect the output measures of performance” [Law, 2015] that are too complex to calculate a result directly either because it is impossible or too computationally expensive. This study

Table 1.1: System, Output, and Stakeholder Examples

System	Output(s)	Stakeholders
Training aircraft	Time to graduate	Students
	Qualified aviators	Deployed Squadrons
	Flight hours	Instructor Corps
	Aircraft life	Program Managers
Water delivery infrastructure	Emergency water	Citizens
	Potable water	Firefighters Business & Industry
Buildings	Rental income	Owners
	Space availability	Tenants
Bridges	Throughput traffic	Communities
	Commute time	Commuters
	Freight weight per hour	Freight Shippers
Electrical power	Delivered power	Producers
	Satisfied customers	Distributors
	Power available on demand	Residents & Industry

uses *model* interchangeably with *analytical model* and *simulation* for *simulation model*.

1.4 Resilience

The Society for Risk Analysis provided a operational definition of resilience:

[[Society for Risk Analysis, 2016](#)]:

Resilience is the ability of a system to reduce the initial adverse effects (absorptive capability) of a disruptive event (stress) and the time/speed and costs at which it is able to return to an appropriate functional-

ity/equilibrium (adaptive and restorative capability). The disruptive events maybe shocking or creeping, endogenous or exogenous.

This statement described the epochs of a cycle of resistance, robustness, and recovery. This study also relied heavily upon the definition for resilience, and its relationship to functional output presented by [Ayyub \[2014a\]](#):

Resilience notionally means the ability to prepare for and adapt to changing conditions and withstand and recover rapidly from disruptions. Resilience includes the ability to withstand and recover from disturbances of the deliberate attack types, accidents, or naturally occurring threats or incidents. The resilience of a system’s function can be measured based on the persistence of a corresponding functional performance under uncertainty in the face of disturbances.

The definition required a resilience model to be sensitive to a system’s functional performance — sometimes called the figure-of-merit [[Henry and Ramirez-Marquez, 2012, 2016](#), [Ramirez-Marquez and Rocco S., 2009](#)]. Functional performance is the desired output of the system as defined by its stakeholders. The functional performance data may come from direct measurement of the system or from a model/simulation of the system. Since informing decisions is a primary motivation for resilience models, simulation is often the primary source for resilience model input data. The resilience models used the system’s functional performance to data to measure the resilience of a system. The resilience models answer the question, “resilience of what to what?” [[Carpenter et al., 2001](#)]

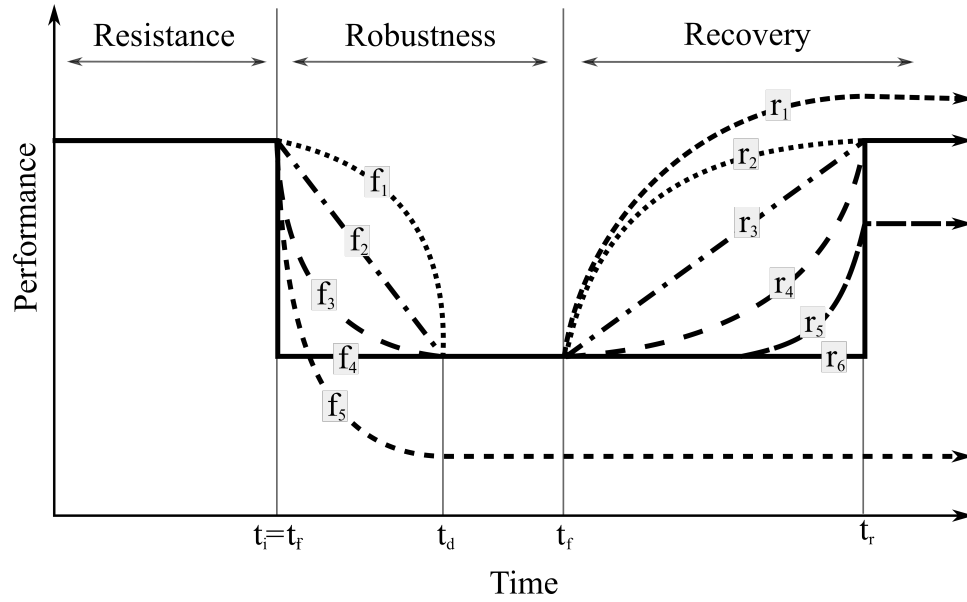


Figure 1.2: Performance trajectories adapted from [Ayyub \[2014a\]](#)

The resilience definition implies three time phases of resilience, also called performance segregation [[Ayyub, 2015](#)], associated with critical events in the system time line:

- Resistance phase (before the disturbance)
- Robustness phase (after the disturbance and before recovery)
- Recovery phase (time from recovery to recovery finish)

After the end of recovery phase, a new resistance phase begins.

1.4.1 Resistance phase

Resistance is a systems ability to successful fend off attacks and withstand disturbances without change in functional performance. The resistance phase of

functional performance occurs prior to a disturbance ($t < t_d$). A system may resist the disturbance with uninterrupted delivery of the functional performance. Time to failure is a characteristic of interest during this time period. Two well established techniques support calculation of time to failure are: stress-strength analysis and reliability analysis. Stress-strength analysis requires knowledge of the intensity and frequency of stresses and system strength over time [McPherson, 2010]. When failure data under operational or accelerated conditions, reliability analysis finds the distribution of the time to failure [Ayyub, 2014c, Modarres et al., 2010, Rausand and Høyland, 2004]).

1.4.2 Robustness phase

Robustness is the remaining performance after the degradation. The robustness phase occurs after a degradation in functional performance. Robustness comprises the failure profile, or trajectory, as well. Failure profiles may be described as brittle, ductile, or graceful failure. The robustness phase lasts from failure initiation until recovery initiation. For long life-span systems, the failure time interval may be insignificant compared to time spent in the normal, degraded, and recovered states, and may be approximated as a step function in many cases [Ayyub, 2014c].

1.4.3 Recovery Phase

Recovery is the return of functional output to a desired level of performance. The recovery phase begins after action is taken to restore the degraded system. The

end of recovery phase can be defined in several ways. Resilience models often end the resilience phase once a stable level of performance is achieved [Ayyub, 2014a, Henry and Ramirez-Marquez, 2012, Tran, 2015, Tran et al., 2017]. Ayyub [2015] defines a time horizon that can be determined by a stakeholder or assigned a value associated with the underlying system such as the return period of the disturbance. After the recovery phase, a new resistance phase begins at the *new normal* level of performance and ability to overcome disturbances.

1.5 Resilience Modeling State of the Art

The literature contained a wide variety of models intended to measure the resilience of a wide variety of systems. The resilience models fell into several broad categories: network resilience models, point-in-time resilience models, and area resilience models. Table 1.2 lists common terms that appear regularly in the different resilience models. The following discussion modified parameters and variables from their original publication appearance to present common symbology across the study.

1.5.1 Point-in-Time Resilience Models

One general method of modeling system resilience used performance values at critical points in time during the resilience cycle. The performance level prior to the failure formed a baseline value, $\varphi(t_0)$, the minimum performance level captured the degradation due to the failure, $\varphi(t_d)$, and the value after restoration activities cap-

Table 1.2: Common Symbology.

Symbol	Definition
$\varphi(t)$	Figure of merit, level of system performance, output of system as a function of time
t_0	Earliest time of interest
t_i	Time of failure initiation
t_f	Time of failure completion
t_d	Time of minimum performance
t_r	Time of recovery
t_h	Time horizon
$Q(t)$	Endogenous preference, desired functional output stakeholder need over time
$\chi(t)$	Intertemporal substitutability

tured the amount of recovered performance, $\varphi(t_r)$. Figure 1.3 depicts common points used in these resilience models.

Quotient resilience was a ratio of differences between performance of the critical points in the resilience timeline [Gama Dessavre et al., 2016, Henry and Ramirez-Marquez, 2012, Pant et al., 2014]:

$$R_{QR} = \frac{\varphi(t) - \varphi(t_d)}{\varphi(t_0) - \varphi(t_d)} \quad (1.1)$$

Quotient resilience captured the fraction of recovery achieved relative to the disrupted state. As such, the model did not capture residual performance after a disruption as a benefit to the system. This provided a high contrast for decision-

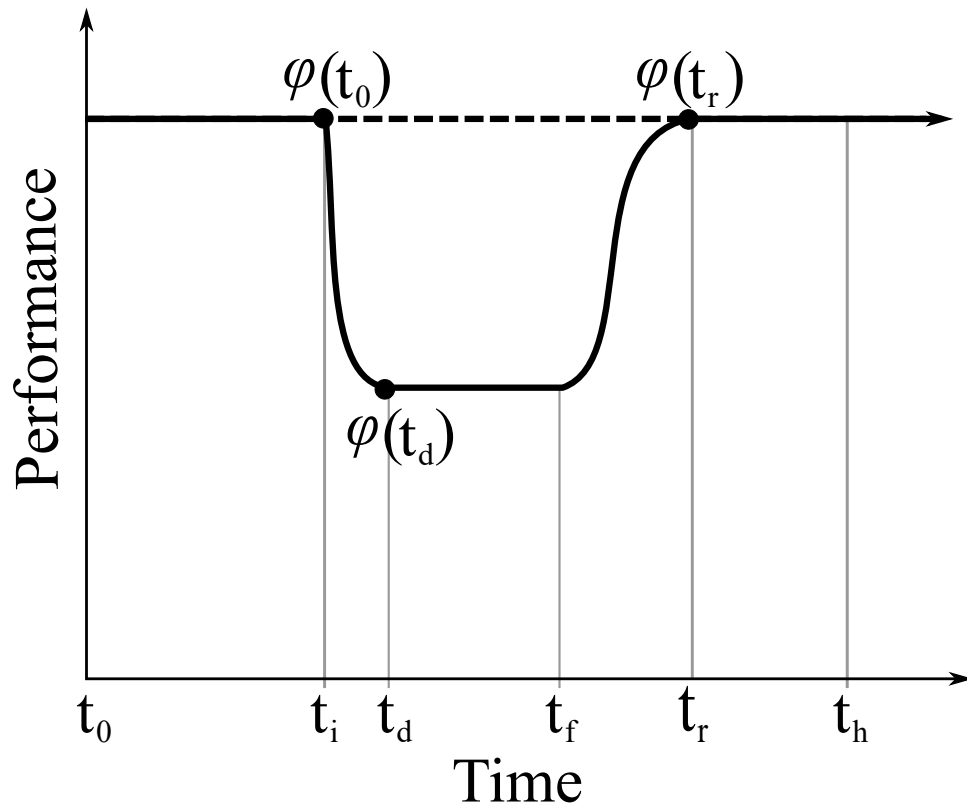


Figure 1.3: General performance and baseline profile for point-in-time models

makers to decide between recovery actions, but did not allow a decision-maker to assess the initial effect of the disturbance. Follow-on studies used quotient resilience to find importance measures for networks [Barker et al., 2013, 2015, Baroud et al., 2014].

Francis and Bekera [2014] proposed a family of models based upon resilience factor (ρ_i):

$$\rho_i(S_p, \varphi(t_0), \varphi(t_d), \varphi(t_r)) = S_p \frac{\varphi(t_r)}{\varphi(t_0)} \frac{\varphi(t_d)}{\varphi(t_0)} \quad (1.2)$$

where the speed factor, S_p , was:

$$S_p = \begin{cases} \frac{t_\delta}{t_r^*} \exp[-a(t_r - t_r^*)] & t_r \geq t_r^* \\ \frac{t_\delta}{t_r^*}, & \text{otherwise} \end{cases} \quad (1.3)$$

In addition to the critical points-in-time, the model included the speed factor, S_p , to include triage recovery activities in the model. Triage activities resulted in an intermediate, improved equilibrium state prior to final recovery. The speed factor for recovery included time between failure and the start of recovery activities ($t_r - t_r^*$), slack time (t_δ), the time to complete the initial recovery actions (t_r^*), and a resilience decay factor applied while the system was in the interim equilibrium state, F_r^* . The model introduced a fragility term and an event probability term to resilience factor to account for the random nature of disturbance events and their associated failures. Fragility was the probability of failure (μ) given a disturbance event i described by a vector of parameters (z). Taking the fragility, resilience factor, and the probability of the event i occurring ($Pr[D_i]$), produced the expected system functionality degradation (ζ) [Francis and Bekera, 2014]:

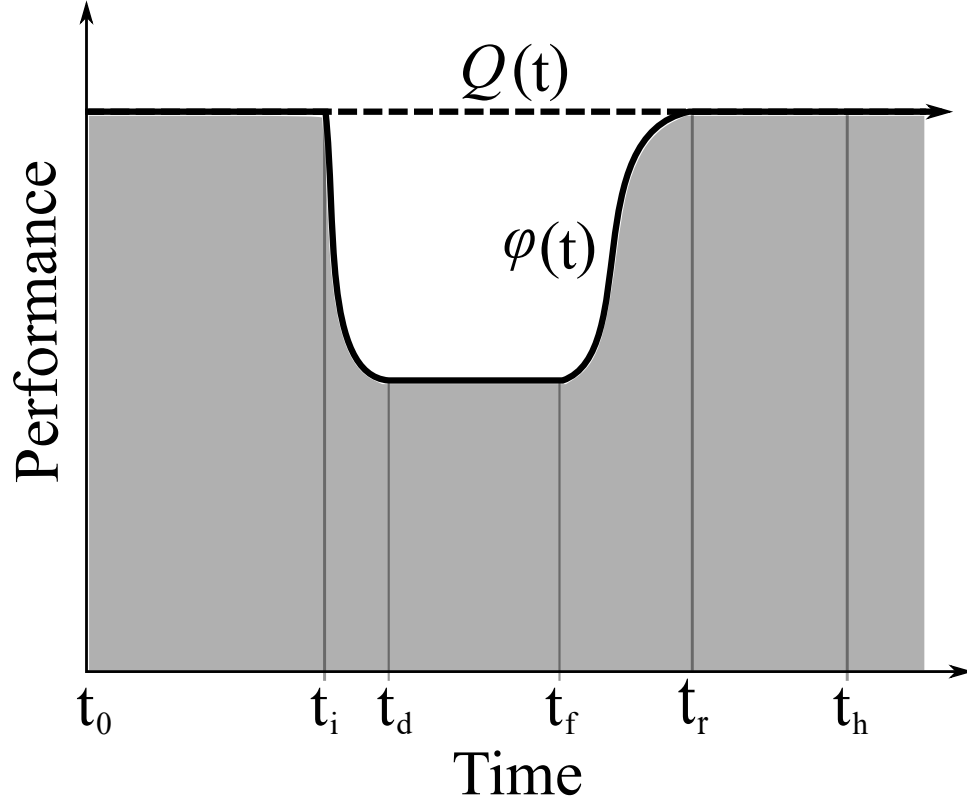


Figure 1.4: General performance and baseline profile for time interval models

$$\zeta = \Pr[D_i] \cdot (\mu|\mathbf{z}_i) \cdot \rho_i(S_p, \varphi(t_r), \varphi(t_d), \varphi(t_0)) \quad (1.4)$$

1.5.2 Time Interval Resilience Models

Another general method to measure the resilience of a system was to compare the performance over time against the baseline performance over the same time period. The model was typically a ratio of the areas under the actual performance (the shaded area under $\varphi(t)$ and the baseline performance (the total area under $Q(t)$ in Figure 1.4).

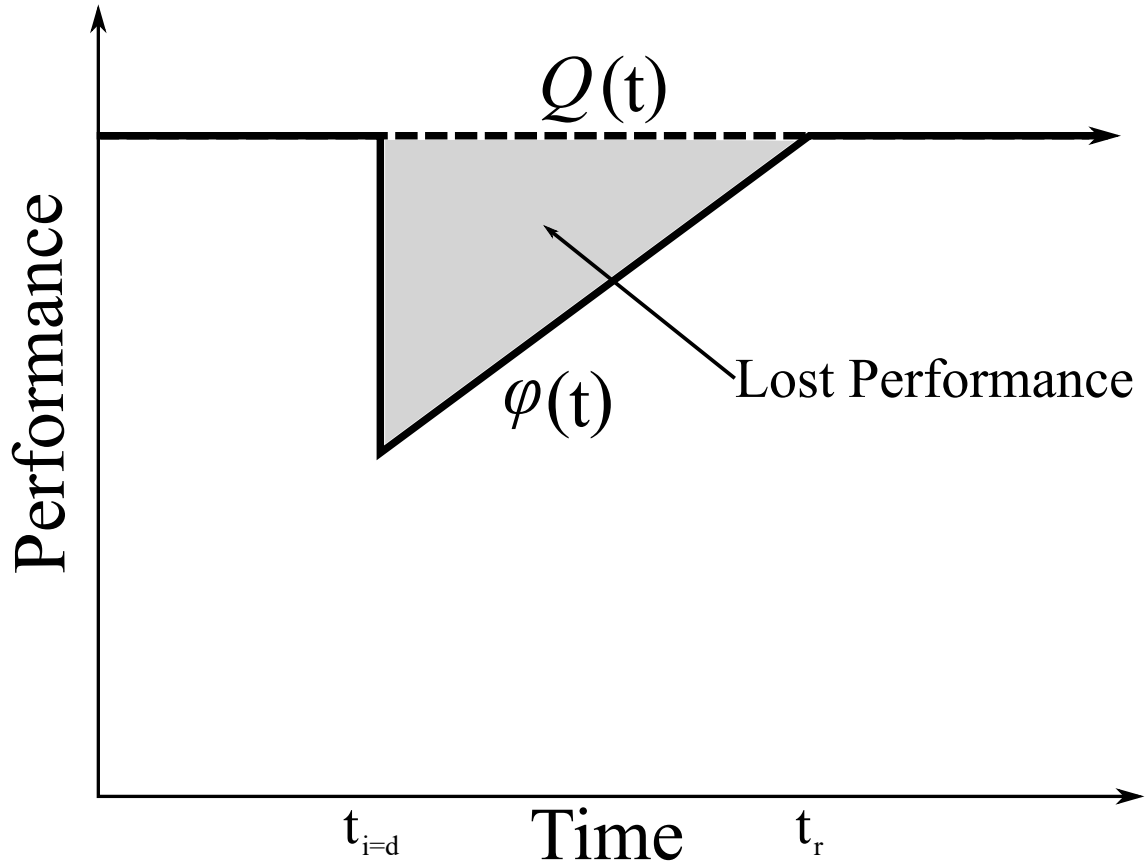


Figure 1.5: Resilience triangle

The resilience triangle defined a special case of Figure 1.4 with instantaneous degradation instantaneously and linear recovery. The *missing* performance is a triangular area. Figure 1.5 depicts a loss in performance given a failure with performance returning to the *status quo* value after recovery [Ayyub, 2014a, Bruneau et al., 2003, Tierney and Bruneau, 2007, Zobel, 2011].

The resilience triangle (R_{Δ}) did not contain the resistance of the system. The mathematical representation of the resilience triangle is [Bruneau et al., 2003]:

$$R_{\Delta} = \int_{t_i=t_d}^{t_r} [Q(t) - \varphi(t)] dt \quad (1.5)$$

A case with no reduction in performance yielded a resilience value of zero, while the minimum resilient (most *unresilient*) system yielded:

$$R_{\Delta_{min}} = \frac{Q}{2}(t_r - t_{i=t_d}) \quad (1.6)$$

Zobel [2011] expanded upon the resilience triangle concept to develop the adjusted resilience triangle, $R_{\Delta_{adj}}$. The variables of the adjusted resilience triangle were the initial loss of functionality, $\varphi(t_d)$, the time to recover, t_r , the failure time ($t_i = t_d$), and an upper bound to the time to recovery (t_r^*). The adjusted resilience triangle ($R_{\Delta_{adj}}$) model was:

$$R_{\Delta_{adj}}(\varphi(t_i = t_d), t_r) = 1 - \frac{\varphi(t_i = t_d)t_r}{2t_r^*}; \quad \varphi(t_i = t_d) \in [0, 1], t_r \in [0, T^*] \quad (1.7)$$

As with the original resilience triangle, the adjusted resilience triangle measured performance did not incorporate resistance. Zobel's formulation accommodated a time horizon, albeit implicitly, with the inclusion of t_r^* .

Ayyub [2014a] generalized the resilience triangle with the integral resilience model. Integral resilience removed the resilience triangle constraints for failure and recovery profiles. Integral resilience also included performance of the system prior to the disturbance. This enabled consideration of the probabilistic nature of disturbances and system failure. The formulation for integral resilience was:

$$R_{IR} = \frac{T_i + F\Delta T_f + R\Delta T_r}{T_i + \Delta T_f + \Delta T_r} \quad (1.8)$$

T_i was the time of the incident or disturbance, ΔT_f was the time from the incident to the system minimum performance, ΔT_r was the time from system minimum performance until the system achieved stable recovery. The failure and recovery profiles, F and R , captured the ratio of performance over time to status quo performance over the same time:

$$F = \frac{\int_{t_i}^{t_f} \varphi(t) dt}{\int_{t_i}^{t_f} Q dt}; R = \frac{\int_{t_f}^{t_r} \varphi(t) dt}{\int_{t_f}^{t_r} Q dt} \quad (1.9)$$

Ayyub [2015] proposed a practical version of Equation 1.8 making the following assumptions:

- Step degradation at $t_i = t_d$
- Linear or step recovery completed at t_r
- Disrupting events followed the Poisson distribution.

These assumptions demonstrated the model versatility by including varying failure and recovery levels. The practical Integral Resilience model was:

$$R_{IR_{prac}} = 1 - \exp(-\lambda t_h(1 - p\bar{R}_f)) + \exp(\lambda t_h) \quad (1.10)$$

\bar{R}_f was the non-resilience per failure for the step failure and linear recovery cases:

$$\bar{R}_{f_{step}} = \frac{(t_r - t_i)(\varphi(t_0) - \varphi(t_r))}{\varphi(t_r)t_h} \quad (1.11)$$

$$\bar{R}_{f_{linear}} = \frac{(t_r - t_i)(\varphi(t_0) - \varphi(t_r))}{2\varphi(t_r)t_h} \quad (1.12)$$

The time, t_h , was the planning horizon for the system stakeholders; λ was the rate of the Poisson process; and p was the probability of failure given a disturbance. The study assigned t_h the value of the return period for the disturbance, $\frac{1}{\lambda}$.

Ouyang *et al.* [Ouyang and Dueñas-Osorio, 2012, Ouyang and Wang, 2015, Ouyang *et al.*, 2012] presented resilience as the ratio of the integrals of the performance profile, $\varphi(t)$, and a target performance profile $Q(t)$:

$$R_{Ouyang} = \frac{\int_0^T \varphi(t) dt}{\int_0^T Q(t) dt} \quad (1.13)$$

Ouyang explicitly stated that the target performance profile $Q(t)$ may vary with time. This model, along with the models in Equations 1.8 and 1.10, captured the ratio of areas under performance curves (Figure 1.4). The numerator was the area under the performance curve of the system when a failure occurs. The denominator was the area under the performance curve with no failure.

Gama Dessavre *et al.* [2016] proposed applying the integral resilience concept to a time-series plot of quotient resilience. The result was Total Quotient Resilience:

$$R_{TQR} = \frac{\int_{t_0}^{t_h} R_{QR}(u) du}{t_h - t_0} \quad (1.14)$$

where t_h was the time horizon, and R_{QR} was the Quotient Resilience (Equation 1.1).

1.5.3 Hybrid Resilience Models

Vugrin et al. [2010] proposed a family of resilience models. The foundational model, systemic impact, was the area between the targeted system performance, Q , and the actual system performance, $\varphi(t)$

$$SI = \int_{t_0}^{t_f} [Q(t) - \varphi(t)] dt \quad (1.15)$$

System impact shared similarities with the resilience triangle. A system with no disturbance recorded a system impact of zero. The final form of resilience was Recovery-Dependent Resilience (RDR):

$$RDR = \frac{SI + \alpha \cdot TRE}{\int_{t_0}^{t_f} |Q(t)| dt} \quad (1.16)$$

When $\alpha = 0$, RDR is similar to the recovery and failure profiles in Equation 1.9 except desired RDR approaches zero rather than one:

$$RDR(\alpha = 0) = \frac{\int_{t_0}^{t_f} [Q(t) - \varphi(t)] dt}{\int_{t_0}^{t_f} |Q(t)| dt} \quad (1.17)$$

One model used aspects of both point-in-time resilience and time interval resilience. The model, proposed by Tran [2015], Tran et al. [2017] included aspects of integral resilience (Equation 1.8) and Expected System Degradation Function (Equation 1.4):

$$R_{Tran} = \begin{cases} \sigma r [\delta + \zeta + 1 - \tau^{r-\delta}] & \text{if } r - \delta \geq 0 \\ \sigma r (\delta + \zeta) & \text{otherwise} \end{cases} \quad (1.18)$$

where

$$\sigma = \frac{\sum_{t=t_0}^{t_h} \varphi(t)}{(t_h - t_0)Q(t_0)} \quad (1.19)$$

and

$$\delta r = \frac{\varphi(t_d)}{Q(t_0)} \frac{\varphi(t_r)}{Q(t_0)} = \rho(S_p = 1) \quad (1.20)$$

The total performance factor, σ , was a time-interval resilience model. The product of absorption factor, δ , and recovery factor, r , were equivalent to the resilience factor in Equation 1.2. The recovery time factor τ , rewarded a system for a quick recovery. The volatility factor, ζ , lowered the resilience value when performance has high volatility.

1.5.4 Network Resilience Models

Chen and Miller-Hooks [2012] defined resilience as, “. . . a network’s capability to resist and recover from disruption or disaster.” The resulting network resilience model produced a ratio (α) between the maximum demand satisfied after a disturbance (d_w for origin-destination pair $w \in \mathbf{W}$) and the maximum demand satisfied before the disturbance (D_w for the origin-destination pair $w \in \mathbf{W}$):

$$\alpha = E \left(\frac{\sum_{w \in \mathbf{W}} d_w}{\sum_{w \in \mathbf{W}} D_w} \right) \quad (1.21)$$

This model explicitly called out satisfied demand as a desired end for a system’s function [Chen et al., 2012]. The study that exercised the model used deterministic

failures and a constant level of demand, but the model could accommodate changing stakeholder demands.

[Alderson et al. \[2015\]](#) defined operational resilience as, “the ability of a system to adapt its behavior to maintain continuity of function (or operations) in the presence of disruptions.” The model used Defender-Attacker-Defender models used commonly in the Operations Research field. A Defender-Attacker-Defender model defined the order and number of actions (moves) taken by notional defenders and attackers

1. A defender chose the assets to defend
2. An attacker selected and destroyed assets
3. The defender re-allocated resources to compensate for the destroyed assets.

The output of the model Was maximum flow after the defender’s final move. Of particular interest was the worst-case maximum flow of the system for a given the number of attacks available to the attacker [[Alderson et al., 2011, 2014, 2015](#)].

1.5.5 Resilience Model Comparisons

Each resilience model in the literature attached a case studies for demonstrating the models impact, but only two studies compared different resilience models using the same case study. [Gama Dessavre et al. \[2016\]](#) compared an integral resilience model to the quotient resilience model. The authors concluded that quotient resilience was the superior model because it showed higher sensitivity during the failure event than integral resilience. Tran compared integral resilience to the hybrid

resilience model while varying recovery time, recovery profile, and volatility. Tran concluded that the hybrid model is more sensitive to these parameters [[Tran, 2015](#), [Tran et al., 2017](#)].

Chapter 2: Gaps, Needs, and Research Objectives

This chapter identifies gaps in the state-of-the-art as reported in Chapter 1. The research objectives for the dissertation derive from these gaps. The gaps, needs, and research objectives inform the methodology and case study selection in following chapters.

2.1 Gap 1 - Stakeholder Preferences

The resilience models reviewed in the preceding chapter satisfy the question: “*Resilience of what to what?*” [Carpenter et al., 2001]. The models require a system (*of what*) and a threat or disturbance (*to what*). Answering these two questions was adequate for ecological systems where continued existence and flourishing of a species or habitat is the goal, but a key piece of context, purpose, was missing when applied to engineered systems. Common definitions of engineered systems emphasize the system’s purpose [INCOSE, 2017, Law, 2015]. One way to frame purpose, is identify the stakeholders and their desires by adding the question “*for whom?*” Table 1.1 shows examples of this context by mapping systems to outputs to stakeholders.

Stakeholders define the purpose of the system [Aven, 2003, Ayyub, 2014a,

[Donaldson and Preston, 1995](#), [Freeman, 1984](#), [Mitroff, 1983](#)]. The role of the stakeholder is implicit in many the resilience models; often status quo performance is the baseline for desired performance. In some situations, a stakeholder may desire more (or less) output from during a disturbance and after recovery. The stakeholder may have period time, past which, the system’s performance becomes unimportant compared to other pressing needs.

Economics defines many of the concepts necessary to include stakeholder preferences in resilience models. The first assumption is to treat the stakeholder as a rational consumer of the functional output of the system of interest. As a rational consumer, the stakeholder makes decisions regarding improvements to the system of interest using preferences. These preferences are the basis to compare system performance after a disturbance. This study explores the impact of changing three preferences: the stakeholder’s preferred time horizon, endogenous preference, and intertemporal substitutability. The following sections describe the three preferences in more detail.

2.1.1 Time Horizon

Time horizon is the “The most remote future period taken into account in making economic decisions, such as investment” [[Black et al., 2017](#)]. Stakeholders define preferred time horizons. The stakeholders’ time horizons impact preferred options. The stakeholder may have a time horizon independent of recovery time. Examples include the lifetime of the system, scheduled replacement of the system,

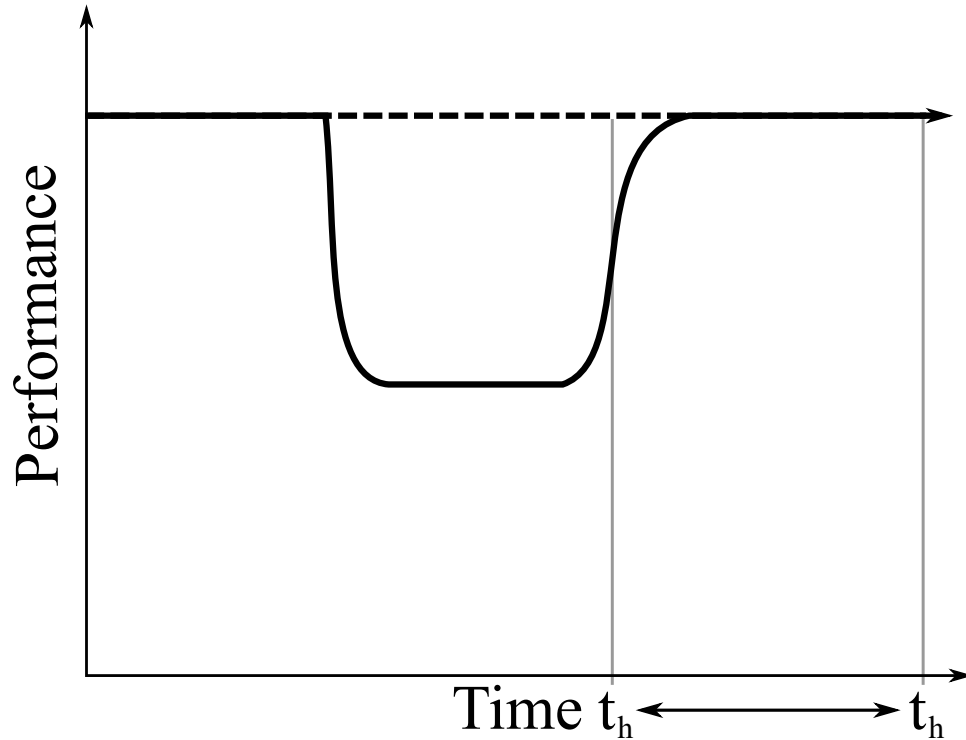


Figure 2.1: Moving time horizon

or the stakeholder’s anticipated period of responsibility for the system. The stakeholders’ time horizons dictate preferred options leading different preferred courses of actions for different stakeholders. A short time horizon may stress reliability or avoidance of failure because time for recovery may be greater than the time horizon [Demsetz, 1996]. Figure 2.1 shows two different time horizons.

2.1.2 Endogenous Preferences

Endogenous preferences are “Individual preferences that form under the influence of the economic, social, legal, and cultural structure of the environment and may change in response to changes in the environment” [Black et al., 2017]. *Status*

quo performance is acceptable in normal operating conditions, but resilience analysis requires examining preferences during times of disturbance. A stakeholder's appetite for a system's output will change during times of crisis. Highway usage during a hurricane illustrates the point. Prior to landfall, outbound traffic may demand more than one hundred percent of outbound capacity. Inbound traffic flow may be reversed to accommodate the demand. During the hurricane, demand for the freeways falls to well below limits as only emergency services use the road. After the hurricane, the highways handle greater freight capacity to deal with inflowing supplies. In the context of system performance, endogenous preference is the level of functional performance desired by the stakeholder at a given time. This coincides with the targeted performance profile, $Q(t)$, used in several resilience models [Ayyub, 2014a, 2015, Kong et al., 2015, Ouyang and Dueñas-Osorio, 2012, Ouyang et al., 2012].

One situation overlooked by the literature is the case with a demand change but no system degradation. This is depicted in Figure 2.2 where the dashed line represents the demanded output from the system. The models described above cannot address this situation as the performance level, $\varphi(t)$, has no critical points in time. The critical time points and values are all part of the endogenous preference, $Q(t)$ which is not explicitly incorporated in the models.

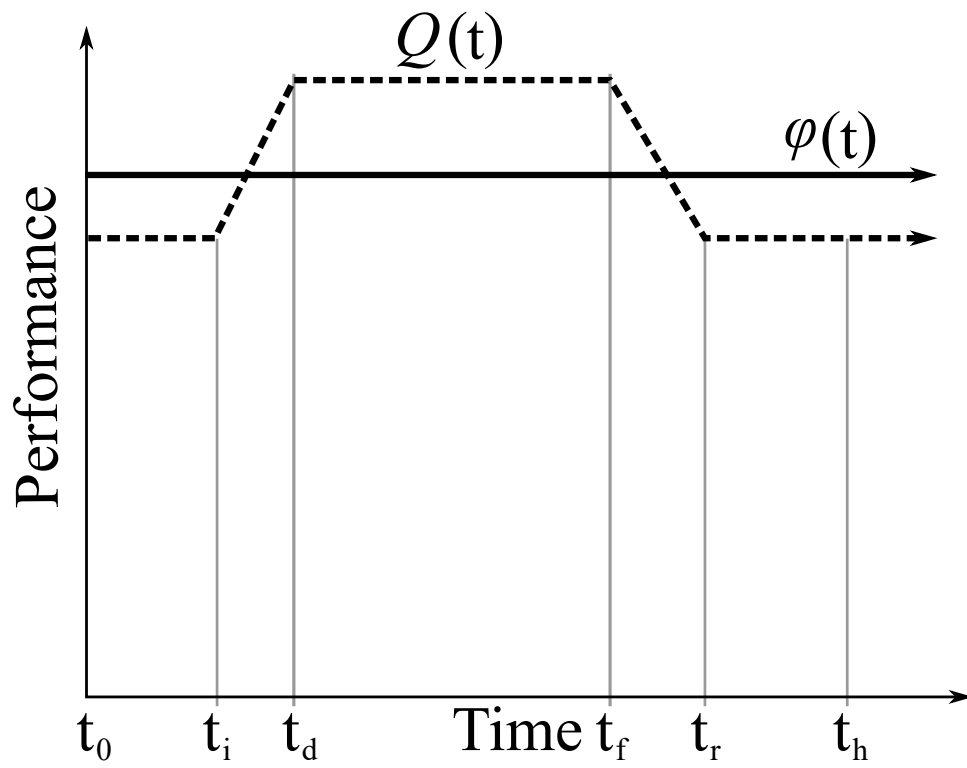


Figure 2.2: Constant performance and changing endogenous preference scenario

2.1.3 Intertemporal Substitutability

Intertemporal substitutability is the “replacement of the consumption of a good or service at one point in time by consumption at a different time” [Black et al., 2017]. In the context of the resilience timeline, intertemporal substitutability quantifies the value of excess performance from the resistance and recovery phases during the robustness phase. If the stakeholder can use surplus production, a resilience model should be able to differentiate between systems. The model of this study will assume that some fraction of excess production can be used at any time during the failure period. Other models may fade out the substitutability as the time of excess production moves further from the failure period. The intertemporal substitutability factor, $\chi(t)$, adjusts the value of the excess production. If surplus is *ephemeral* ($\chi = 0$), then excess production during that period has no value outside of that time. An example of this is excess electricity production without backup capacity. If surplus is *permanent* ($\chi = 1$), all excess output may be applied to shortfalls. An example of this situation is excess electricity with a storage system that has no loss. A value between zero and one identifies some loss in value when exchanging its time output. Intertemporal substitutability may also be time- and event-dependent.

2.2 Gap 2 - Model Comparison

The literature has few studies comparing the outputs of competing resilience models. In general, the resilience model literature focuses upon development

and application of a resilience model with little direct comparison among models. Few instances of resilience model comparison in support of decision-making. The reader is left with little in the way of guidance for choosing an appropriate resilience model or the limitations of a resilience model.

2.3 Gap 3 - Common Framework for Resilience Assessment

The resilience literature focuses upon resilience model development or identifying system-specific characteristics of a system that improve resilience. A gap in the state of the art is a methodology for conducting a resilience analysis that allows an analyst to apply the same methodology to cross-domain systems. This capability is critical when considering a complex, interconnected system of systems such as the infrastructure and operation of a city after a natural disaster.

2.4 Research Objective 1 - Develop Hybrid Resilience Framework

Research objective 1 defines a methodology for conducting a resilience analysis. The methodology should accommodate multiple system functional outputs and stakeholder preferences. The methodology applies to a wide variety of systems and data generation methods by separating the system model from the resilience model.

One task extends a set of resilience models to include three key stakeholder preferences: time horizon, endogenous preference, and intertemporal substitutability. The result is a mathematical framework for quantifying resilience as a decision support model incorporating the preferences of primary stakeholders. The exten-

sion will explicitly incorporate the stakeholder needs identified in Gap 1: endogenous preference, time horizon, and intertemporal substitutability.

2.5 Research Objective 2 - Conceptual Validation of the Resilience Models in the Context of the Hybrid Resilience Framework

Conceptual validation builds trust in the outputs of resilience models. A key task is developing fundamental profiles of functional performance and stakeholder preference. The fundamental models are the inputs to the resilience models that cause a change in resilience that can be determined by inspection. For instance, by varying robustness of a system after failure and holding the other parameters constant, as robustness increases, resilience should increase. This will be done for all phases of resilience and for the stakeholder preferences. Comparisons of the resilience models' behaviors form the basis for assessing each model's ability to support decision and communicate uncertainty.

2.6 Research Objective 3 - Apply Hybrid Resilience Framework to Case Studies

Case studies identify systems of interest and their associated simulations provide the inputs to exercise the decision-support capability of the resilience model. The case studies will demonstrate the effects of changes in stakeholder preferences and selected courses of action. The case studies' systems of interest for suffer disturbances of uncertain strength at uncertain intervals. The level of degradation

after a failure may vary. The speed and level of recovery may vary. The hybrid resilience methodology case studies will be in unrelated domains and demonstrate compatibility with system of system analysis.

Chapter 3: Methodology

The overarching methodology comprised four steps. The first step selected the resilience models and identified the input metrics and parameters for the models. The second step extended, or modified, the models to include stakeholder preferences. Completion of step one and two satisfied research objective 1. The third step conceptually validated the resilience models using fundamental models of system performance and stakeholder need. Step three satisfied research objective two. The fourth step applied the resilience models to simulation case studies. Two different types of simulations provided input to the resilience models. Step four satisfied the third research objective. Figure 3.3 shows the high-level methodological flow.

3.1 Defining the Hybrid Modeling Framework

Resilience requires context. [Carpenter et al. \[2001\]](#) summarized the context of resilience in socio-ecological problems with the question “... resilience of what to what?” Studies in engineering proposed adding “for whom?” when discussing engineered systems [[Emanuel, 2017](#), [Emanuel and Ayyub, in press](#)]. [Ayyub \[2014b\]](#) defined the method for measuring resilience: “The resilience of a system’s function can be measured based on the persistence of a corresponding functional perfor-

mance under uncertainty in the face of disturbances.” One or multiple stakeholders’ preferences provide the context for assessing the value of the system’s functional output. The stakeholder preferences answer the questions “How much is enough?”, “How long must the system perform?”, and “What value will today’s surplus output have when the system suffers a disturbance in functional output?” [Emanuel, 2017, Emanuel and Ayyub, in press]

Shanthikumar and Sargent [1983] described four types of hybrid models composed of analytical models and simulations. In a class I hybrid model, an analytical model and a simulation worked independently to provide analyst’s solution. A class II model used an analytic model to scope the sampling space for the simulation. A class III model used simulation results as an input to an analytical model (Figure 3.1). The roles reversed in a class IV model with the analytic model providing results to the simulation.

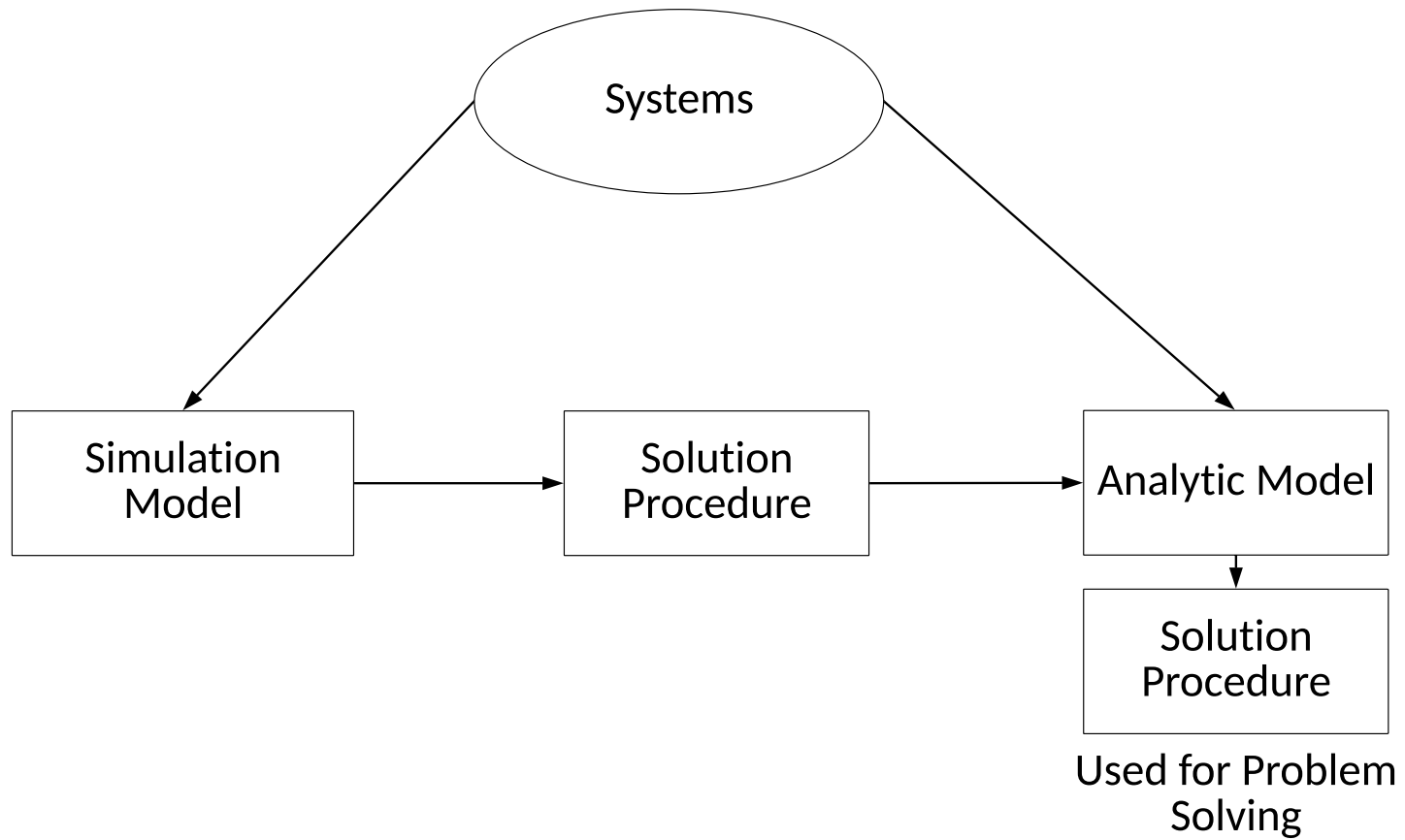


Figure 3.1: Class III hybrid simulation/analytic model [Shanthikumar and Sargent, 1983]

Simulation and analytical models each have their own advantages for resilience analysis. The composition of system, systems of systems, and their associated data vary greatly across domains, but the attributes of resilience apply across domains. The class III hybrid model provided the flexibility to produce appropriate data for the system, system of systems, threats, and scenarios, while maintaining a common analytical model for calculating resilience. The class III hybrid model served as the framework for identifying system characteristics, data of interest, and the stakeholder preferences.

The class III hybrid model explicitly separates the system data and the resilience analytical model as shown in Figure 3.1. The system splits into the system and the stakeholder shown in Figure 3.2. The system informed the data generation method. Data generation methods included data collected from the system in operation; data collected from similar systems or systems under test; or a simulation of the system. Endogenous preference, time horizon, and intertemporal substitutability populated the stakeholder model. Some data generation methods could include portions of the stakeholder profile; for instance, a simulation could model the storage capacity of the system. The stakeholder preference profile must take this into account.

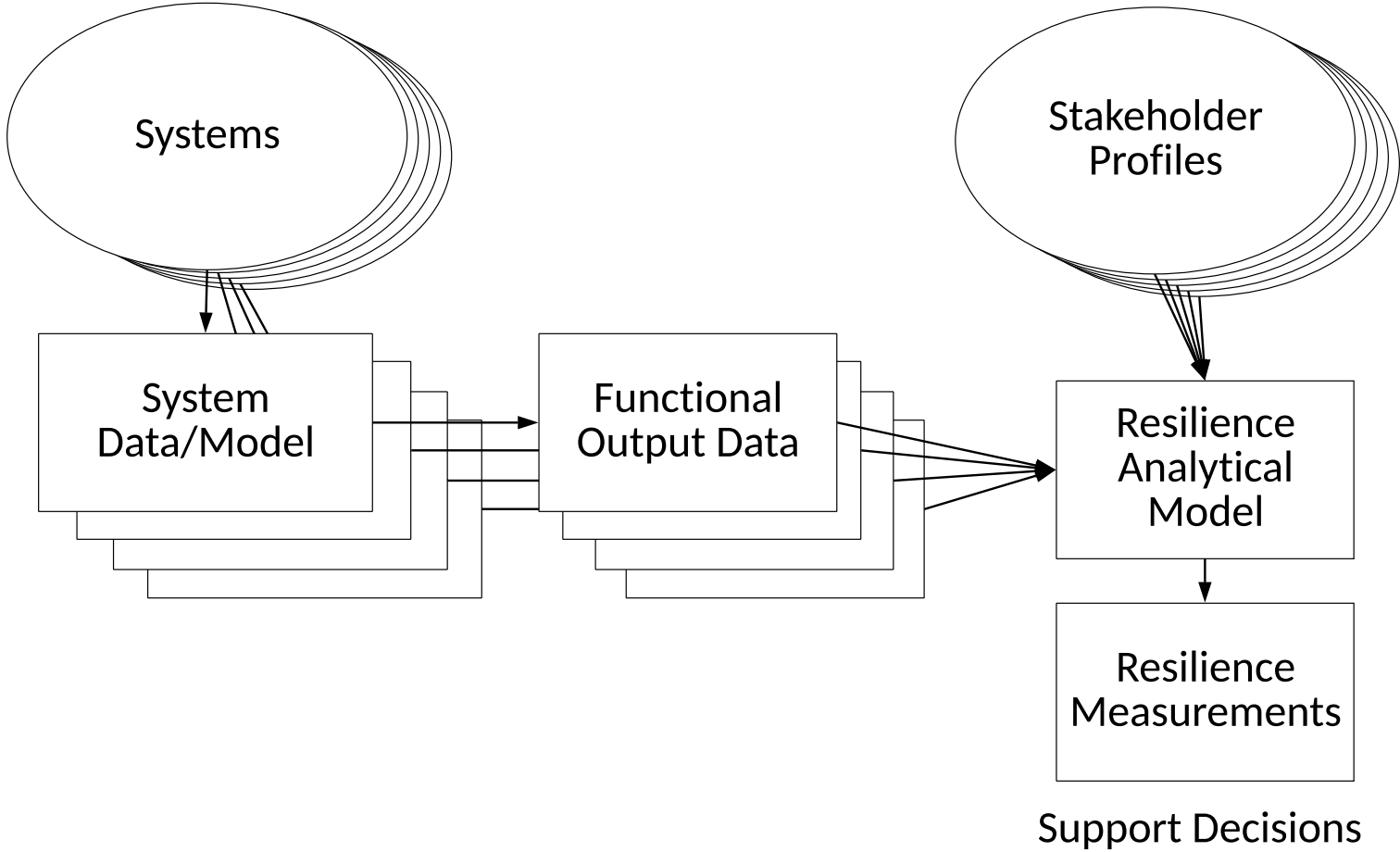


Figure 3.2: Class III model modified for the hybrid resilience framework

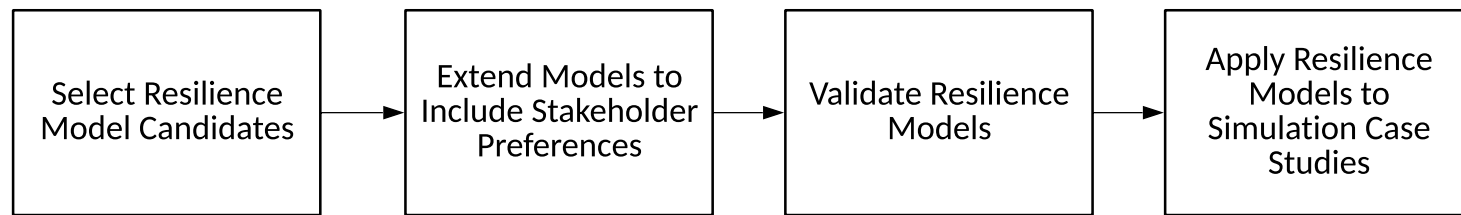


Figure 3.3: General methodology

The hybrid resilience framework guides the analyst through the analysis:

1. Identify the system of interest
2. Identify system representation, for example:
 - System in its operating environment
 - System in a test environment
 - Surrogate system
 - System simulation
3. Collect functional output data, such as:
 - Direct measurement from operating system
 - Direct measurement from test system
 - Outputs from system simulation
4. Define stakeholder preference profiles:
 - Time horizon
 - Endogenous preference
 - Intertemporal substitutability
5. Produce resilience measurements

3.1.1 System Identification and Functional Output Measurement

The analyst first identifies the system(s) of interest and the functional output(s). This activity sets the scope of the study which drives the physical and functional definition of the system(s) of interest. Stakeholders have requirements for output from the system of interest. Selecting the system and functional models should always be performed in this context. The analyst defines the external layers interfacing with the system of interest. The external layers provide context for the normal operating environment of the system and disturbance type, frequency, and magnitude to the system [Egli et al., 2015].

The functional outputs of the system of interest provide the measures for the resilience analytic model [Ayyub, 2014a]. The symbol φ represents functional performance. The functional performance is a key input for the resilience analytical model.

3.1.2 Stakeholder Preference Profiles

The stakeholder preference profiles provides the context for the functional output data. A stakeholder must determine the quantity of output that satisfies stakeholder needs, the overall time period the system must operate to be useful to the stakeholder, and the ability to time-shift surplus functional output to periods of shortage.

3.2 Select Resilience Model Candidates

The literature identified several potential models to use to measure resilience incorporating stakeholder preferences. Figure 3.4 shows the criteria for selecting resilience models for this study. The first requirement is the resilience models must satisfy the definition of resilience. That is, the resilience model must encompass the resistance, robustness, and recovery phases, or be amenable to extension.

The resilience model must support a class III hybrid simulation/analytic framework. The resilience model must be separable from the system, and it must use the functional output of the system as an input. These two requirements ensure the resilience model will be portable among different systems and data types.

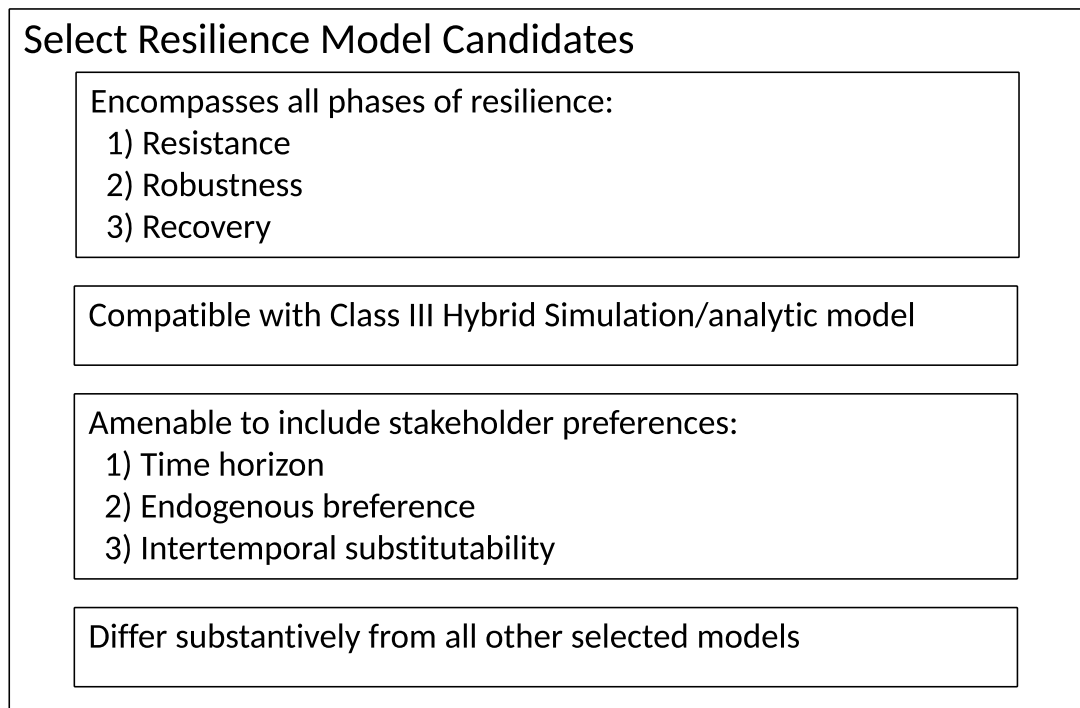


Figure 3.4: Resilience model selection criteria

The resilience analytic model must account for the stakeholder preferences defined in Section 2.1 or be modifiable to incorporate the preferences as parameters in the model.

Table 3.1 summarizes the desired characteristics of a resilience model. Some models, such as network models and resilience triangle-type models, focus upon the robustness, or robustness and recovery of the system. Network models couple tightly with the simulation and models of the network itself. This makes network models difficult to extract for use on non-network type systems. The time-based resilience models cover all phases of resilience, are separable from the model of the system, and are based upon the output of the system.

The study selected Integral Resilience, Resilience Factor, Quotient Resilience, and Total Quotient Resilience (Table 3.2). Each of these models satisfied the requirements listed above.

Table 3.1: Model Criteria Assessment.

Model Name and Reference	Resistance	Robustness	Recovery	Separable from System	Based upon Functional Output	Unrestricted Performance
Resilience Triangle (Eq. 1.5)		X	X	X	X	
Adjusted Resilience Triangle (Eq. 1.7)		X	X	X	X	
Quotient Resilience (Eq. 1.1)	X	X	X	X	X	X
Network Resilience (Eq. 1.21)		X			X	
Current Potential Resilience (Eq. 1.13)	X	X	X	X	X	X
Resilience Curve [Alderson et al., 2011]		X			X	
Integral Resilience (Eq. 1.8)	X	X	X	X	X	X
Practical Integral Resilience (Eq. 1.10)	X	X	X	X	X	
Expected System Degradation Factor (Eq. 1.4)	X	X	X		X	X
Resilience Factor (Eq. 1.2)	X	X	X	X	X	X
Recovery Dependent Resilience (Eq. 1.16)	X	X	X	X	X	X
Total Resilience (Eq. 1.14)	X	X	X	X	X	X

3.3 Extend the Models to Include Stakeholder Preferences

After selecting the candidate models, the next step is identifying where the models include stakeholder preferences and extending the metrics to include the preferences they are missing. Figure 3.5 shows the three stakeholder preferences and the symbology used throughout the study.

Table 3.2: Resilience models used in this study.

Model Name	Analytical Model
Quotient Resilience (Eq. 1.1)	$R_{QR} = \frac{\varphi(t) - \varphi(t_d)}{\varphi(t_0) - \varphi(t_d)}$
Total Quotient Resilience (Eq. 1.14)	$R_{TQR} = \frac{\int_{t_0}^{t_h} R_{QR}(u) du}{t_h - t_0}$
Resilience Factor (Eq. 1.2)	$\rho = S_p \frac{\varphi(t_r) \varphi(t_d)}{\varphi(t_0) \varphi(t_0)}$
Integral Resilience (Eq. 1.8)	$R_{IR} = \frac{T_i + F\Delta T_f + R\Delta T_r}{T_i + \Delta T_f + \Delta T_r}$

3.3.1 Incorporate Time Horizon

The integral resilience models implicitly assume the time horizon ends with recovery [Ayyub, 2014a, Francis and Bekera, 2014, Gama Dessavre et al., 2016, Henry and Ramirez-Marquez, 2012] or explicitly with the return period of the stressor [Ayyub, 2015]. While these are two reasonable points for a time horizon, the stakeholder may have other motivations for setting a time horizon such as the reasonable lifetime of the system, an anticipated operational capability of a replacement system, or the return period of a random process.

The resilience model currently ends at the recovery time. The stakeholder defined time horizon is t_h . Time horizon is naturally included in the Resilience Factor and Quotient Resilience models. One simply records the resilience value at

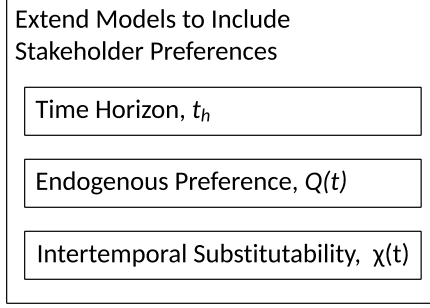


Figure 3.5: Extend resilience models to incorporate stakeholder preferences

the time of interest, t_r , for Resilience Factor and t for Quotient Resilience.

$$\rho_i(S_p, \varphi(t_0), \varphi(t_d), \varphi(t_h)) = S_p \frac{\varphi(t_h)}{\varphi(t_0)} \frac{\varphi(t_d)}{\varphi(t_0)} \quad (3.1)$$

$$R_{QR} = \frac{\varphi(t_h) - \varphi(t_d)}{\varphi(t_0) - \varphi(t_d)} \quad (3.2)$$

Integral resilience supports this method for times less than the recovery time, but an additional factor is necessary to accommodate time horizons that extend beyond the recovery time. $\Delta T_h = t_h - t_r$ is the time period from recovery to the stakeholder's time horizon. Adding ΔT_h changes the resilience model to:

$$R_{IR} = \frac{T_i + F\Delta T_f + R\Delta T_r + \Delta T_h}{T_i + \Delta T_f + \Delta T_r + \Delta T_h} \quad (3.3)$$

3.3.2 Stakeholder Endogenous Preference

The change to resilience factor is straightforward. The initial performance level, $\varphi(t_0)$, is replaced by the stakeholder need at the appropriate time in the

denominator. Rather than take the values at the minimum performance level, t_d , is the maximum shortfall in desired performance during the degradation period.

Resilience Factor becomes:

$$\rho_i = S_p \frac{\varphi(t_d) \varphi(t_r)}{\varphi(t_d) \varphi(t_r)} \quad (3.4)$$

Quotient Resilience incorporates stakeholder need by substituting $\varphi(t)$ with a ratio of figure of merit and need $\frac{\varphi(t)}{Q(t)}$. Quotient Resilience becomes:

$$R_{QR} = \frac{\frac{\varphi(t)}{Q(t_h)} - \frac{\varphi(t_d)}{Q(t_d)}}{\frac{\varphi(t_0)}{Q(t_0)} - \frac{\varphi(t_d)}{Q(t_d)}} \quad (3.5)$$

A pre-disturbance profile, M , and a post-recovery profile, H , capture the excess performance and shortfalls before failure and after recovery. They are defined as:

$$M = \frac{\int_{t_0}^{t_i} \varphi(t) dt}{\int_{t_0}^{t_i} Q dt}; R = \frac{\int_{t_r}^{t_h} \varphi(t) dt}{\int_{t_r}^{t_h} Q dt} \quad (3.6)$$

Applying the coefficients to the appropriate time interval results in the following Integral Resilience model:

$$R_{IR} = \frac{M\Delta T_i + F\Delta T_f + R\Delta T_r + H\Delta T_h}{\Delta T_i + \Delta T_f + \Delta T_r + \Delta T_h} \quad (3.7)$$

3.3.3 Incorporate Intertemporal Substitutability

Intertemporal substitutability, χ , is the “replacement of the consumption of a good or service at one point in time by consumption at a different time” [Black et al., 2017]. Intertemporal substitutability takes values from zero to one. The value of χ may be constant for the entire time horizon, or it may be dependent upon time or events. Two special values of χ are the *ephemeral* and *permanent* cases. The *ephemeral* case ($\chi = 0$) allows no substitution across time. When the system has a shortage at time t_j , surplus from time t_i has no value. The *permanent* case ($\chi = 1$) where a surplus retains its full value or utility throughout the time horizon. Any surplus at time t_i has full value at time t_j .

The following expression incorporates intertemporal substitutability into the performance to need ratios used in Resilience Factor and Quotient Resilience:

$$\Phi_\chi(t) = \begin{cases} \frac{\varphi(t)}{Q(t_{d,r})} & \text{for } \varphi(t) < Q(t) \\ 1 + \chi(t) \frac{\varphi(t) - Q(t)}{Q(t_{d,r})} & \text{for } \varphi(t) \geq Q(t) \end{cases} \quad (3.8)$$

Resilience Factor becomes:

$$\rho_E = S_p \Phi_\chi(t_d) \Phi_\chi(t_h) \quad (3.9)$$

The same performance ratios add intertemporal substitutability to the Quotient Resilience model:

$$R_{EQR}(t) = \frac{\Phi_\chi(t) - \Phi_\chi(t_d)}{\Phi_\chi(t_0) - \Phi_\chi(t_d)} \quad (3.10)$$

Extending total quotient resilience merely changes the integrand in the numerator of the equation from quotient resilience to extended quotient resilience. Extended quotient resilience is:

$$R_{ETQR} = \frac{\int_{t_0}^{t_h} R_{EQR}(t) dt}{\int_{t_0}^{t_h} Q(t) dt} \quad (3.11)$$

Integral Resilience must incorporate time substitutability into each of the profiles, M , F , R , and H . The time substitutability factor applies the same way for each profile. For all t where φ is less than $Q_r(t)$, the profile value remains unchanged:

$$\begin{aligned} M_\chi(t_0 \leq t \leq t_i) &= \begin{cases} M & \varphi(t) < Q(t) \\ 1 + \chi(t)(M - 1) & \varphi \geq Q(t) \end{cases} \\ F_\chi(t_0 \leq t \leq t_i) &= \begin{cases} F & \varphi(t) < Q(t) \\ 1 + \chi(t)(F - 1) & \varphi \geq Q(t) \end{cases} \\ R_\chi(t_0 \leq t \leq t_i) &= \begin{cases} R & \varphi(t) < Q(t) \\ 1 + \chi(t)(R - 1) & \varphi \geq Q(t) \end{cases} \\ H_\chi(t_0 \leq t \leq t_i) &= \begin{cases} H & \varphi(t) < Q(t) \\ 1 + \chi(t)(H - 1) & \varphi \geq Q(t) \end{cases} \end{aligned} \quad (3.12)$$

The Extended Integral Resilience becomes:

$$R_{EIR} = \frac{M_{\chi}\Delta T_i + F_{\chi}\Delta T_f + R_{\chi}\Delta T_r + H_{\chi}\Delta T_h}{\Delta T_i + \Delta T_f + \Delta T_r + \Delta T_h} \quad (3.13)$$

Table 3.3 summarizes the naming conventions and equations for all resilience analytical models, original and extended, that are part of this study.

Fundamental deterministic and stochastic simulations provided the scenarios for considering the merits of each resilience metric. Scenarios were a set of inputs to develop the data for performance of a notional system and for notional stakeholders that are inputs for the resilience models. The scenarios were fundamental in the sense that, through the understanding of the definition of resilience, the direction of the change in the resilience value can be determined by inspection. For example, if the robustness of a system increased, one should expect the resilience to increase as well. Figure 3.6 shows the process for conceptually validating the models.

A series of foundational models of system performance and stakeholder need provided the scenarios for measurement. The assessment covered the models' ability to distinguish between different performance models and their consistency. The baseline deterministic performance and preference profiles are:

- Step failure without recovery (Figure 4.1a)
- Step failure with step recovery (Figure 4.1b)
- Step failure with linear recovery (Figure 4.1c)
- No failure with step increase in endogenous preference (Figure 4.1d).

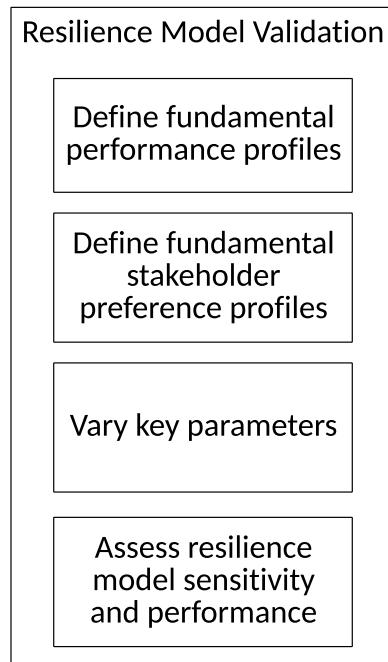


Figure 3.6: Steps to conceptually validate the original and extended resilience models

Table 3.3: Summary of the Eight Resilience Analytical Models

Model Name	Analytical Model
Quotient Resilience	$R_{QR} = \frac{\varphi(t) - \varphi(t_d)}{\varphi(t_0) - \varphi(t_d)}$
Extended Quotient Resilience	$R_{EQR}(t) = \frac{\Phi_\chi(t) - \Phi_\chi(t_d)}{\Phi_\chi - \Phi_\chi(t_d)}$
Total Quotient Resilience	$R_{TQR} = \frac{\int_{t_0}^{t_h} R_{QR}(u) du}{t_h - t_0}$
Extended Total Quotient Resilience	$R_{ETQR} = \frac{\int_{t_0}^{t_h} R_{EQR}(t) dt}{\int_{t_0}^{t_h} Q(t) dt}$
Resilience Factor	$\rho = S_p \frac{\varphi(t_r) \varphi(t_d)}{\varphi(t_0) \varphi(t_0)}$
Extended Resilience Factor	$\rho_E = S_p \Phi_\chi(t_d) \Phi_\chi(t_h)$
Integral Resilience	$R_{IR} = \frac{T_i + F\Delta T_f + R\Delta T_r}{T_i + \Delta T_f + \Delta T_r}$
Extended Integral Resilience	$R_{EIR} = \frac{M_\chi \Delta T_i + F_\chi \Delta T_f + R_\chi \Delta T_r + H_\chi \Delta T_h}{\Delta T_i + \Delta T_f + \Delta T_r + \Delta T_h}$

Table 3.4: Scenarios for Deterministic Fundamental Profiles

Scenario	Constant Parameters	Varied Parameters
Step Failure without Recovery	Initial Performance	Time to Failure Level of Failure Time Horizon Endogenous Preference Intertemporal Substitutability
Step Failure with Step Recovery	Initial Performance Time to Failure	Level of Failure Time to Recover Level of Recovery Time Horizon Endogenous Preference Intertemporal Substitutability
Step Failure with Linear Recovery	Initial Performance Time to failure Time to recover	Time Horizon Endogenous Preference Intertemporal Substitutability
No Failure with Changing Need	Initial Performance Profile of Endogenous Preference	Time Horizon Intertemporal Substitutability

3.4 Case Studies

Two case studies will satisfy Research Objective 3: “Exercise the decision-support capability of the resilience in two case studies using different types of models to simulate the behavior of the systems.” The models simulated how inputs were turned into functional outputs. Each case study defined scenarios, stakeholders, disruptive events, functional outputs, and basis of analysis. Stakeholder perspectives defined the functional outputs of interest and their associated preferences. Disruptive events caused degradation in functional output and may be external or internal to the system. External disruptive events were changes to the input variable or the stakeholder preferences whereas internal disruptive events are failures to the working of the system that cause degradation of the functional output.

For all cases, the study developed indicators in the resilience software to enable analysts to spot-check the operation of the resilience model. Before generating complex time-series data of the system’s functional output, the resilience models used fundamental models. Ad hoc stakeholder and performance parameter sensitivity studies built confidence that the model responded appropriately.

3.4.1 Infrastructure Resilience Case Study

To demonstrate the hybrid methodology, a system dynamics model of the critical infrastructure systems of Austin, Texas provides the functional outputs for the resilience model (Figure 3.7). The infrastructure case study has three phases. The first phase investigates a deterministic electrical failure and its impact on water

supply from the perspective of three stakeholders. The second phase studies an electrical failure's impact on seven other critical infrastructures each with their own stakeholder preference profiles. The third phase applies a probabilistic electrical failure defined by a Monte Carlo simulation of hurricane arrival times and strength to stresses the electrical system output in the system dynamics model. The resilience model captures the resilience of all critical infrastructures identified in the model relative to their stakeholders' preferences, and the storm impact to the electrical system. The study applies the hybrid methodology to produce a post hoc analysis of the electrical grid resilience of post-Maria Puerto Rico.

3.4.2 Fleet Resilience Case Study

The US Department of Defense has many long-lived systems with multiple stakeholders with different preferences. The fleet resilience case study applied the hybrid resilience framework to a squadron of training aircraft (Figure 3.8). Key stakeholders were the program manager and the squadron commanding officers. The study calculated the resilience of several functional outputs of the training squadron (graduation rates, satisfaction rates, daily ready aircraft) with the intent to allow stakeholders to quantify the impact of three courses of action. Stakeholder profiles explored different values for time horizon, endogenous need, and intertemporal substitutability. Further development of the intertemporal substitutability enabled time and event based stakeholder preference profiles. A discrete event simulation developed provided the time-series functional data input for the resilience analytical

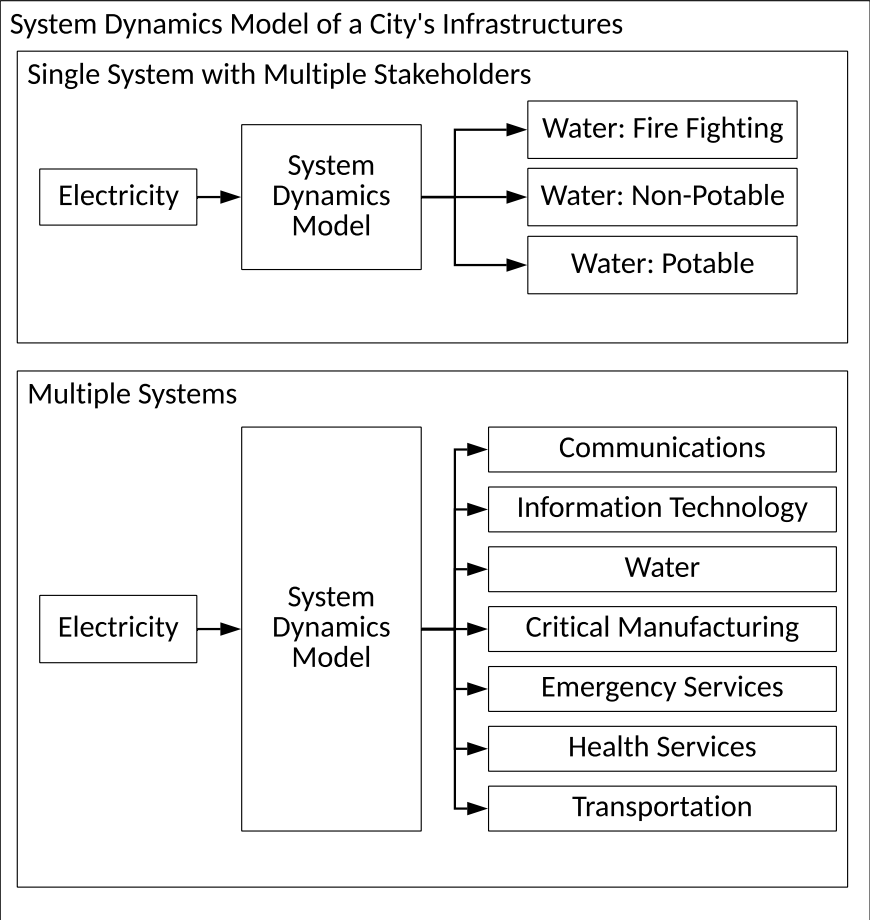


Figure 3.7: Infrastructure resilience case study

model.

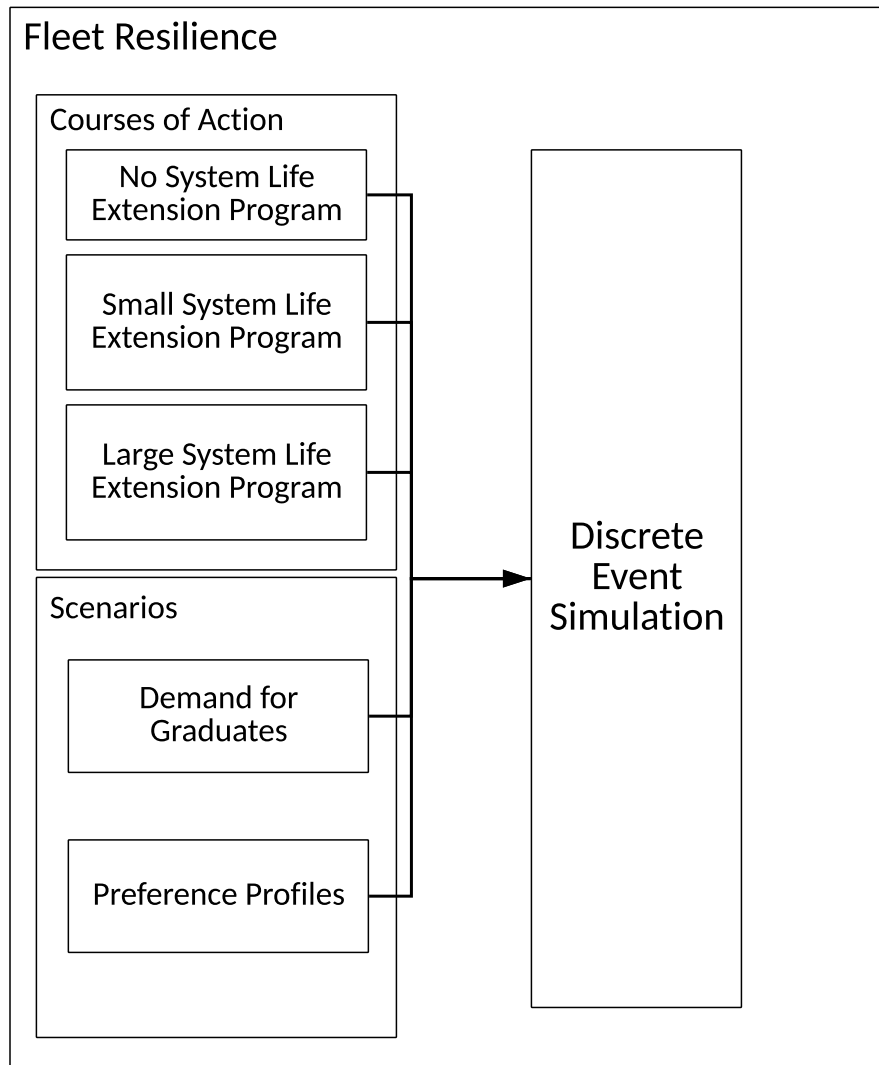


Figure 3.8: Fleet resilience case study

3.5 Methodology Review

This overall study has four sections of action. The first step selected the resilience models best capable of:

- Using the functional output of the system as an input
- Compatible with a class III hybrid simulation/analytic model to ensure compatibility with a broad spectrum of data sources
- Encompasses all phases of resilience
- Incorporates or is amenable to modification to incorporate three stakeholder preferences
- Differ substantively from the other selected models.

The second step modified the models to include the time horizon, endogenous preference, and intertemporal substitutability stakeholder preferences. The third step conceptually validated the models by assessing their resilience measurements using fundamental models of performance. The fourth and final step exercised the models in two different case studies, infrastructure resilience and fleet resilience. Figure 3.9 lays out the methodological flow of this study.

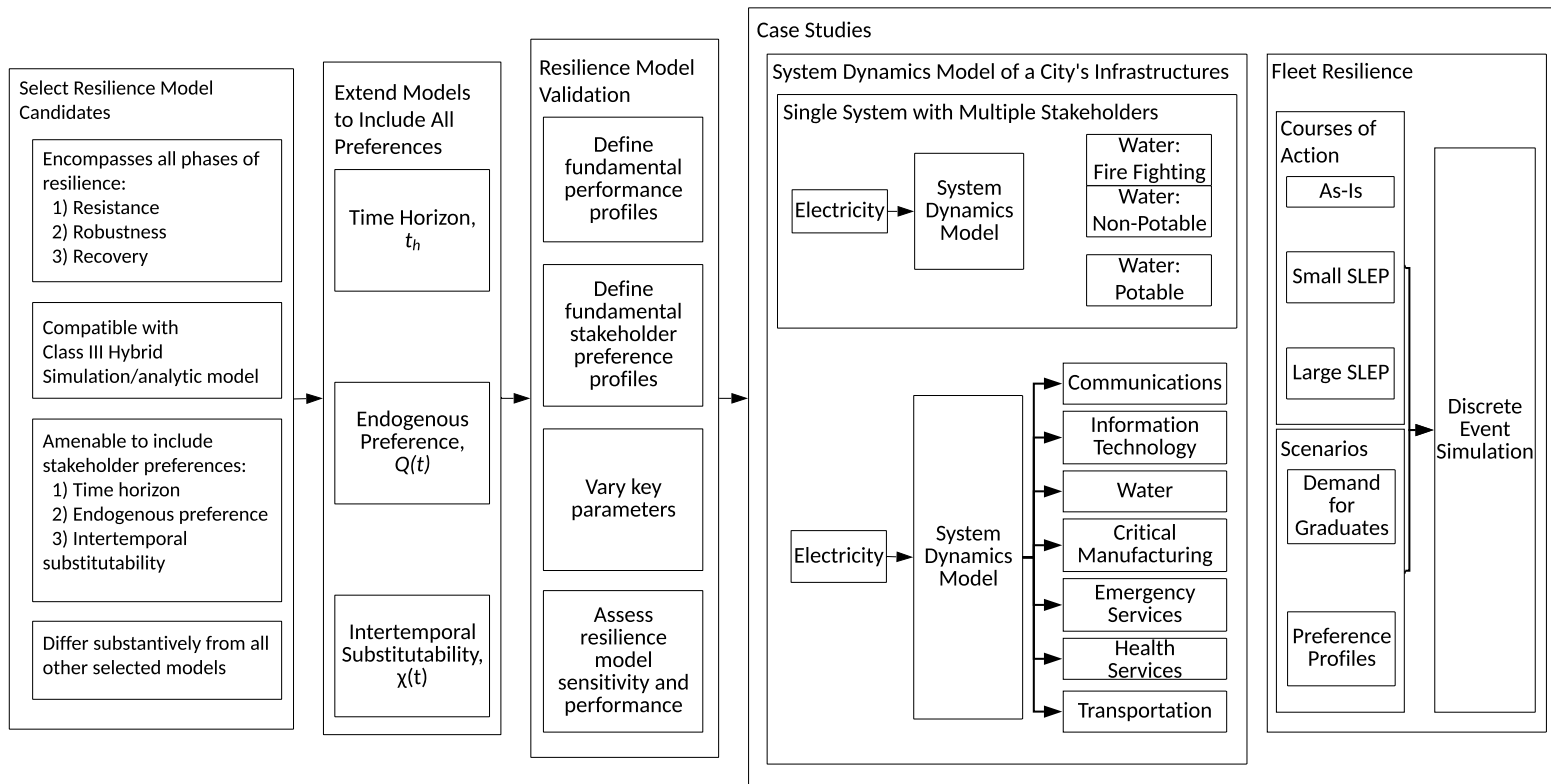


Figure 3.9: Flow of the methodology from model selection to case studies

Chapter 4: Resilience Model Comparison

The resilience model comparison study applied fundamental performance and stakeholder preference profiles to the eight resilience models defined in the previous chapter. The study progressed, one factor at a time, through the key aspects of the performance and stakeholder models to identify situations where the models yield undesirable results, such as insensitivity. The performance scale was set so normal operations is 1.0 and the time scale is from 0 to 100 and was indifferent to the units of the functional output.

4.1 Fundamental performance and preference profiles

Deterministic, fundamental profiles of performance and preference enabled a parametric analysis of the resilience models. The performance profiles were:

1. Step failure without recovery with constant endogenous preference,
2. Step failure with step recovery with constant endogenous preference,
3. Step failure with linear recovery with constant endogenous preference,
4. Step increase in endogenous preference with constant system performance.

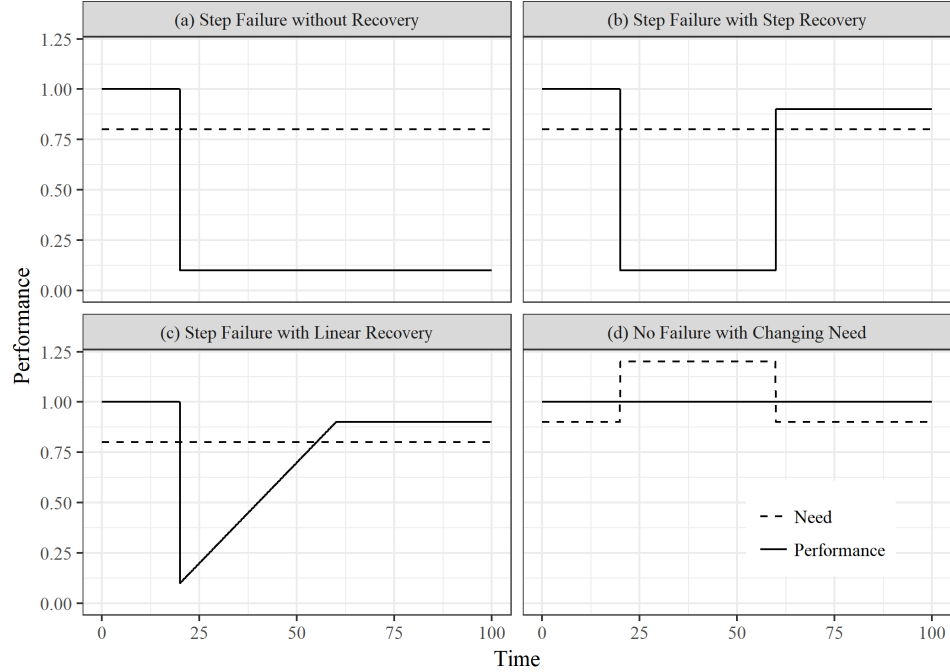


Figure 4.1: Fundamental performance and endogenous preference profiles

The fundamental performance profiles allowed the analyst to assess the resilience models' sensitivity and behavior in response to parameter variation. The performance profile parameters varied for system performance (e.g., time to failure, recovery level) and stakeholder preferences. The parameters defining the performance of the system were: time to failure (t_d), robustness ($\varphi(t_d)$ and F), time to recover (t_r), and recovery level ($\varphi(t_r)$, R , and H). All profiles assumed an instantaneous failure, so failure initiation time, failure completion time, and minimum performance time were the same for all profiles ($t_i = t_d = t_f$). The stakeholder preference parameters were time horizon (t_h), endogenous preference ($Q(t)$), and intertemporal substitutability (χ). Table 4.1 lists the parameter values for all fundamental profiles.

Table 4.1: Parameters for Fundamental Profiles

Parameter	Time to Failure	Robustness	Recovery Time	Recovery Level	Time Horizon	Endogenous Preference	Intertemporal Substitutability
(1)	(2)	(3)	(4)	(5)	(6)	(7)	(8)
$\varphi(t < t_i)$	1.0	1.0	1.0	1.0	1.0	1.0	1.0
$\varphi(t_d < t < t_r)$	0.1	0 - 1.0	0.1	0.1	0.1	0.1	0.1
$\varphi(t_r)$			0.9	0.1 - 1.2	0.9	0.9	0.9
t_d	20 - 60	20	20	20	20	20	20
t_r			20 - 60	60	60	60	60
t_h	80	80	80	80	0 - 100	80	80
$Q(t)$	0.8	0.8	0.8	0.8	0.8*	0 - 1.0	0.8*
χ	0	0	0	0	0	0	0 - 1.0

BLANK entries do not apply to the profile

* Except the changing need model

4.1.1 Time to Failure

Figure 4.2 shows the the resilience value from the models as time to failure varies from 20-60 using profile 4.1(a). Resilience Factor and Quotient Resilience are insensitive to the time to failure while Extended and Integral Resilience increase as the time to failure increases.

4.1.2 Robustness

Robustness is the amount of performance remaining after failure [Ayyub, 2014a, 2015]. The robustness performance profile varied the failure level, $\varphi(t > t_d)$, of Figure 4.1(a) from zero (complete failure) to one (no failure). Figure 4.3 shows the resilience models' behavior. Extended Total Quotient Resilience stepped from a resilience of 0.5 to a resilience of 1.0 when $\varphi(t_d) \geq 0.8$. Extended Resilience Factor and extended Integral Resilience were greater than or equal to their corresponding original resilience models for the entire profile and level off once the $\varphi(t_d) \geq Q(t)$.

Quotient Resilience and Total Quotient Resilience were insensitive to changes in the failure level. Inspecting Quotient Resilience, which is at the base of all four models, revealed the reason for this insensitivity. For all constant failure levels, $R_{QR} = 0$ because the numerator is the difference between the performance at time t and the minimum performance. This occurs whether the performance in the failed state is 90% of desired or completely failed. Because of this, the Quotient Resilience family of models cannot capture robustness.

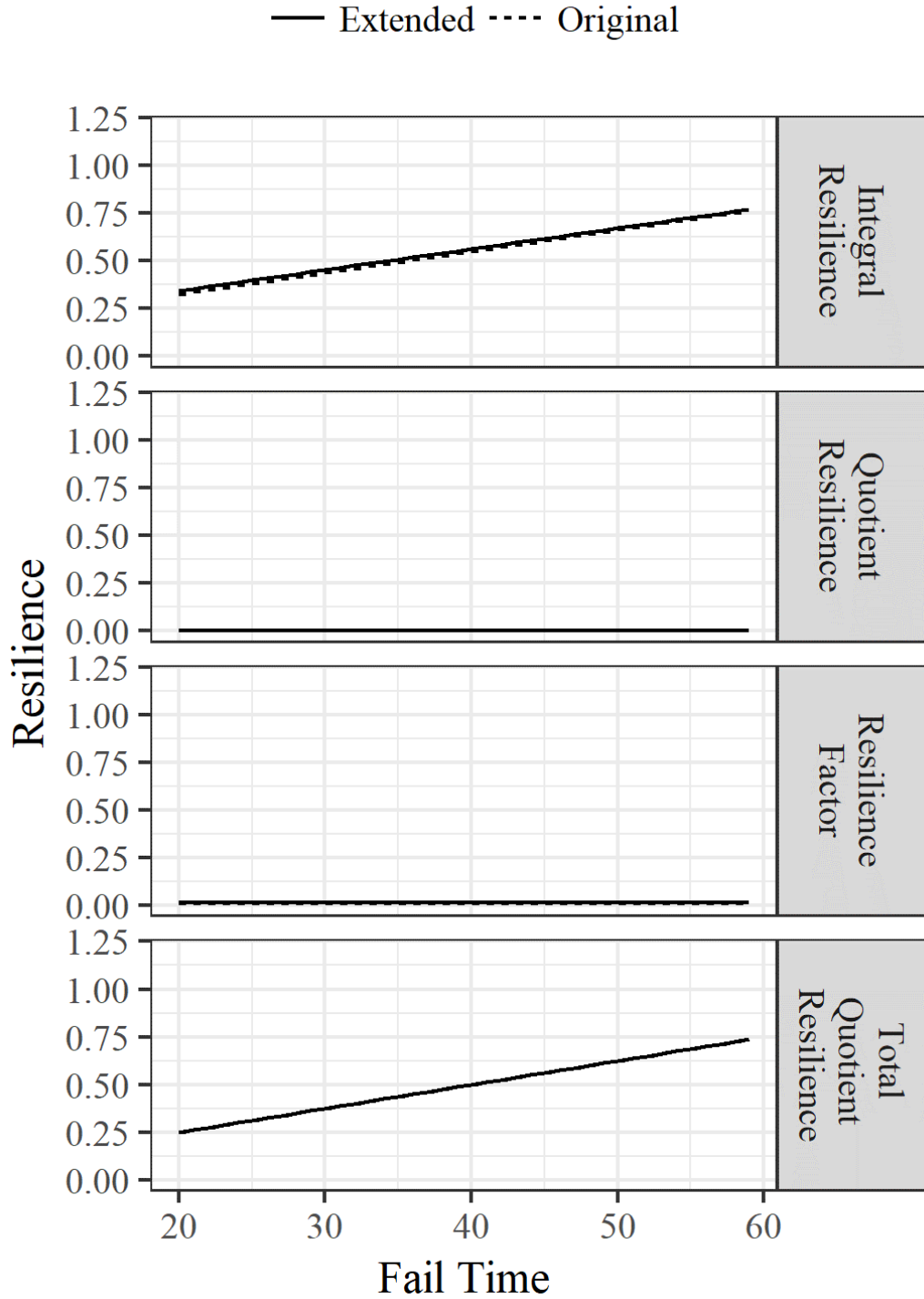


Figure 4.2: Resilience model responses to time to failure in the step failure without recovery performance profile

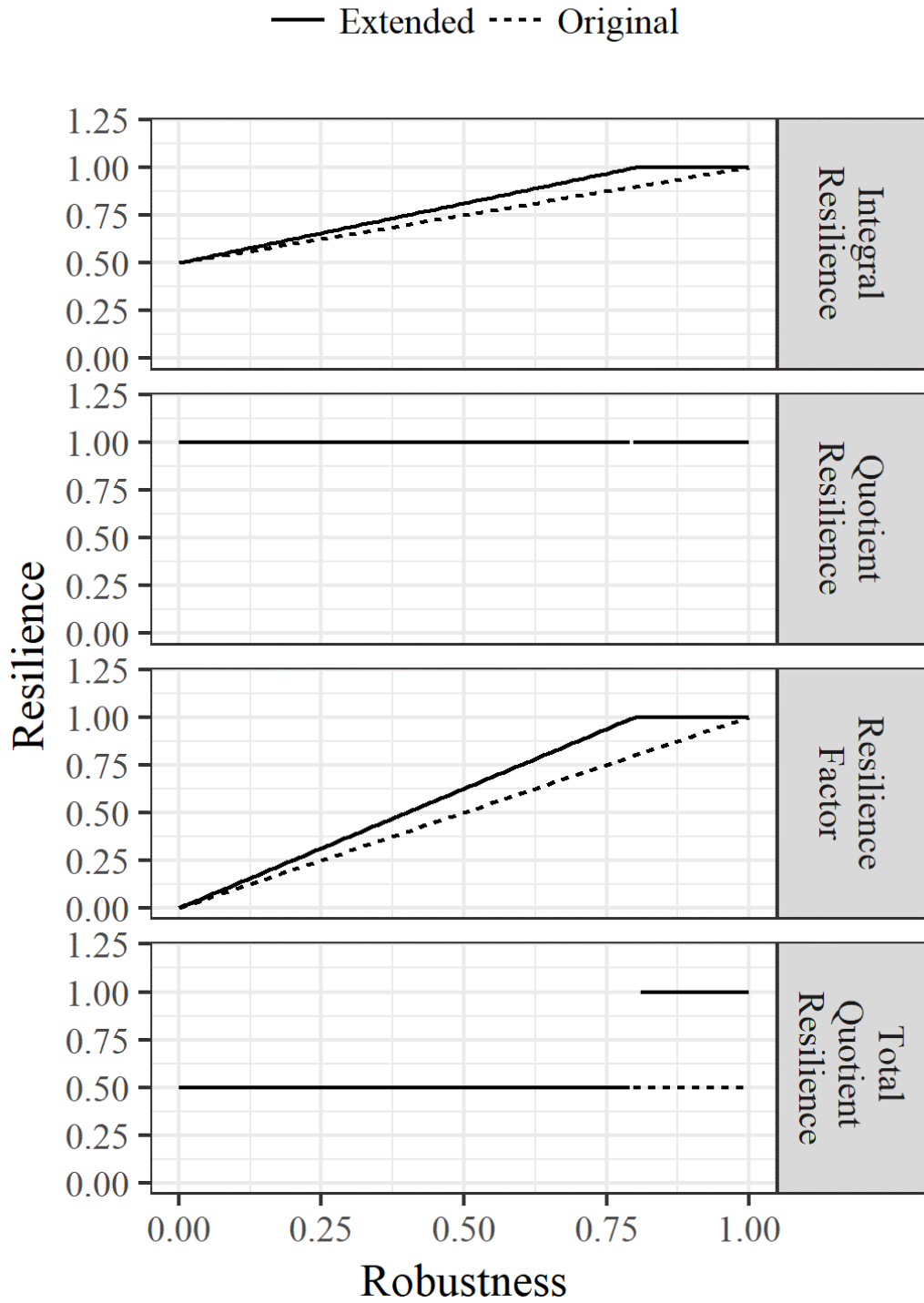


Figure 4.3: Resilience model responses to robustness

4.1.3 Recovery Time

The recovery time performance profile varied the recovery time in Figure 4.1(b) from 21 to 60. Figure 4.4 shows Resilience Factor and Quotient Resilience models were insensitive to the change in recovery time. Both Integral Resilience and Total Quotient Resilience showed decreasing resilience as the time in the degraded state increased.

4.1.4 Recovery Level

The recovery level profile varied the recovery level in Figure 4.1(b) from $\varphi(t_r) = 0.1$ (no recovery) to $\varphi(t_r) = 1.2$. Figure 4.5 shows all resilience models are sensitive to recovery level. The original resilience models increased linearly as recovery levels rise. The extended resilience models increase linearly until the recovery level surpassed stakeholder desired output ($\varphi(t_r) \geq 0.8$).

4.1.5 Time Horizon

The time horizon sensitivity assessment used the four fundamental profiles depicted in Figure 4.1. The time horizon varies from 0 to 100. Figure 4.6 shows the resilience model responses as time horizon varies for each failure model.

Figure 4.6(a) shows the responses of the resilience models to the step failure without recovery profile. Extended and Original Quotient Resilience values fell from one to zero despite a robustness of 0.1 in the degraded state. Extended and Original Resilience Factor fell at the time of failure. Integral Resilience showed a slow drop

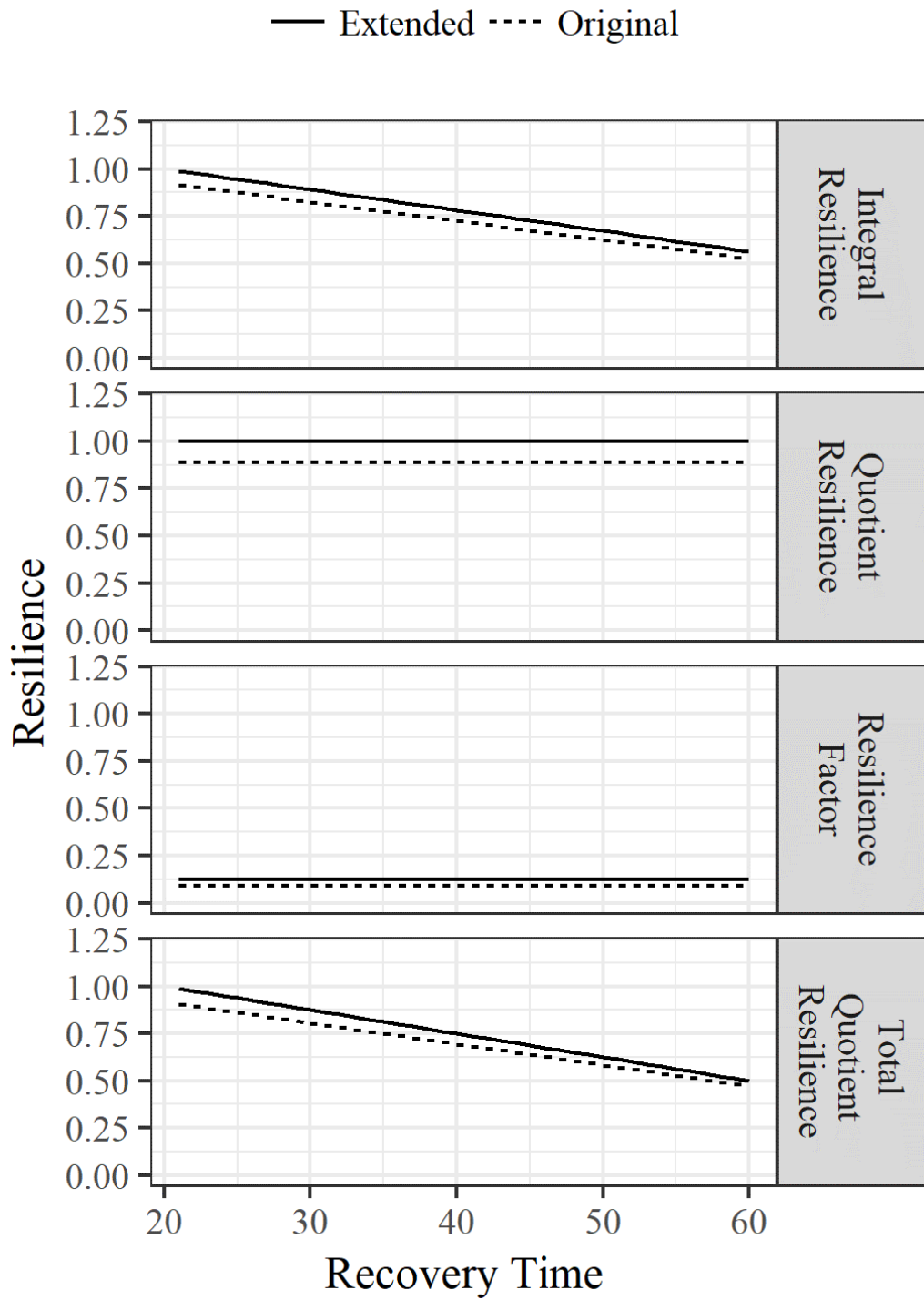


Figure 4.4: Resilience model responses to time to recover

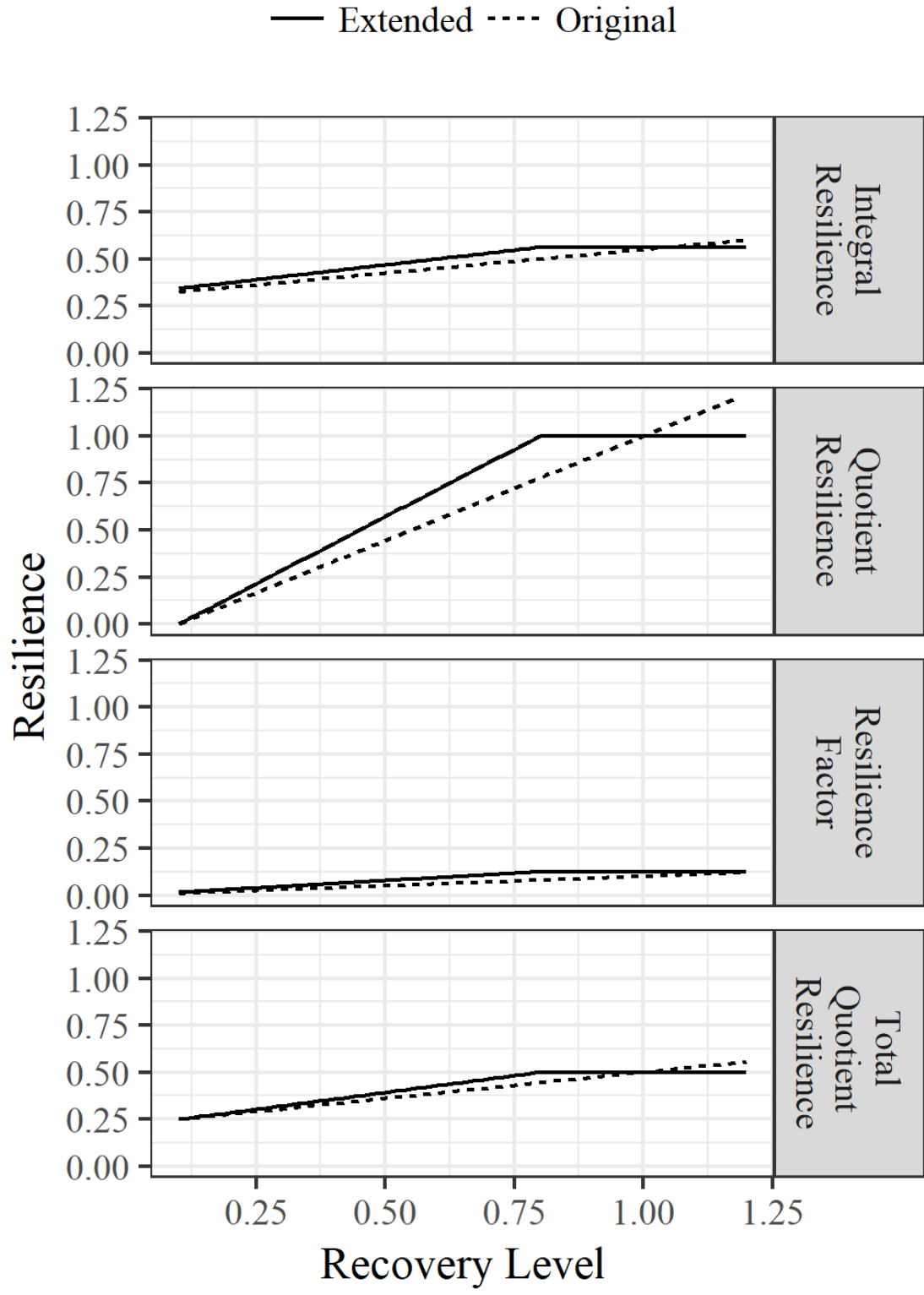


Figure 4.5: Resilience model responses to recovery level

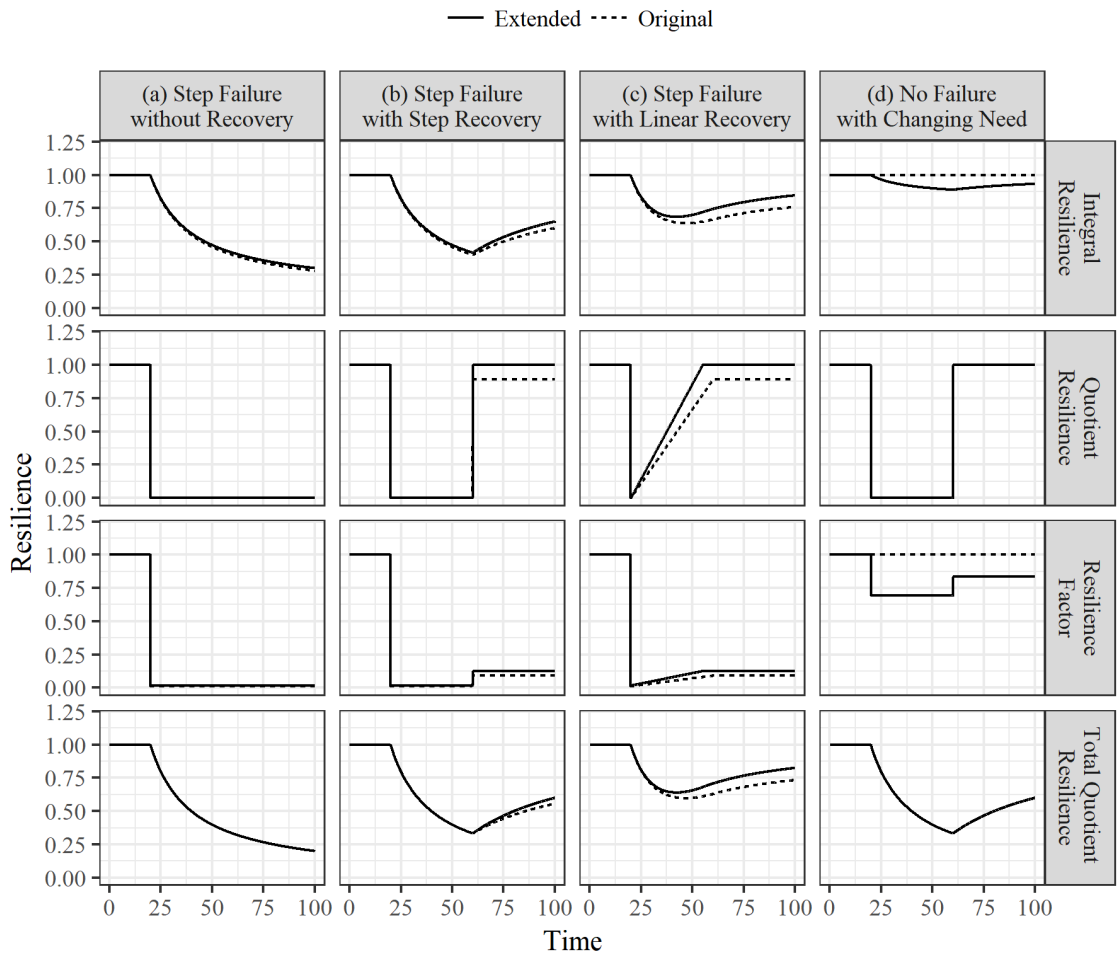


Figure 4.6: Resilience model response to step failure and recovery with varying time horizon

off in value for both models as the time horizon increases.

Figure 4.6(b) showed the responses of the resilience models a to the step failure with step recovery profile. The extended resilience models were equal to or greater than their original counterpart. The Resilience Factor and Quotient Resilience models responded only at the failure (t_d) and recovery (t_r) times. The Integral Resilience Models and Total Quotient Resilience Models responded to failure and recovery values over the entire post-disturbance time.

Figure 4.6(c) shows the resilience model responses to the step failure with linear recovery profile. In each case, the value of the extended resilience model was equal to or greater than the original model. Resilience Factor and Quotient Resilience models responded at failure and rose linearly during the recovery period. Both Integral Resilience Models showed nonlinear response over the profile.

Figure 4.6(d) shows resilience model responses to the profile with no system failure and a step change in stakeholder endogenous preference. Both Original Quotient Resilience and Original Total Quotient Resilience were undefined for the profile. Original Integral Resilience and Original Resilience Factor had constant resilience value of one. The other models expressed responses similar to the step failure with step recovery time horizon profile in Figure 4.6(b).

4.1.6 Endogenous Preference

The endogenous preference case varied a constant endogenous need from zero to one for profiles in Figure 4.1(a), (b), and (c). All original resilience models were

insensitive to changing the endogenous preference (Figure 4.7). Quotient Resilience was sensitive to satisfied endogenous preference, $Q(t) \geq \varphi(t_d)$, but largely insensitive to the degree of satisfaction. Extended Integral Resilience, Extended Resilience Factor, and Extended Quotient Resilience showed distinction between small changes in endogenous preference for much of the profile.

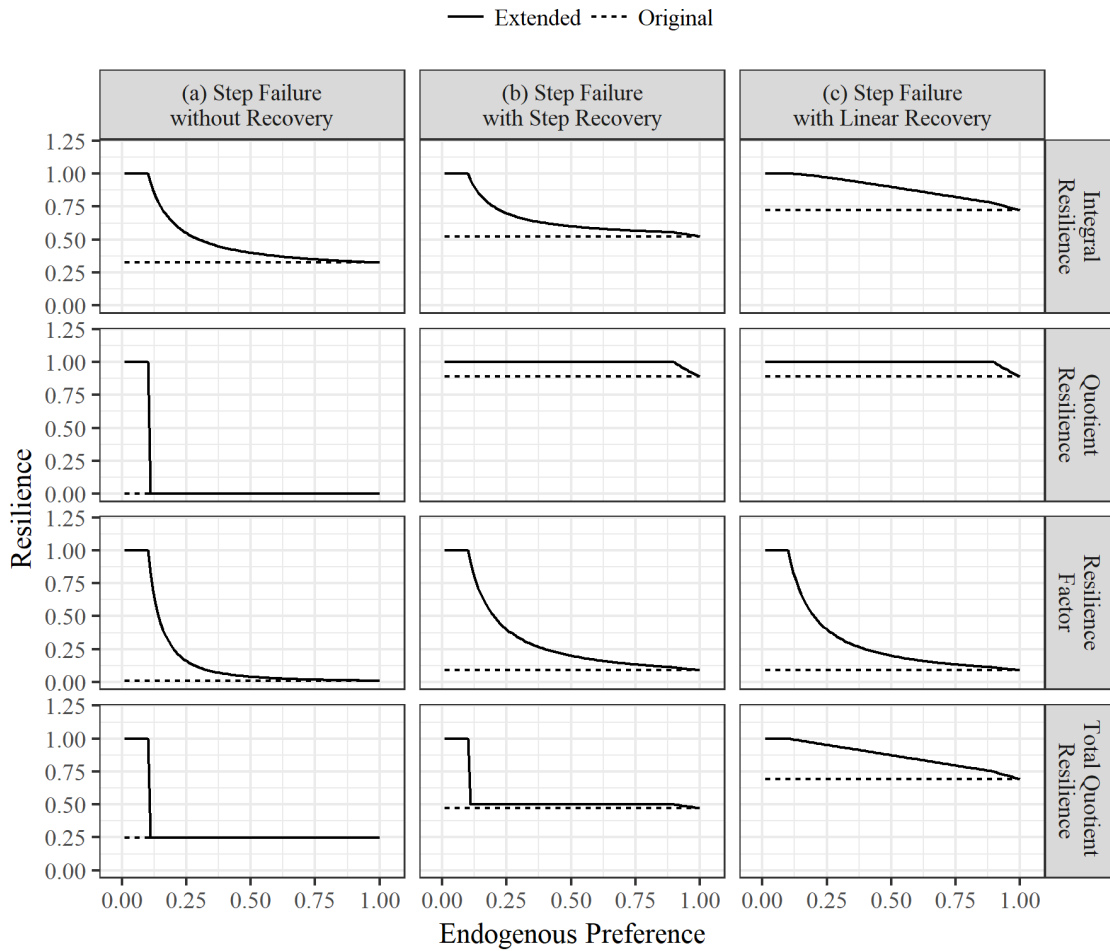


Figure 4.7: Step failure and recovery to endogenous preference

4.1.7 Intertemporal Substitutability

The intertemporal substitutability assessment used all four fundamental profiles in Figure 4.1. Figure 4.8 depicts the resilience model results while varying the intertemporal substitutability (χ) from zero to one for the four profiles. The original resilience models were insensitive to changes in intertemporal substitutability. Extended Integral Resilience and Extended Resilience Factor rose with increasing χ , while Extended Quotient Resilience and Extended Total did not change.

4.2 Results from Fundamental Performance and Preference Profiles

This study developed performance/preference profiles capable of varying parameters critical system performance and stakeholder preference. Table 4.2 aggregates the sensitivities of the original and extended resilience models. The study first found insensitivity of the original models to endogenous preference and time substitutability. The study also found Extended Integral Resilience to be the only model sensitive to all profile and preference parameters.

4.3 Conclusion

This chapter assessed the sensitivity of eight resilience models to parameters based on fundamental performance and preference profiles. One resilience model, Extended Integral Resilience, showed sensitivity to all parameter changes. The other resilience models showed insensitivity to parameters that are critical to selecting a

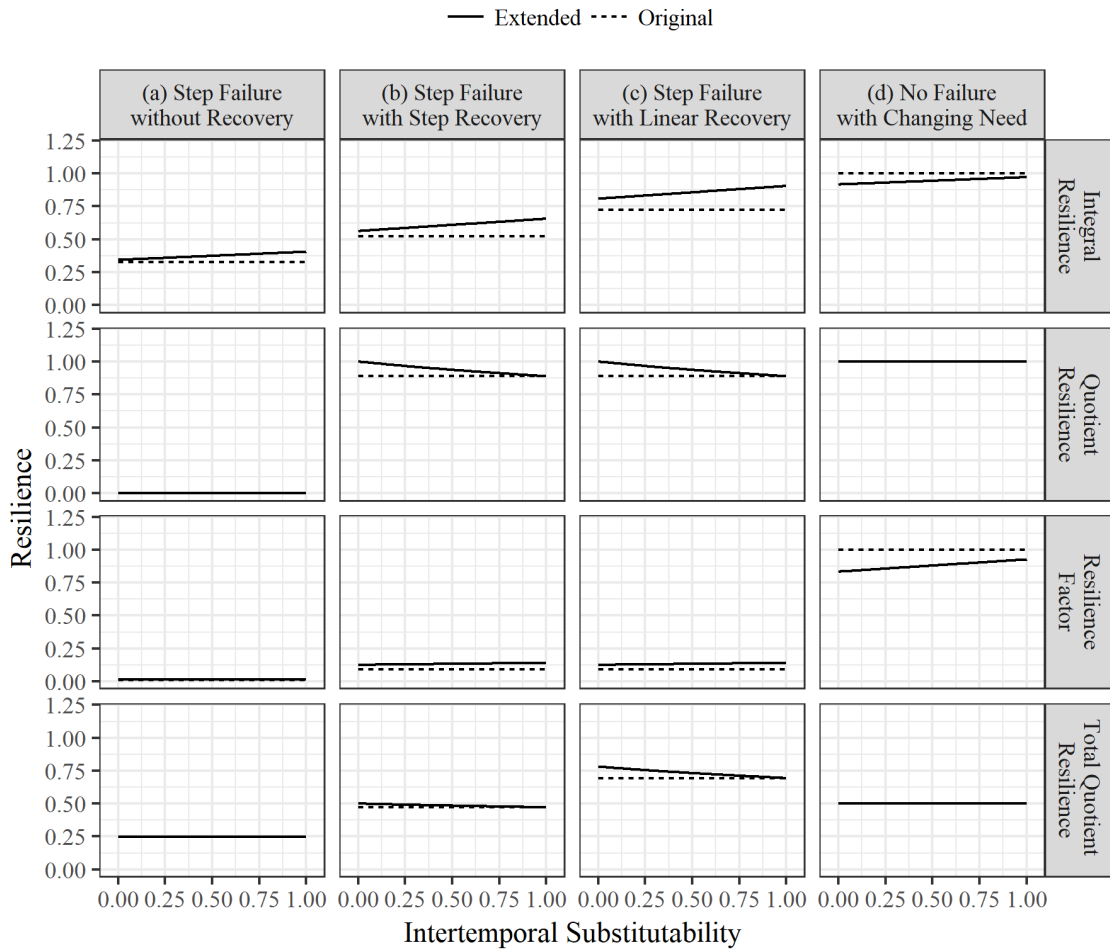


Figure 4.8: Resilience model responses to intertemporal substitutability

Table 4.2: Resilience Model Sensitivity to Fundamental Profiles

Model	Parameter	Resilience Factor		Integral Resilience		Quotient Resilience		Total Quotient Resilience	
		Original	Extended	Original	Extended	Original	Extended	Original	Extended
(1)	(2)	(3)	(4)	(5)	(6)	(7)	(8)	(9)	(10)
Step Failure without Recovery	t_d, t_i	I	I	S	S	I	I	S	S
	t_h	S	S	S	S	S	S	S	S
	$Q(t)$	I	S	I	S	I	S	I	S
	χ	I	I	I	S	I	I	I	I
Step Failure with Step Recovery	$\varphi(t_d)$	S	S	S	S	I	I	I	S
	t_r	I	I	S	S	I	I	I	S
	$\varphi(t_r)$	S	S	S	S	S	S	S	S
	t_h	S	S	S	S	S	S	S	S
	$Q(t)$	I	S	I	S	I	S	I	S
	χ	I	S	I	S	I	S*	I	S*
Step Failure with Linear Recovery	t_h	S	S	S	S	S	S	S	S
	$Q(t)$	I	S	I	S	I	S	I	S
	χ	I	S	I	S	I	S*	I	S*
Variable Endogenous Preference	$Q(t)$	I	S	I	S	I	S	I	S
	χ	I	S	I	S	I	I	I	I

* Counter-intuitive behavior

I = Insensitive to parameter; S = Sensitive to parameter; t_d = Disturbance time; t_i = Disturbance initiation time; t_h = Time horizon; $Q(t)$ = Endogenous preference; χ = Intertemporal substitutability factor; $\varphi(t_d)$ = Performance at disturbance time; $\varphi(t_r)$ = Performance at recovery time

course of action. The case studies highlighted the Quotient Resilience-based models' inability to distinguish among courses of action where performance drops to zero for any amount of time.

Chapter 5: Infrastructure Resilience Case Study

The case study demonstrated the application of the hybrid resilience framework to a system of systems. The infrastructure resilience case study satisfies the definition of a system of systems defined earlier [Jamshidi, 2009]. The case study had three sections. The first two sections focus on assessing the resilience models within the hybrid framework using the critical infrastructures of a city. The first section investigated the water infrastructure resilience to electrical power disruption. The water distribution system had three stakeholders with different preference profiles. The second section analyzed the impact of electrical disruption on all critical infrastructures. Each critical infrastructure had a unique stakeholder preference profile. The first two sections applied all original and extended metrics defined in the previous sections (Table 3.3).

The third section focused upon applying the hybrid framework using the extended Integral Resilience model. The study investigated the failure and recovery of the electrical system in the context of hurricane damage to a city's electrical infrastructure. The section applied the Extended Integral Resilience R_{EIR} model exclusively. First, the study used data collected from Puerto Rico in the aftermath of Hurricane Maria to calculate resilience. Second, the study investigated the re-

silience of the simulated city for the duration and recovery from a single storm. The Third, the study investigated the city resilience over a ten year time period with randomly assigned storm arrival times and strengths. Figure 5.2 shows inputs and outputs of the system dynamics case studies.

5.1 City of Austin Infrastructure System Dynamics Model

In response to requests by stakeholders in Austin, TX, and the Department of Homeland Security (DHS), The Johns Hopkins University Applied Physics Laboratory (JHU/APL) designed a system dynamics model simulating the interrelations among the critical infrastructure systems. Figure 5.1 shows a map of the Travis County, TX, and Austin, total population 1.2 million. Stakeholders identified their relationships with other infrastructure systems. The model provided visual feedback of the consequences of the many relationships to the group. The visual output facilitated scenario-based discussions to identify weak points in the overall infrastructure and potential solutions. The model excluded geographic information in order to prevent disclosure of sensitive, critical nodes in the infrastructure [Egli et al., 2015]. This study added data extraction methods and the ability to conduct batch runs of the simulation with stochastic variables.

The simulation included the following critical infrastructures: Energy, Transportation, Water, Health, Emergency Services, Communications, Information Technology, and Critical Manufacturing. A series of stakeholder interviews and conferences provided the basis for the system dynamics simulation with the intent to

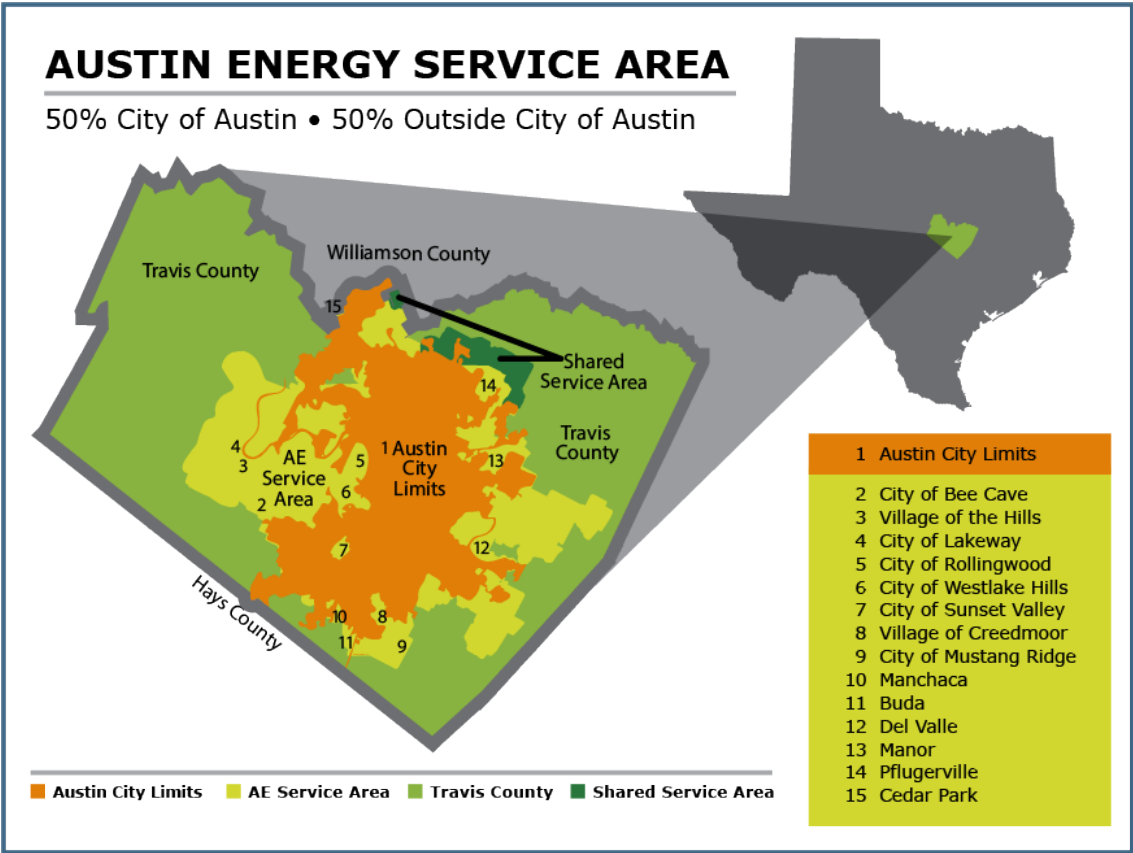


Figure 5.1: Map of electricity service for Travis County, Texas from [Austin Energy \[2013\]](#)

show interdependencies across sectors at a system level relationships rather than component level. The system dynamics linked the critical infrastructure sectors using stocks and flows. Stocks are the accumulations of a state variable of the system. Flows are rates of change in the system. The system dynamics model allows an analyst to define functionality profiles that vary over time to produce time-series data to use as inputs to the resilience models.

Within the simulation, each sector produced functional output at a rate determined by itself and its contributors. This functional output determined the sector functionality. Based on the production, the sector contributed to other sectors. A function comprising base production capability, contributing sector inputs, and assigned degradation from user controls determined the production of the sector. When a sector's output degraded, affected sectors saw a loss of functionality through a reduced contribution from the sector. A priority function defined which dependent sectors receive the input sector's functionality. In the absence of a priority function, all sectors experienced a proportional loss of functionality based upon the degraded contribution. If the affected sectors had reserve capacity of the contributing sector (e.g., an energy reserve or a water reserve) these reserves compensated for the degradation until exhausted. Each sector followed this basic construct with variations based upon input sectors, output sectors, and available reserves.

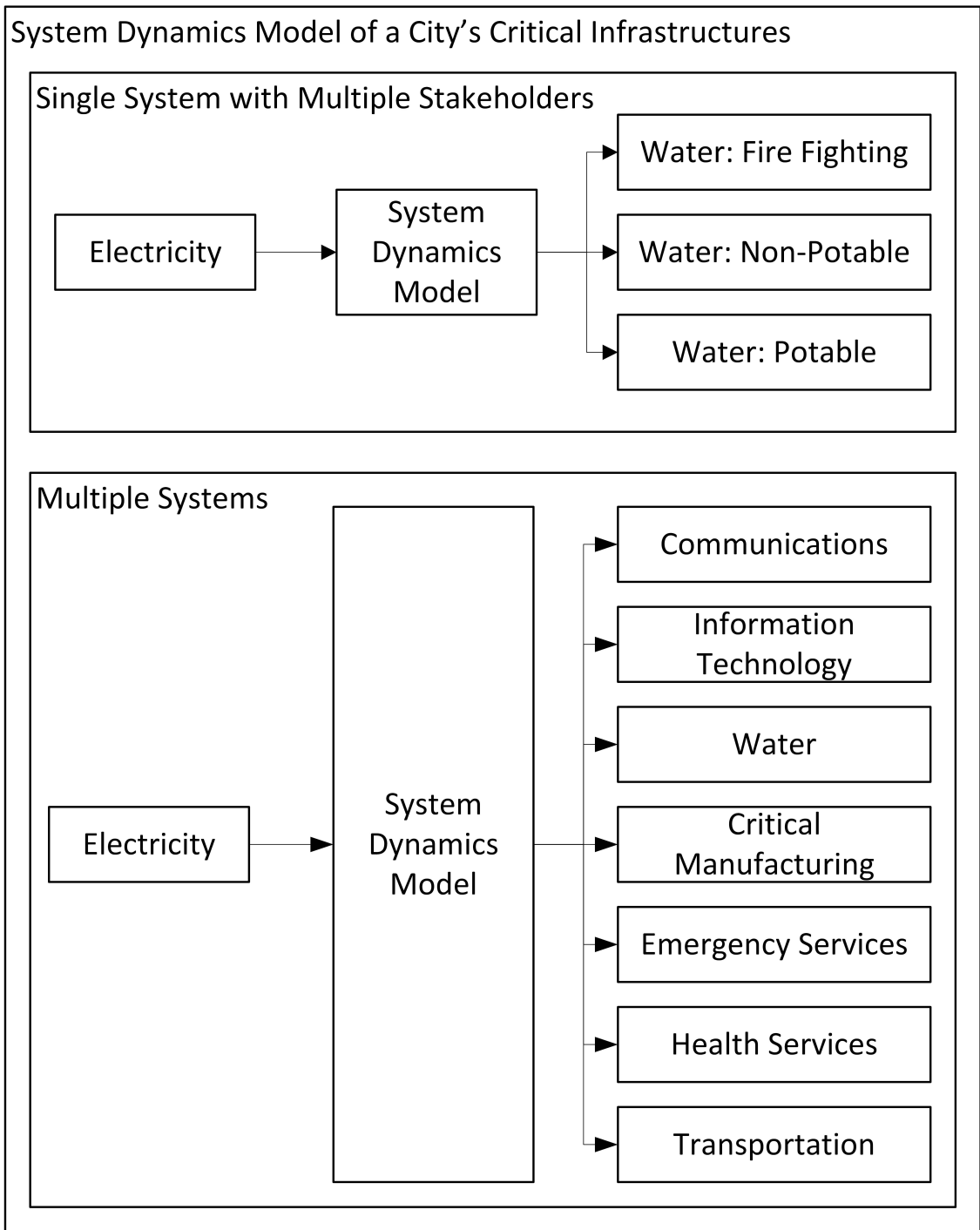


Figure 5.2: City infrastructure case studies

5.2 Water System Stakeholder Perspective

Studies of water deliver performance after major disruptive events identified multiple stakeholders: firefighters, users that can purify non-potable water, and users of potable water [Davis et al., 2012, Davis, 2014]. The water system scenario used the water system’s dependency upon electrical power to show the resilience impact of implementing different options for modifying the electrical system for each water system stakeholder. The resilience results enabled an informed discussion among the stakeholders to select an appropriate course of action.

The system dynamics model simulated a two week period with an electrical disturbance at the end of the first day. The model captured the impact of electrical power performance on the water system performance. The electricity stakeholder had several courses of action available (Table 5.1). The disturbance under consideration was a failure of the electrical system for several days followed by restoration to 60% of *status quo* performance. The electricity infrastructure stakeholder considered four courses of action. Course of action “A” left the system in the *status quo* or “as-is” condition. Course of action “B” improved the robustness of the electrical system. Course of action “C” reduced the time to recover. Course of action “D” produced a full recovery, as opposed to the 80% recovery in alternatives “B” and “C”. Figure 5.3 shows the simple step function behavior of the electrical system. Due to the interconnectivity of the infrastructures, the water system’s functional output was more complicated for all courses of action.

The water system provided water for firefighting, non-potable water for in-

Table 5.1: Electrical System Courses of Action

Scenario	Description	Failure Time	Robustness	Recovery Time	Recovery Level
(1)	(2)	(3)	(4)	(5)	(6)
A	Current System	1 Day	0	~8 Days	60%
B	Improved Robustness	1 Day	25%	~8 Days	60%
C	Improved Time to Recover	1 Day	0	~5.5 Days	60%
D	Full Recovery	1 Day	0	~8 Days	100%

Table 5.2: Water System Stakeholder Preferences

Stakeholder Perspective	Endogenous Preference	Intertemporal Substitutability
(1)	(Q)	(χ)
(1)	(2)	(3)
Fire Fighting	30%	0
Non-Potable Water	70%	0.2
Potable Water	90%	0.5

dustrial, public health, and horticultural purposes, and potable water for human consumption. Firefighters, industrial users (non-potable water supply), and citizens (potable water supply) each had their own preference values (Table 5.2). The resilience models calculated resilience using the functional outputs and the stakeholder preference profiles defined.

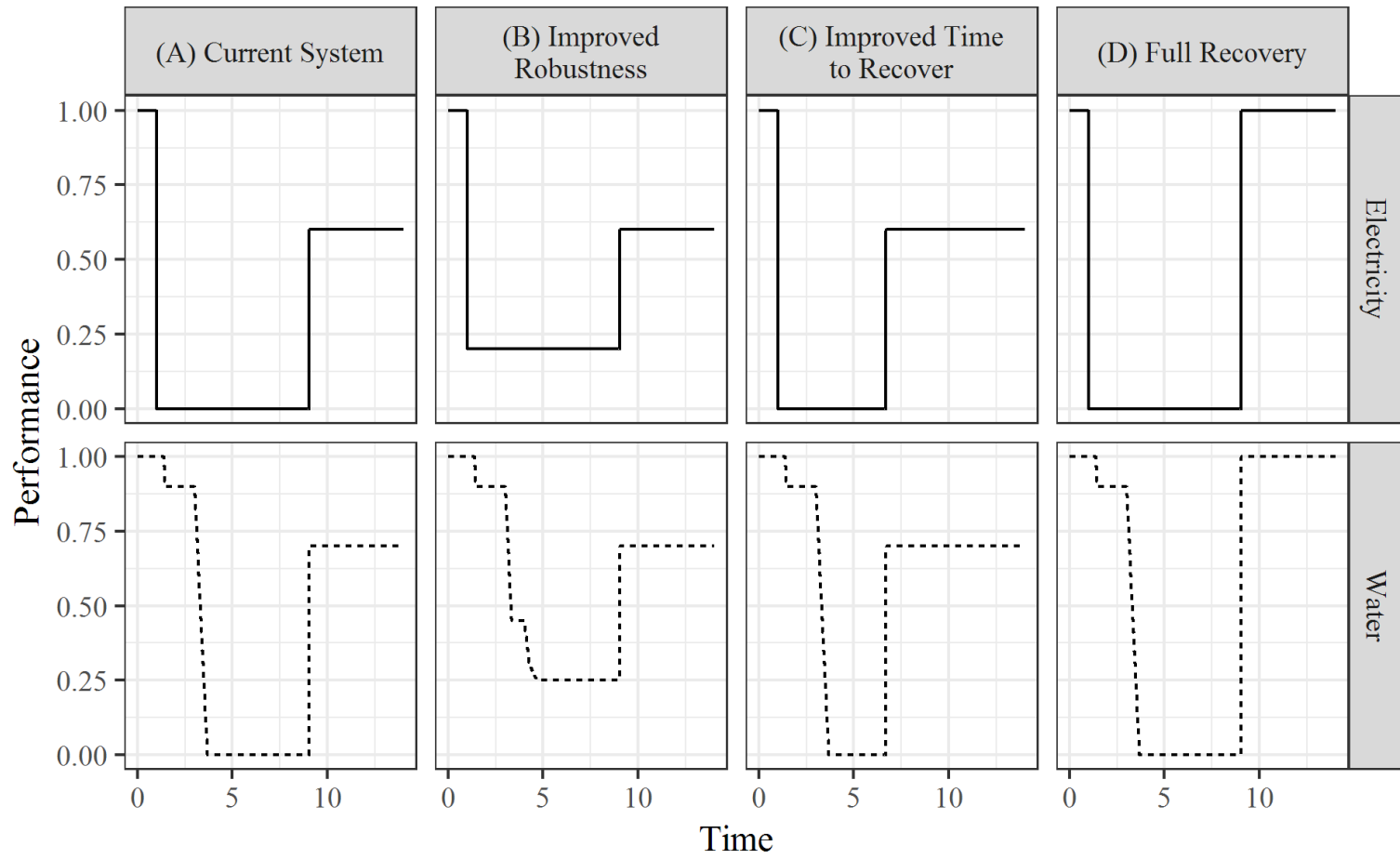


Figure 5.3: Performance profiles from electrical system courses of action

Table 5.3: Water Stakeholder Scenario Resilience

Stakeholder	Integral Resilience	Quotient Resilience	Total Quotient Resilience	Resilience Factor
(1)	(2)	(3)	(4)	(5)
No Stakeholder*	$C > B > D > A$	$D > A = C > B$	$C > D > A > B$	$B > A = C = D$
Fire Fighting	$B > C > D > A$	$A = B = C = D$	$C > B > A > D$	$B > A = C = D$
Non-Potable	$C > B > D > A$	$D > A = C > B$	$C > D > B > A$	$B > A = C = D$
Potable	$C > B > D > A$	$D > A = C > B$	$C > D > A > B$	$B > A = C = D$

Courses of Action:

A - Current System B - Improved Robustness
C - Reduced Time to Recover D - Full Recovery

* "No stakeholder" is equivalent to the original versions of each resilience model

5.2.1 Conclusions from Water Stakeholder Perspective

By inspection of Figure 5.3, courses of action B, C, and D improve upon A, the *status quo*, for electricity. Table 5.3 shows the ranked results of the courses of action using each resilience model. Quotient Resilience and Total Quotient Resilience failed to rank the *status quo* course of action (A) last. The Integral Resilience and Resilience Factor models ranked Scenario A as the worst alternative for all stakeholders.

The Resilience Factor column in Figure 5.4 exposed a weakness in the Resilience Factor models. The model assigned any system with a moment of complete failure ($\varphi = 0$) zero resilience. This held true for momentary failures and for long failure periods. The $\varphi(t_d)$ in the numerator of Equations 1.2 and 3.9 made this true for all cases. The inability to distinguish among courses of action with complete failure for some period of time is a shortcoming in the information provided by the Resilience Factor model. This prevented Resilience Factor from providing any information to the stakeholder as recovery parameters or time to failure parameters improve.

The Integral Resilience model results showed different ordering of the courses of action for different stakeholders. The Fire Fighting stakeholder preferred course of action B (improved robustness) while the other stakeholders preferred course of action C (faster recovery). With this information, the different stakeholders could bring trade-offs to negotiations regarding selecting a course of action. This demonstrated the value of incorporating stakeholder preferences into the resilience

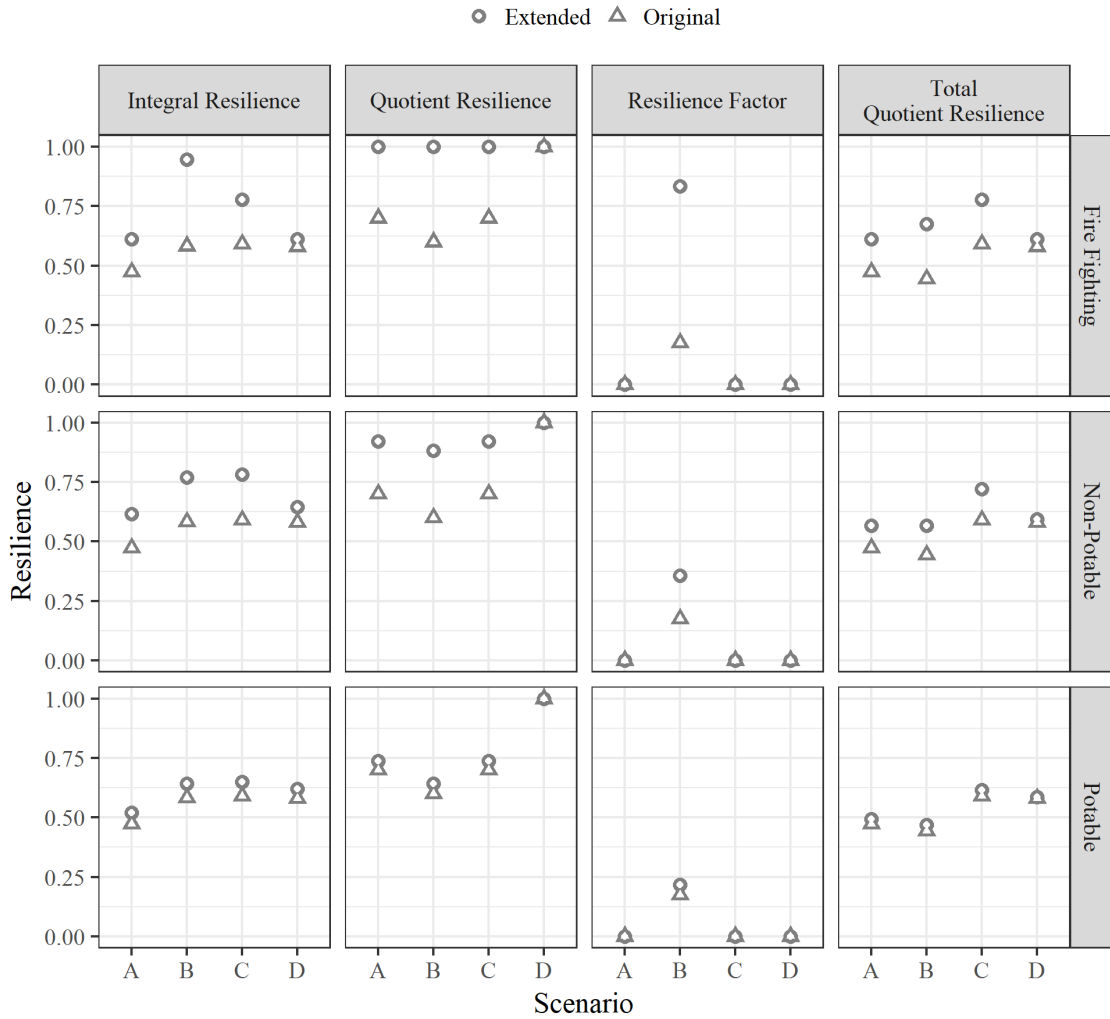


Figure 5.4: Resilience model responses to water stakeholder case study

model.

The Extended Integral Resilience model best represented the comparative resilience of different courses of action. Quotient Resilience and Total Quotient Resilience failed to rank *status quo* as the worst alternative, and Resilience Factor lacked resolution among solutions that allow performance to reach zero. This finding was consistent with the results from the fundamental models section (Table 4.2) where the extended Integral Resilience model (Equation 3.13) showed sensitivity to all varied parameters.

5.3 City Infrastructure Stakeholder Perspective

The City Infrastructure Stakeholder Perspective case study assigned stakeholder preferences for each critical infrastructure system using the same electrical infrastructure courses of action (Table 5.1). Table 5.4 shows the preference values for each infrastructure's stakeholder. Figure 5.5 shows each of the critical infrastructures' performance over time for each proposed course of action.

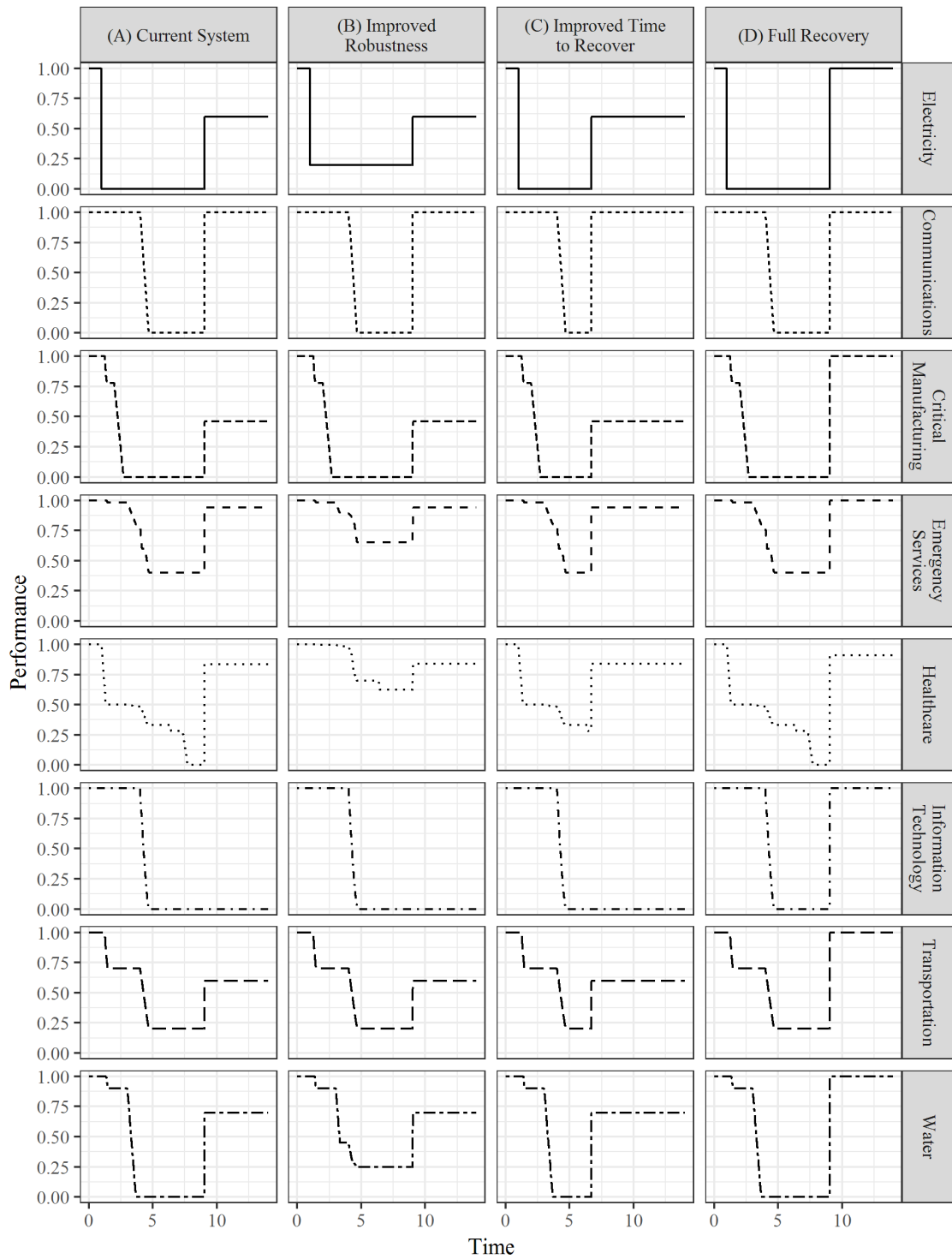


Figure 5.5: All infrastructures performance for a given course of action

Table 5.4: Stakeholder Preferences for All Critical Infrastructures

Stakeholder	Endogenous Preference (Q)	Intertemporal Substitutability (χ)
(1)	(2)	(3)
Electricity	90%	0
Communications	50%	0.2
Information Technology	50%	0.5
Healthcare	90%	0.05
Transportation	75%	0.2
Critical Manufacturing	95%	0.2
Emergency Services	80%	0
Water	90%	0.2

Table 5.5: Infrastructure Stakeholder Scenario Resilience

Stakeholder	Integral Resilience	Quotient Resilience	Total Quotient Resilience	Resilience Factor	Model Type
(1)	(2)	(3)	(4)	(5)	(6)
Electricity	$D > B > C > A$	$D > A = C > B$	$D > C > A > B$	$B > A = C = D$	Original
	$B > D > C > A$	$D > A = C > B$	$D > C > A > B$	$B > A = C = D$	Extended
Communications	$C > A = B = D$	$A = B = C = D$	$C > A = B = D$	$A = B = C = D$	Original
	$C > A = B = D$	$A = B = C = D$	$C > A = B = D$	$A = B = C = D$	Extended
Information Technology	$D > A = B = C$	$D > A = B = C$	$D > A = B = C$	$A = B = C = D$	Original
	$D > A = B = C$	$D > A = B = C$	$D > A = B = C$	$A = B = C = D$	Extended
Healthcare	$B > C > D > A$	$D > A > C > B$	$D > C > A > B$	$B > C > A = D$	Original
	$B > C > D > A$	$D > A > C > B$	$C = D > B > A$	$B > C > A = D$	Extended
Transportation	$D > C > A = B$	$D > A = B = C$	$D > C > A = B$	$D > A = B = C$	Original
	$D > C > A = B$	$D > A = B = C$	$D > C > A = B$	$D > A = B = C$	Extended
Critical Manufacturing	$D > C > B = A$	$D > A = B = C$	$D > C > B = A$	$A = B = C = D$	Original
	$D > C > B = A$	$D > A = B = C$	$D > C > B = A$	$A = B = C = D$	Extended
Emergency Services	$B > C > D > A$	$D > A = C > B$	$C > D > A > B$	$B > D > A = C$	Original
	$B > C > D = A$	$A = B = C = D$	$C > B > D = A$	$B > A = C = D$	Extended
Water	$C > B > D > A$	$D > A = C > B$	$C > D > A > B$	$B > A = C = D$	Original
	$B > C > D > A$	$A = B = C = D$	$C > B > A > D$	$B > A = C = D$	Extended

5.3.1 Conclusions from City Infrastructure Study

The city infrastructure resilience model results were consistent with the earlier water system analysis. The Integral Resilience and Resilience Factor models ranked course of action A, (*status quo*), as the least preferable option in every case. Integral Resilience model provided more resolution than Resilience Factor as several of the infrastructure stakeholders (Communications, Information Technology, Critical Manufacturing) had no preferred course of action using the Resilience Factor models. In Figure 5.6, the Resilience Factor values were zero for Communications, Critical Manufacturing, Information Technology across the board. While it may be true that a complete failure is unacceptable, in those cases, complete failure should be the decision criterion *not* resilience. In this situation, the more complex test of the resilience models yielded more information about their behavior.

5.4 Hurricane Threat Case Study

The previous study applied the resilience models to a single disturbance with properties assigned by the analyst. The following hurricane threat study applied data collected from a devastated area, random threat arrival times, random threat strengths, and a distribution of responses to the threat. The study also investigated the impact of stakeholder preferences changing over time.

The major hurricanes striking the Caribbean in 2017 underscored the need for long-term planning for infrastructure maintenance and resilience to major storms [Hernández et al., 2017, Lu and Alcantara, 2018]. Hurricane Maria passed directly

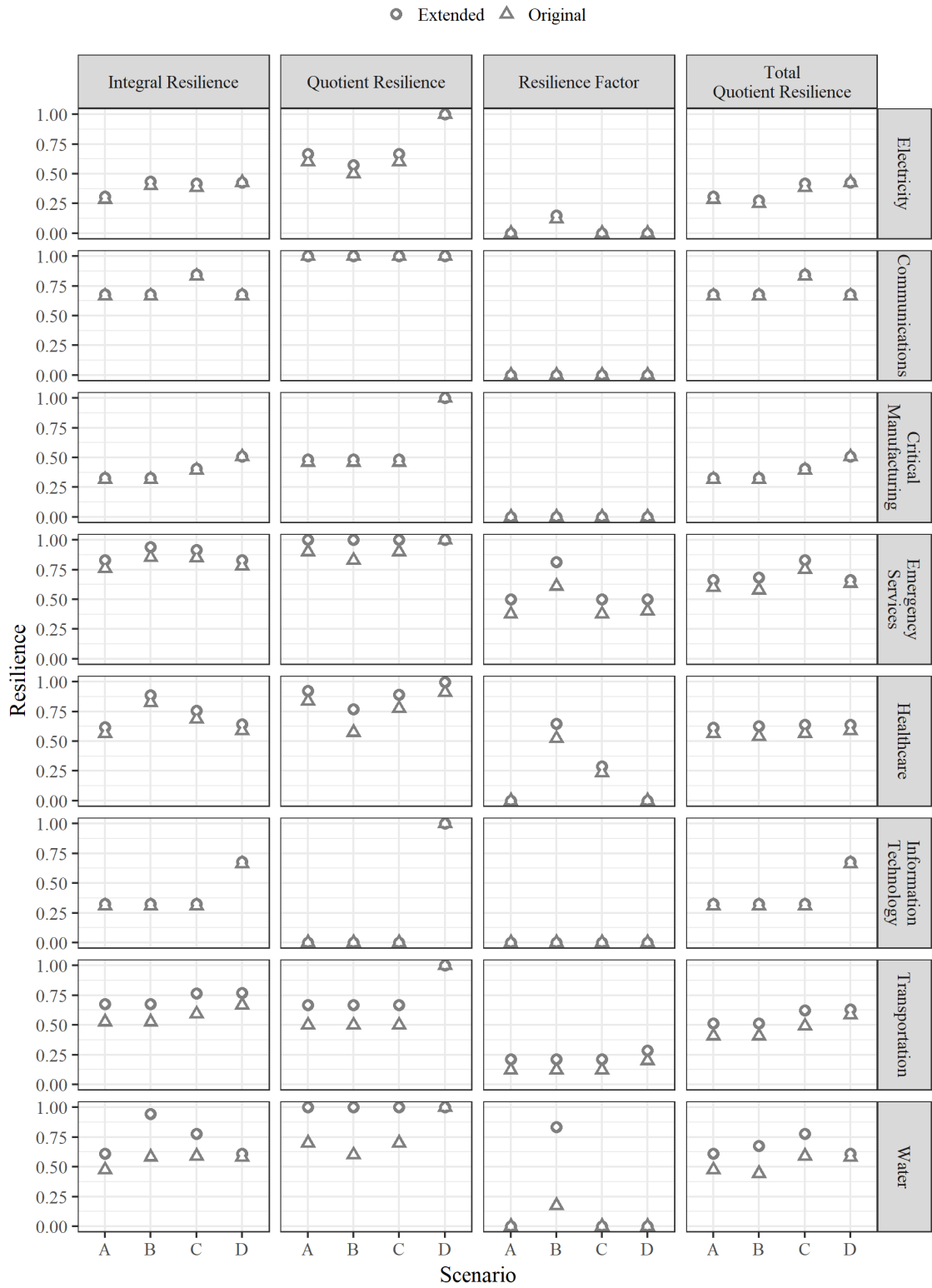


Figure 5.6: Resilience model response to different courses of action

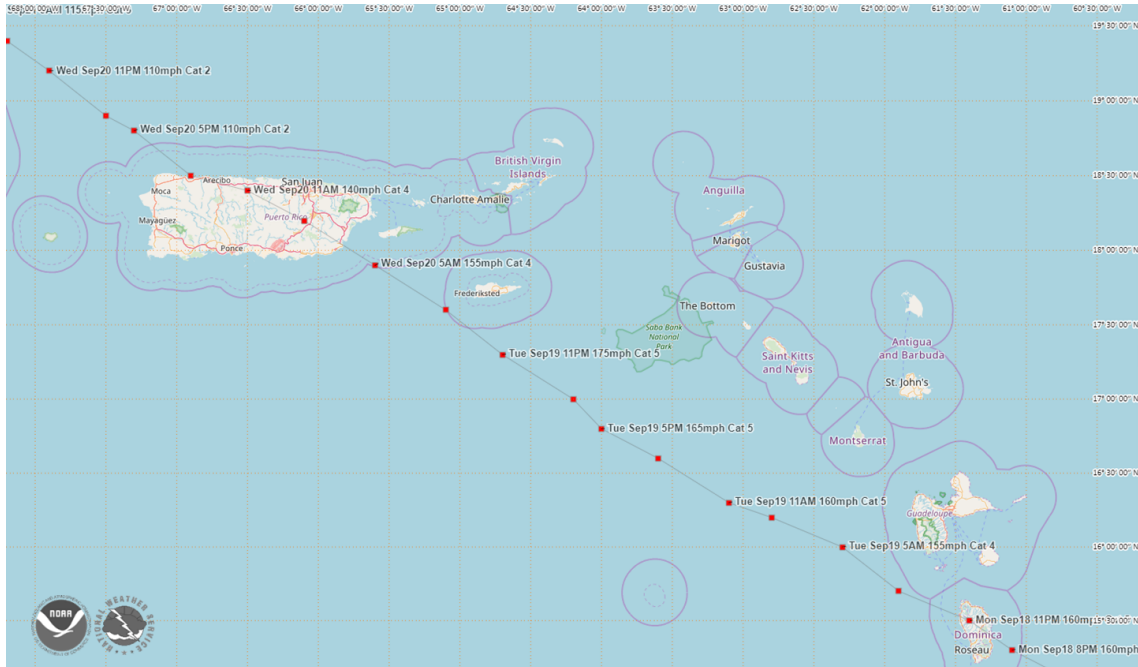


Figure 5.7: Hurricane Maria’s track across the Caribbean Sea [Weather Forecast Office, 2017]

over Puerto Rico (Figure 5.7) causing an incredible amount of damage to the island’s infrastructure. Figures 5.8 and 5.9 show examples of the extensive damage inflicted during the storm across Puerto Rico [Weather Forecast Office, 2017]. The resilience literature provide decision makers a context for making these long-term decisions, allowing stakeholders of different systems to appreciate the impact of decisions on long-term resilience of their system.

5.4.1 Hybrid Resilience Framework Application

Figure 5.10 depicts the structure of the analysis using the hybrid model. The two system-threat pairings of interest are the Puerto Rican electrical grid in the af-



Figure 5.8: Powerline damage in Mayaguez, PR [[Weather Forecast Office, 2017](#)]



Figure 5.9: Road and powerline damage in Canovanas, PR [[Weather Forecast Office, 2017](#)]

termath of Hurricane Maria (*post hoc* resilience observation) and the City of Austin infrastructure response power outages due to hurricane damage (projected resilience assessment). Aggregated data from the Department of Energy (DOE) reports produced the functional outputs for use in the extended Integral Resilience model. The stakeholder for the Puerto Rico case study desires a return to status quo, and the time horizon is the observed recovery time. The city infrastructure stakeholders each have their own long-term and storm-dependent endogenous preferences. The projected resilience assessment used the city of Austin system dynamics model using the threat model described below to generate the functional outputs for the extended Integral Resilience model. The stakeholders had endogenous preference varying with time and multiple time horizons.

In 2017 Hurricane Maria devastated Puerto Rico [Schmidt et al., 2017] and its electrical infrastructure [Redacted, 2017]. Less than half of the 3.4 million Puerto Ricans had access to electrical power two months after the hurricane. Sections of Puerto Rico’s power grid had not yet recovered six months after the storms [U.S. Department of Energy, 2018]. Figure 5.11 depicts the island’s key power plants, transmission lines, and centers of population. When major outages occur on the mainland U.S., personnel and supplies arrive via relatively fast, using high-volume transportation such as railroads or highways. Puerto Rico’s resupply comes via fast, low-volume airlifts or slow, high-volume cargo shipping. This isolation hindered progress to restore electrical capacity [Lu and Alcantara, 2018].

The Department of Energy (DOE) published reports on the service level of the electrical grid of Puerto Rico from September 20, 2017 until April 4, 2018.

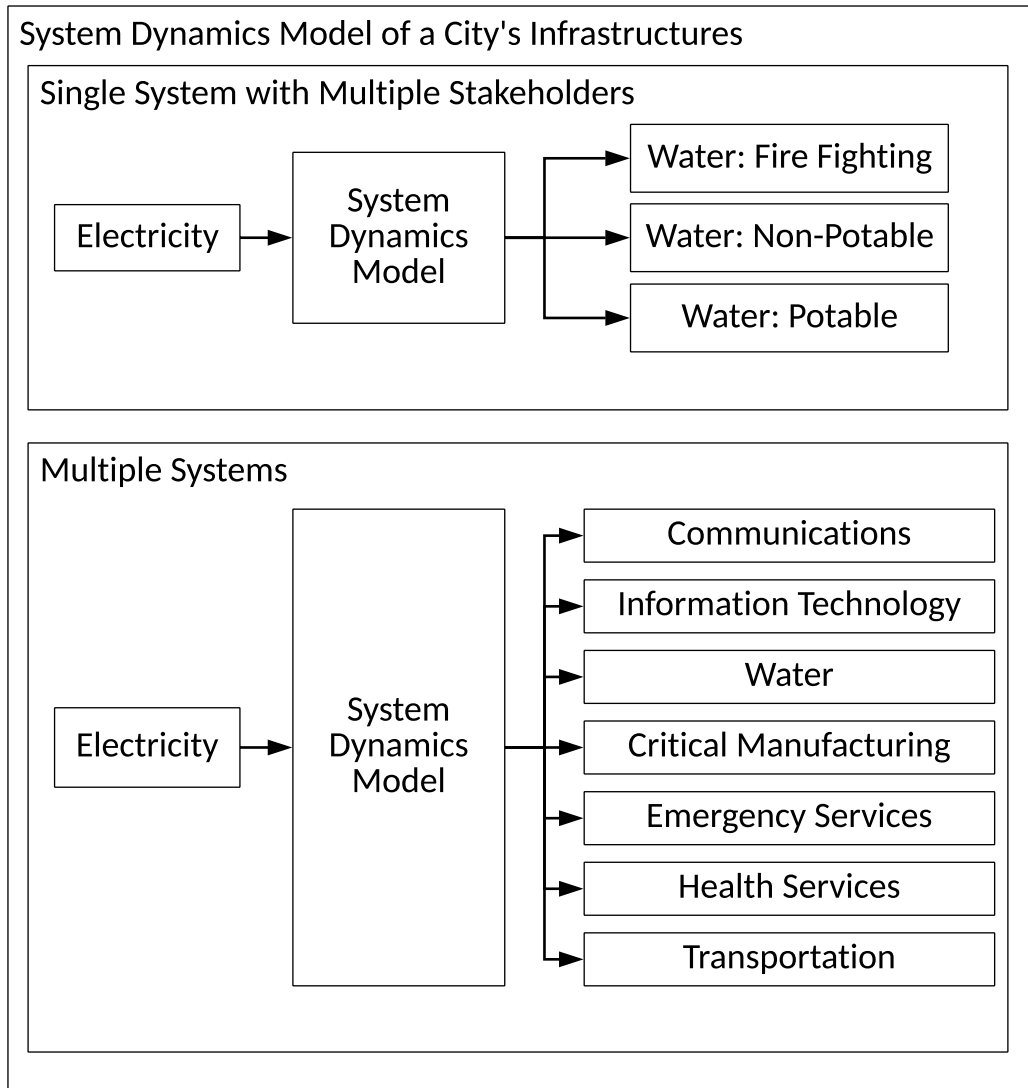


Figure 5.10: Data flow through hybrid model

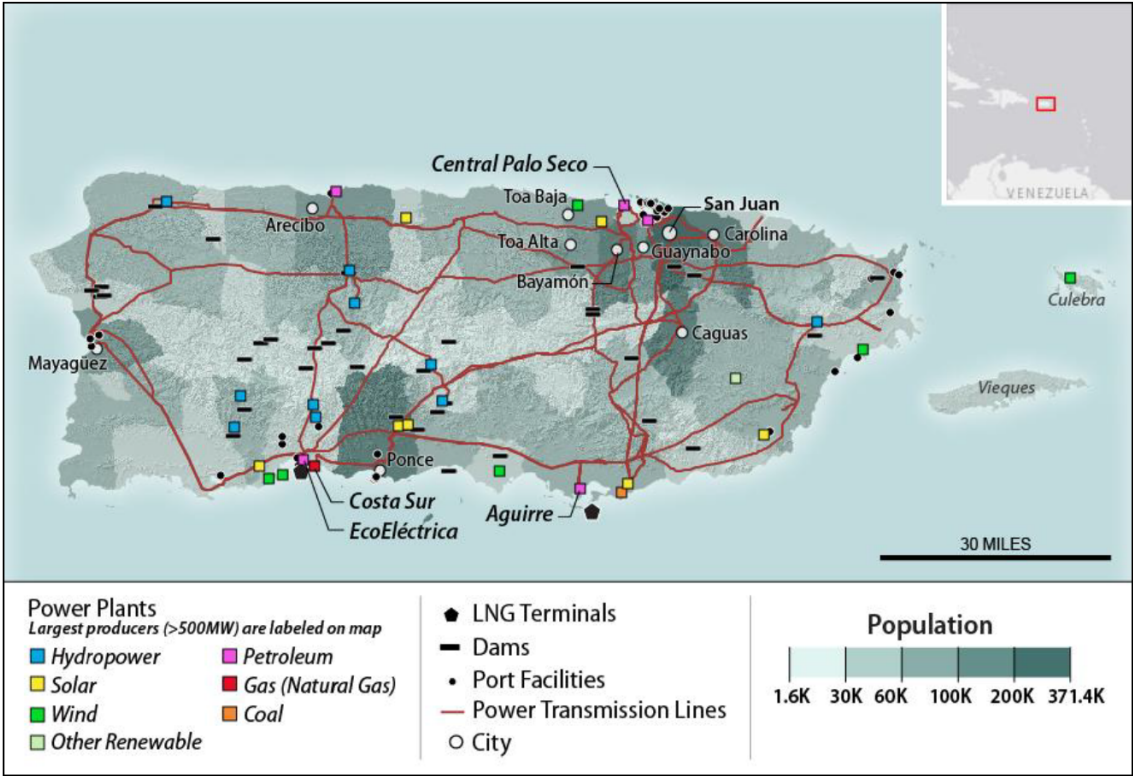


Figure 5.11: Map of Puerto Rico's energy infrastructure

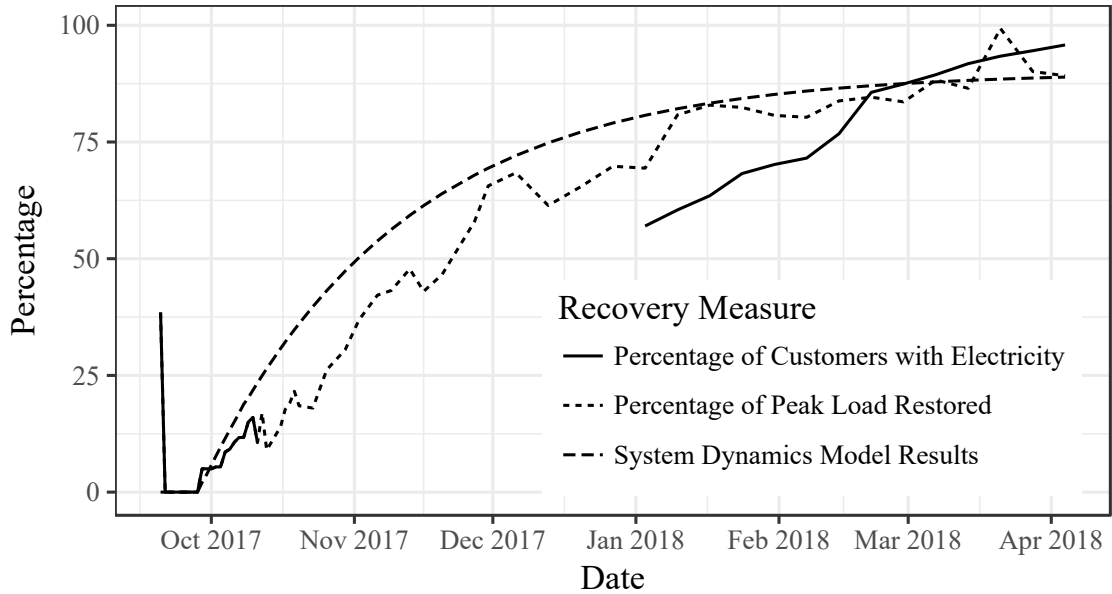


Figure 5.12: Peak load and customer services recovery after Hurricane Maria

From the beginning of reporting until October 11, 2017, the DOE provided the percentage of Puerto Rican customers with electricity. From October 12, 2017 through December 27, 2017, percentage of peak load restored served as a proxy for percentage of customers served. From January 3 to April 4, 2018, the DOE reported peak load and customers served. Figure 5.12 shows the trajectories of customers serviced and peak load for the duration of the reporting period [U.S. Department of Energy, 2018].

The peak load power sufficed for the demonstration of the hybrid model. The electrical grid stakeholders would have preferences for peak power and percent of customers served. Each customer, as stakeholders themselves, would prefer to measure percentage of their particular electrical needs met per day. The DOE data did not allow that level of differentiation, so the study proceeded the available data to

demonstrate the hybrid resilience framework’s flexibility to ingest live data. The stakeholders preferences were status quo restoration of the project for endogenous preference and the time period from landfall to recovery as the time horizon. Intertemporal substitutability was zero.

The resilience of the electrical grid in response to Hurricane Maria was 0.61. The resilience analytic model ingested the peak load percentage values to calculate resilience. The Single Storm Experiment (Section 5.4.4) was a simulation analog to the real-world data collected from Puerto Rico. The Hurricane Maria result appears as larger circle in Figures 5.14 and 5.15.

5.4.2 Projected Resilience Analysis

5.4.2.1 Stochastic Threat Model

The threat model required a frequency of storm occurrence, a distribution of storm strengths, and impact on the electrical system functional output given the strength of a storm. Broward County, FL, a high-susceptibility region with a 25% probability of a Category 1 Hurricane or higher in a given year [Jagger et al., 2001], served as the basis for developing the storm frequency and strength model. The model used an exponential distribution for the arrival times of storms.

The Saffir-Simpson scale rates hurricanes based upon their sustained wind speeds and provides a high-level assessment of the damage for each category of hurricane (Table 5.6) [Schott et al., 2012]. The simulation assumed instantaneous damage to the electrical system so $t_i = t_f$. The simulation drew from triangular

Table 5.6: Hurricane Properties and Effects on Electrical Infrastructure

Category	Wind Strength	Probability of Category
1	74 to 95	54%
2	96 to 110	26%
3	111 to 129	14%
4, 5	130+	6%

Table 5.7: Parameters for Electrical System Behavior

Hurricane Category		1	2	3	4 & 5
Failure Level (%)	Minimum	0	0	0	0
	Mode	70	50	0	0
	Maximum	90	70	40	0
Recovery Level (%)	Minimum	100	90	80	70
	Mode	100	100	95	90
	Maximum	100	100	100	100
Recovery Time (days)	Minimum	3	7	14	28
	Mode	4.5	17	28	75
	Maximum	5	21	35	100

distributions to define the performance parameters of the electrical infrastructure including failure time (t_f), failure level($\varphi(t_f)$), recovery time (t_r), and recovery level ($\varphi(t_r)$). recover. The damage descriptions for a given hurricane strength from the National Hurricane Center were the basis for minimum, maximum, and mode values of the triangular distribution parameters in Table 5.7 [Schott et al., 2012].

The electrical system functional output over time after the initial damage from a hurricane was:

$$\varphi(t) = -\varphi(t_r) - (\varphi(t_r) - \varphi(t_f))^{-bt} \quad (5.1)$$

which supported derivation of the restoration parameter, b by setting

$$\varphi(t) = 0.99\varphi(t_r):$$

$$b = -\frac{1}{t_r} \ln \left(\frac{0.01\varphi(t_r)}{\varphi(t_r) - \varphi(t_f)} \right) \quad (5.2)$$

derived from work by [Reed et al. \[2009\]](#).

The parameters defined above describe the behavior of the electrical infrastructure system. The system dynamics simulation of the city infrastructure used this as an input to simulate the functional performance of the other seven infrastructure systems.

5.4.3 Time-Dependent Stakeholder Models

The stakeholder models included endogenous preference $Q(t)$, time horizon t_h , and intertemporal substitutability $\chi(t)$. The endogenous preference had two components. The first component was a trend over the time, independent of storm arrivals. The second component was a demand spikes in response to an impending or occurring storm. The general trend over time established a starting value representing the current usage of the infrastructure. The endogenous preference for ten years was a percentage of use given current capacity. The study assumed linear growth in usage from t_0 to t_h . The growth could project to be greater than 100% of the current capacity. [Table 5.8](#) shows the values used for “current” and “ten year” endogenous preference. The profiles demonstrated a mix of excess capacity and unmet demand for the time period.

[Table 5.8](#) shows the endogenous preferences at the start of the simulation and

Table 5.8: Endogenous Preference Profiles (% of current capacity)

Infrastructure	Start	10 Years
Electricity	100	100
Communications	100	120
Information Technology	95	95
Healthcare	90	120
Transportation	105	120
Emergency Services	90	110
Critical Manufacturing	100	130
Water	100	110

after ten years. Each infrastructure also had its own surplus (or deficit) functional output. For instance, healthcare had an excess capacity of 10% while transportation is already at a shortfall of 5% representing traffic gridlock. The stakeholders generally assumed demand growth over the simulation period.

The perturbing event could change the demand on certain infrastructures. The stakeholder model reflected this through dynamic endogenous preference spikes in the event of a storm. The transportation sector’s demand, for example, increased before a Category 4 storm as residents evacuated the area. The demand remained high for a period after the storm as first responders and emergency supplies rushed to the area. The emergency services and healthcare systems experienced a spike in demand after the storm and returned to normal. Table 5.9 shows the value used for each of the systems given a strength of the storm. The spike magnitude changed along with the of the projected figure of merit of the system. That is, if the spike was 120% and it occurred at year 5 when the endogenous need was 110%, the value of the spike was 132%.

The system dynamics model simulated the electrical power reserves available

Table 5.9: Endogenous Preference Spikes Due to Storm

Infrastructure	Storm Strength	Start(Days)	End (Days)	Percentage
Healthcare	Cat 1	0	4.5	120
	Cat 2	0	17	120
	Cat 3	0	28	120
	Cat 4,5	0	75	120
Transportation	Cat 1	-2	4.5	120
	Cat 2	-5	17	180
	Cat 3	-5	28	180
	Cat 4,5	-5	75	200
Emergency Services	Cat 1	0	5	120
	Cat 2	0	17	120
	Cat 3	0	28	120
	Cat 4,5	0	75	120

for each infrastructure. In this case, the model of the system, rather than the stakeholder model, captured an aspect of intertemporal substitutability. When applying the hybrid resilience framework, analysts must be sensitive to this possibility to avoid double-counting preferences. For the remainder of this study, $\chi(t) = 0$ to prevent double counting electrical storage.

5.4.4 Single Storm Experiment

The first experiment investigated the resilience of the city infrastructures for the duration of a single storm. The system dynamics model simulated 1000 different storms drawn from the distributions described above. Resilience results for each critical infrastructure satisfied stopping criterion of less than 1% standard error on the mean [Sandborn, 2013].

Every storm struck on day six of the simulation. The time horizon was eight

days after the recovery time. Figure 5.13 shows the time-series data of a single simulation run with a category 4 hurricane. The solid line is the the performance of the infrastructure system, and the dotted line is the stakeholder endogenous preference ($Q(t)$). This experiment was similar to the *post hoc* resilience analysis of Hurricane Maria.

Figure 5.14 shows a boxplot of the resilience for each infrastructure. Figure 5.15 breaks out the boxplots for each infrastructure by the strength of the storm. For all boxplots in this study, the lower and upper edges of the box were the first and third quartiles. The solid bar in the box was the median resilience value.

Profile — Need - - Performance

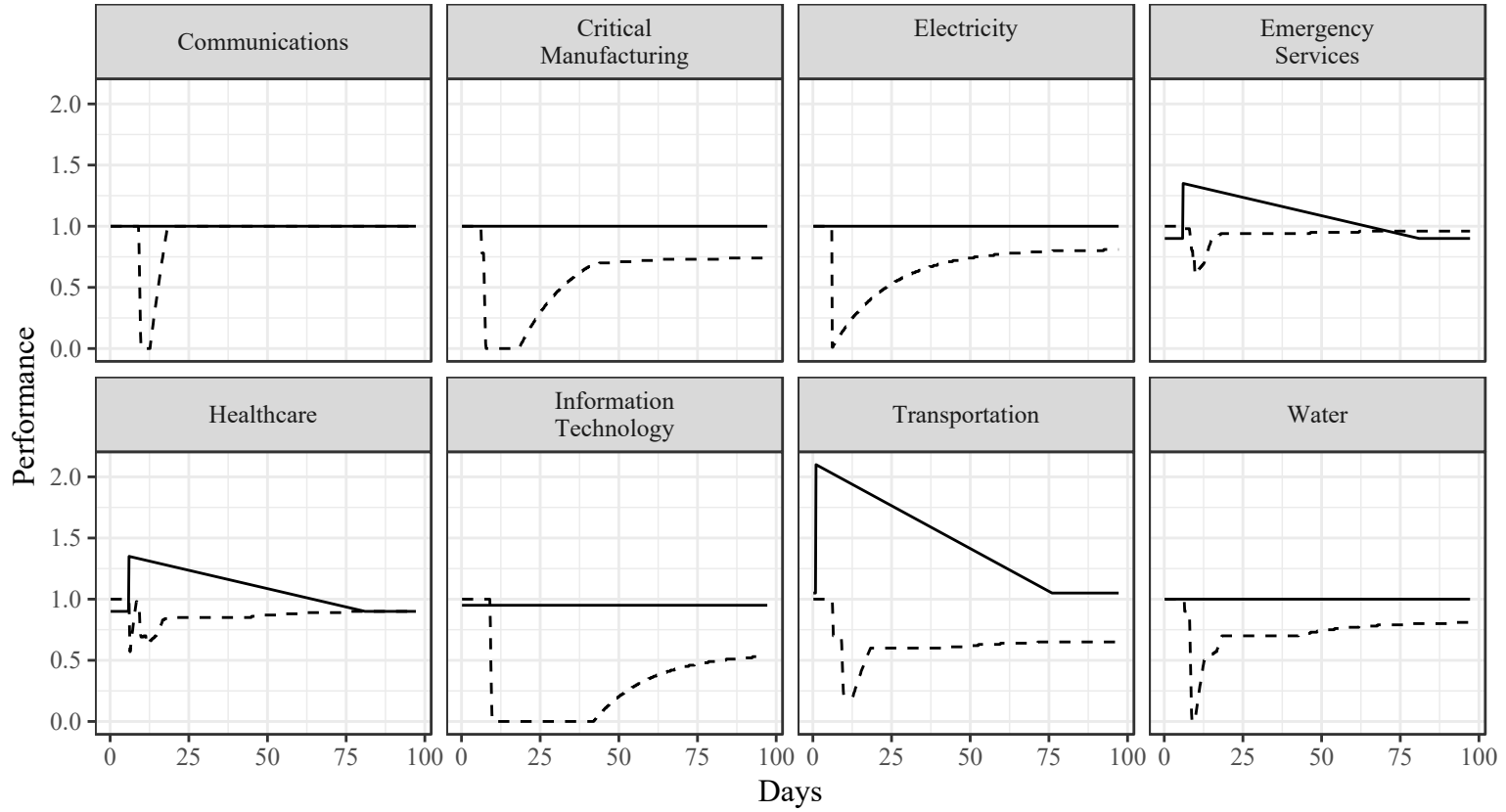


Figure 5.13: Time-series example for a category 4 storm

5.4.5 Multiple Time Horizons Experiment

The experiment comprised 300 simulation runs. Each run had ten random samples drawn from an exponential distribution with a 25% probability of a storm within a 12 month period. The sequential sums of the draws assigned the hurricane landfall times. The experiment discarded all landfall times greater than ten years. Resilience results for each critical infrastructure satisfied stopping criterion of less than 1% standard error on the mean [Sandborn, 2013].

The system dynamics model assigned hurricane strength, failure level, recovery level, and recovery time in accordance with the distributions described in the section above (Table 5.7). The time horizons were six months, one, two, five, and ten years. Table 5.10 shows the maximum number of storms per run, average number of storms per run, average storm strength, and number of runs with no storms. Degradation accumulated in the electrical system by multiplying follow-on storm degradations by the state of the system. For instance, if a previous hurricane had resulted in a recovery level of 0.80, a subsequent hurricane with recovery level would lead to a recovery level of 0.64. This allowed investigation of the trade-offs between short term strength against storm damage and the rising endogenous preferences that are storm-independent.

The simulation recorded a performance value for all eight infrastructure systems every four hours. Figure 5.16 shows time-series data for a single run for the entire ten year time horizon. Vertical gray bars denote the time horizons at 6 months, 1, 2, and 5 years. Table 5.11 and Figure 5.17 summarize the resilience

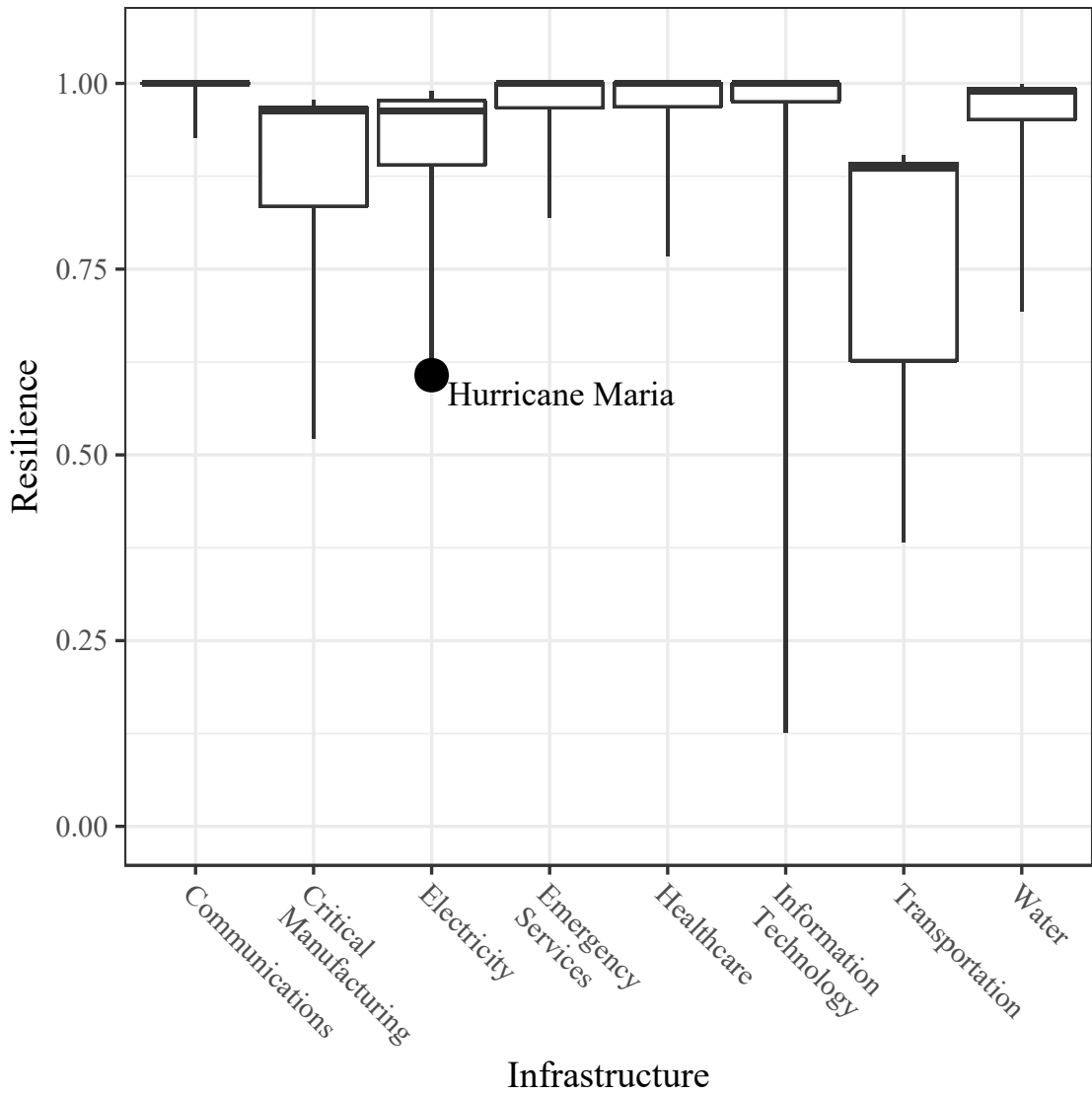


Figure 5.14: Infrastructure resilience values for 1000 simulation runs

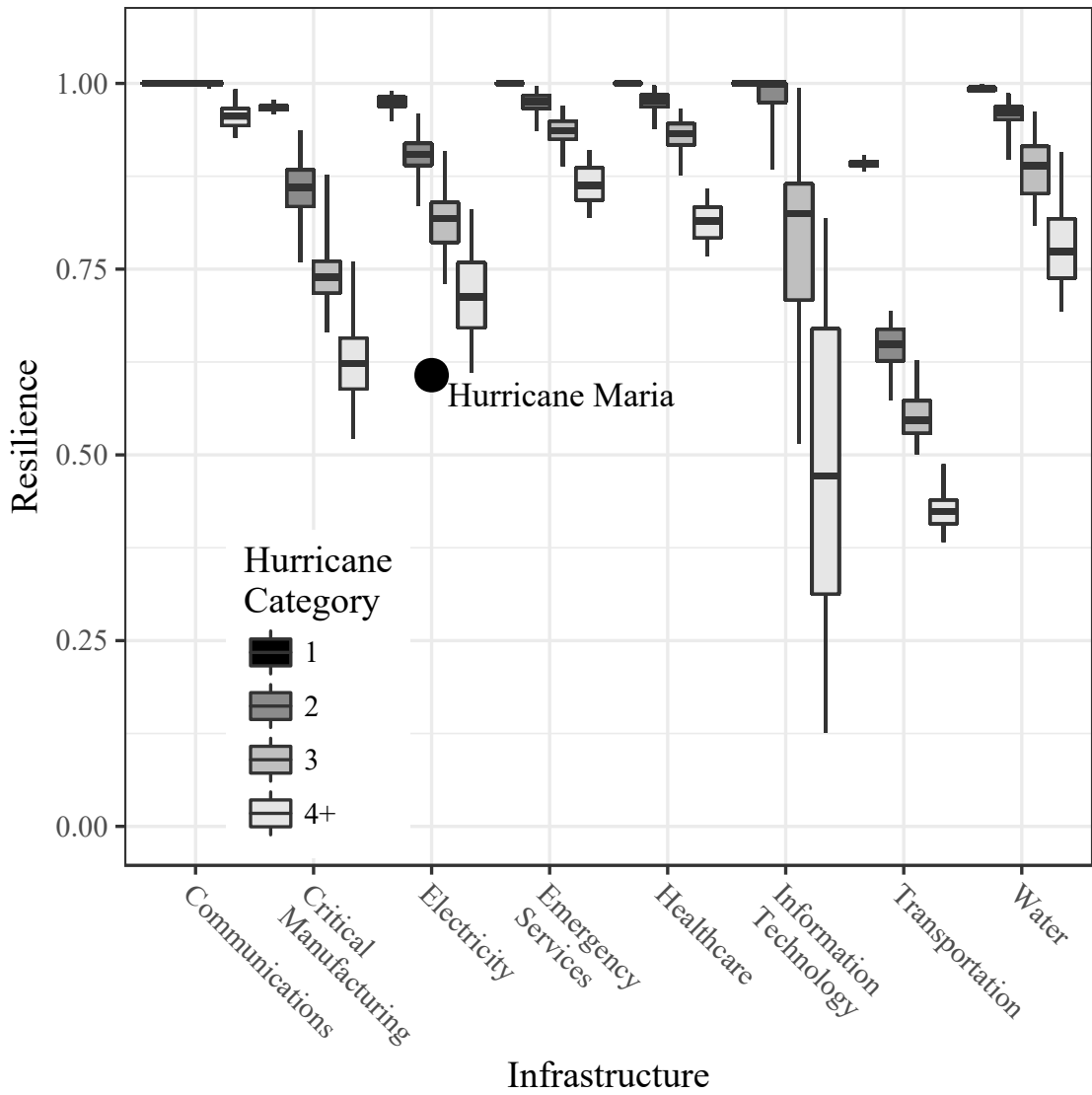


Figure 5.15: Infrastructure resilience values by hurricane category

Table 5.10: Storm Data for Each Time Horizon

Time Horizon	Maximum Number of Storms per Run	Average Number of Storms	Average Storm Strength	Runs with No Storms
6 months	2	0.14	0.24	259
1 year	3	0.30	0.44	224
2 years	4	0.62	0.92	157
5 years	5	1.36	1.57	68
10 years	7	2.73	2.27	18

results for each run, infrastructure, and time horizon combination.

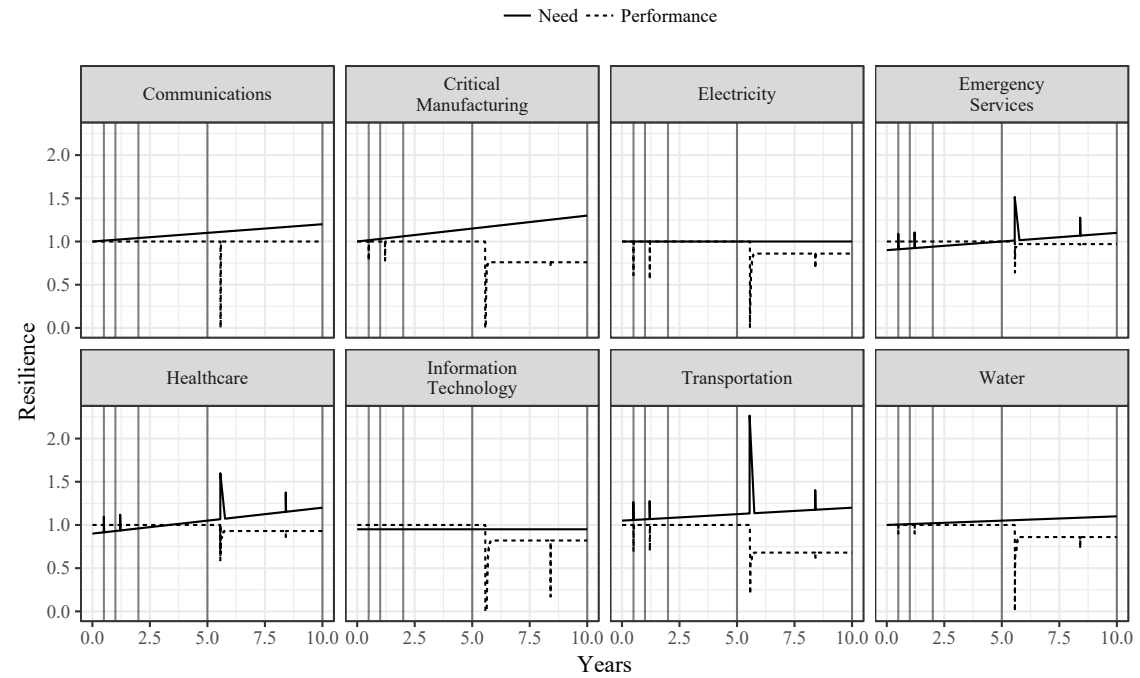


Figure 5.16: Performance and endogenous preference for a ten year time horizon

5.4.6 Hurricane Threat Case Study Discussion and Conclusion

The single storms experiment showed the expected decrease in resilience as storm strength increases. The Hurricane Maria data lies at the edge of the resilience values in Figure 5.14.

When the resilience data was differentiated by storm strength, the infrastructure system showed strong resilience to category 1 and 2 storms (Figure 5.15). Information technology showed a great difference between category 2 storms and stronger storms where the resilience value begins to decrease. From a stakeholder perspective, information technology and transportation stakeholders may consider improving electrical storage capacity when faced with longer lasting power outages.

The resilience decreased for the longer time horizon for all infrastructures (Figure 5.17). Communications, emergency services, and healthcare exhibited very little spread in resilience for all time horizons which suggested that changes in the endogenous preference are resilience drivers rather than hurricanes. This finding would effect the negotiation framework when capital must be allocated for the different infrastructures. Stakeholders for communications, emergency services, and healthcare would argue for more capacity independent of storm arrival as opposed to improving the electrical grid in response to hurricane caused power outages. On the other hand, critical manufacturing and transportation stakeholders would argue for improved electrical buffers for their infrastructures and/or improvement in the electrical grid response to storms, especially the category 3, 4, and 5 storms.

This hurricane threat study demonstrated the hybrid resilience framework in

Table 5.11: Resilience Results

Stakeholder Profile	6 Month		1 Year		2 Year	
	Mean	Range	Mean	Range	Mean	Range
Infrastructure						
Communications	0.99	0.98–0.99	0.99	0.98–0.99	0.98	0.97–0.98
Critical Manufacturing	0.99	0.77–0.99	0.97	0.76–0.98	0.95	0.75–0.97
Electricity Availability	1.00	0.86–1.00	0.99	0.87–1.00	0.99	0.82–1.00
Emergency Services	1.00	1.00–1.00	1.00	1.00–1.00	1.00	1.00–1.00
Healthcare	1.00	1.00–1.00	1.00	1.00–1.00	1.00	0.96–1.00
Information Technology	1.00	0.87–1.00	1.00	0.76–1.00	0.99	0.49–1.00
Transportation	0.94	0.64–0.95	0.93	0.64–0.95	0.91	0.64–0.94
Water	1.00	0.88–1.00	0.99	0.87–0.99	0.98	0.82–0.99

Stakeholder Profile	5 Year		10 Year		Post-Maria Puerto Rico
	Mean	Range	Mean	Range	
Infrastructure					
Communications	0.95	0.95–0.95	0.91	0.91–0.91	
Critical Manufacturing	0.89	0.69–0.93	0.80	0.63–0.87	
Electricity Availability	0.98	0.77–1.00	0.96	0.75–1.00	0.61
Emergency Services	1.00	1.00–1.00	0.99	0.95–1.00	
Healthcare	1.00	0.90–1.00	0.95	0.83–0.96	
Information Technology	0.98	0.32–1.00	0.96	0.25–1.00	
Transportation	0.87	0.60–0.92	0.80	0.56–0.89	
Water	0.96	0.76–0.98	0.92	0.72–0.95	

the context of critical infrastructure response to extended power outages from hurricanes. The hybrid resilience framework was unique in that it explicitly considered stakeholder preferences including the quantity of functional output and the time horizon of consideration. The study included simulated data and data collected from the field in Puerto Rico in the aftermath of Hurricane Maria. The hybrid model enabled resilience analysis comparison among different types of systems and types of modeling techniques for the systems.

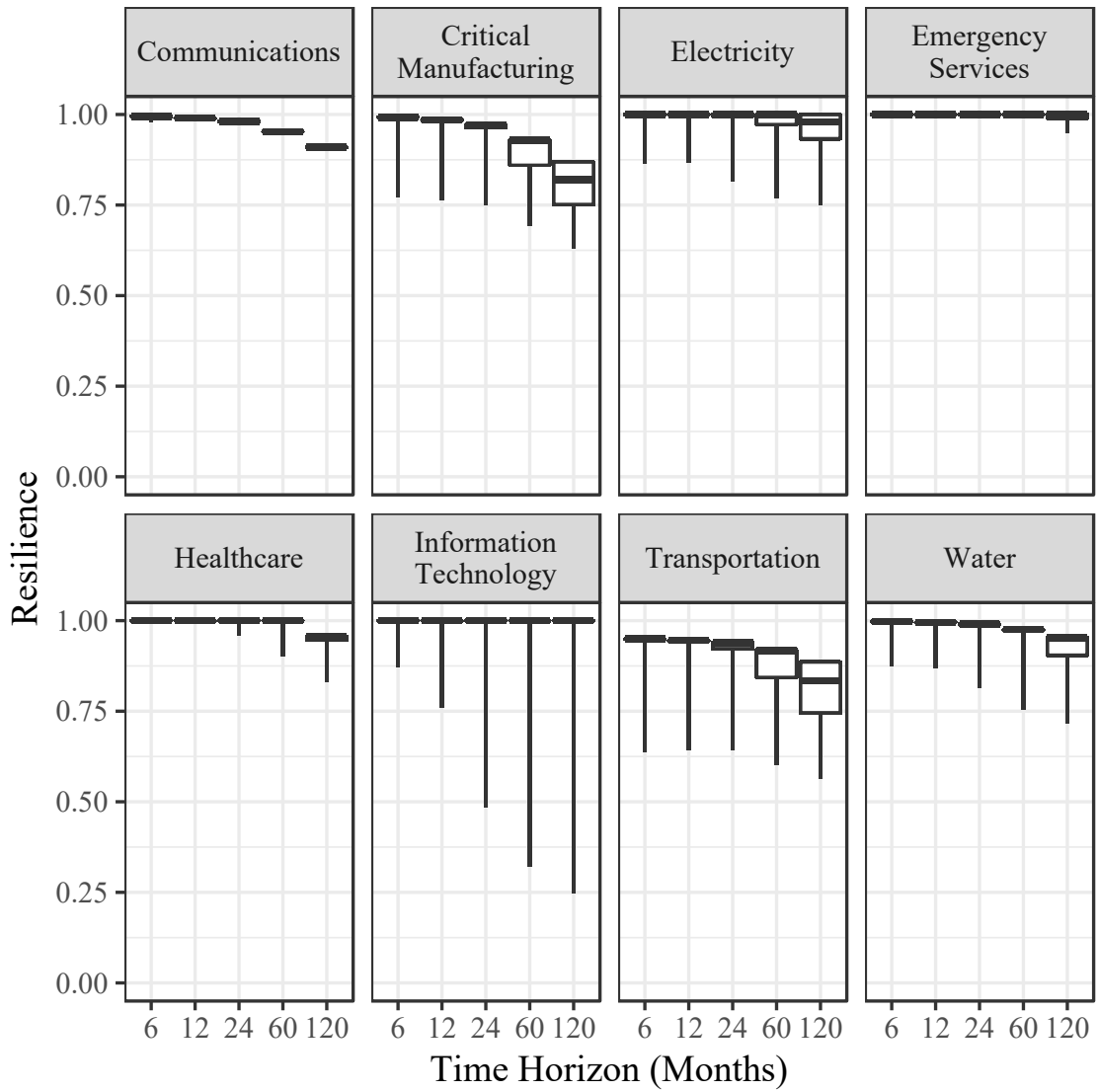


Figure 5.17: Resilience values for each time horizon and infrastructure pair

Chapter 6: Fleet Resilience Case Study

6.1 Department of Defense Sustainability Challenges

Aging systems must operate past their planned lifetimes to compensate for these delays. This life extension has reliability, safety, and operational implications. One method to deal with the problems of aging systems is a System Life Extension Program (SLEP). A SLEP extends the lifetime and often adds capability to an aging system. Many government systems are undergoing SLEP including the Army Tactical Missile System [[The Office of the Director of Operational Test and Evaluation, 2017](#), [Zacks Equity Research, 2015](#)], weather radars [[Radar Operations Center, 2018](#)], ships [[Eckstein, 2018](#), [Naval Sea Systems Command, 2018](#)], and aircraft [[Garbarino, 2018](#), [Jennings, 2018](#), [Lockheed Martin Public Relations, 2017](#), [Tirpak, 2015](#)]

This case study developed a discrete event simulation for the flight operations of a squadron of aircraft; defined the critical functional outputs of the simulation in the context of two stakeholders' preferences; and defined stakeholder preference profiles informed by the key functional outputs of the system and threats to mission assurance. Stakeholder preferences profiles included time horizon, endogenous preference, and intertemporal substitutability. The discrete nature of the functional

outputs of the simulation required modification of the extended Integral Resilience model. The case study also expanded the options for modeling stakeholder intertemporal substitutability to include event- and time-dependent values for χ . The study demonstrated the impact of changes to a stakeholder's preference model to the resilience of the system.

6.2 Case Study: Training Squadron of Aircraft

This case study was based upon current jet trainers, the T-45 Goshawk (Figure 6.1) and T-38 Talon (Figure 6.2), in the U.S. Navy and U.S. Air Force. These aircraft, along with instructor pilots, provide training to prepare pilots for flying advanced tactical aircraft. Trainer aircraft require less maintenance, and less cost than tactical aircraft. The T-X aircraft is the oft-delayed replacement for the T-38 [Mehta, 2013, Roberts, 2011]. No replacement yet exists for the T-45; The T-45 is undergoing SLEP to increase its operational lifetime. The T-45 SLEP includes detailed inspections, preventive parts replacement, corrosion control, and crack control [Jennings, 2018].

When possible, the study used unclassified US Navy documents available via official DoD websites to guide development of the simulation. In cases where information is missing, the authors made simulation decisions consistent with personal experience and with the goal of making the simulation tractable.

One course of action to mitigate the current DoD challenges regarding aging systems and delayed acquisitions [Burgess, 2015, LaGrone, 2016] is SLEP of the aging



Figure 6.1: T-45 Goshawks on the flightline [Sgt. Dengrier M. Baez, 2015]

system. SLEP can mitigate a host of problems:

- Parts obsolescence [Tomczykowski, 2001]
- Part wear-out [Jennings, 2018]
- Capability improvement [Burgess, 2015]

A SLEP defines the systems to modify, amount of life to add, number of systems to SLEP, and when the SLEP should occur in the lifetime of the system. The impact of the decisions often occur well beyond the careers of the people who make them. Therefore, considering the time horizon of the individuals is important.

Figure 6.3 depicts the hybrid resilience framework for the training squadron



Figure 6.2: T-38 Talon [Roberts, 2011]

case study. The system of interest was the training squadron comprising aircrew and aircraft. Threats to the system were delays in fielding a replacement aircraft and a surge in graduate pilot production. The two stakeholders, program managers and squadron commanding officers, shared two functional outputs: graduation per quarter and satisfaction rate. Program managers were also concerned with the daily aircraft ready for flight. The stakeholders had different preference profiles (time horizon, endogenous preference, and intertemporal substitutability) for each functional output. The resilience analytical model calculated resilience of each functional output-stakeholder preference pairing.

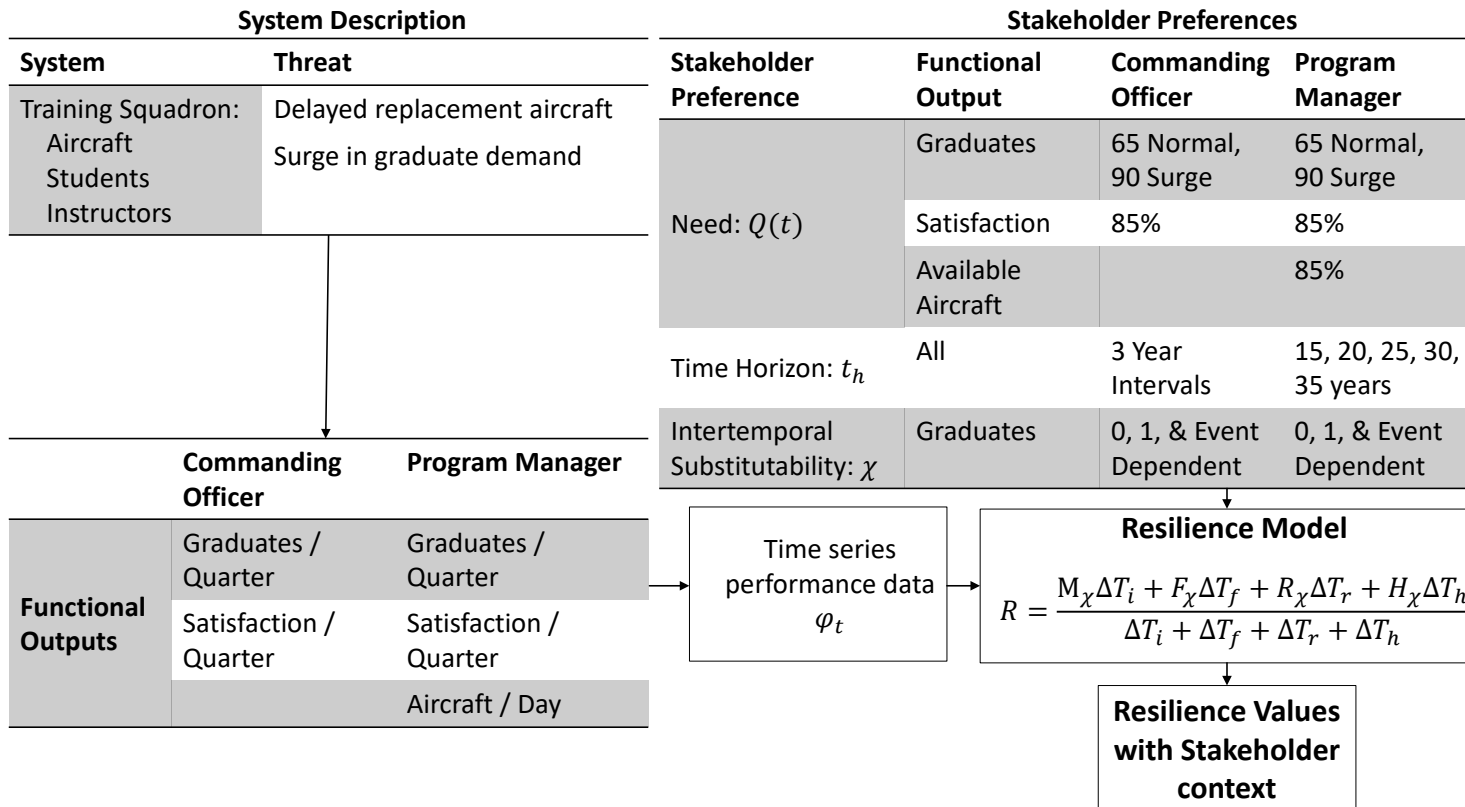


Figure 6.3: Case study hybrid resilience framework

6.3 Training Squadron Simulation

The simulation used the SimPy [Lünsdorf and Scherfke, 2018] package in Anaconda Python 3.5 [Anaconda Inc., 2016]. SimPy contains capability to define a simulation environment, processes, and resources. The squadron simulation comprised two primary objects: aircrew and aircraft. Multiple processes, defined by a scheduler object, determined which aircraft and aircrew were available for a slot in the flight schedule, and matched the available aircraft and aircrew to conduct a training event.

Figure 6.4 depicts the simulation flow. The simulation revolved around flight events. A flight required a student, an instructor, and an aircraft. At the completion of the flight, each component of the aircraft was either ready to fly in the next event (up) or required a maintenance action (down). If a component was down, maintenance personnel repaired the aircraft to return it to the flightline. After a flight, the component's expended life could trigger aircraft retirement or move to the SLEP queue. Instructors graded students after each flight. The grades were pass/fail. After a certain number of passing flights, the student graduated and placed in the graduate pool for assignment to a tactical squadron.

The scenarios defined the possibilities for system behavior and threats to the system under consideration. The system was a fleet of 50 aircraft with a monthly matriculation of 25 students. Matriculation numbers were drawn from a uniform distribution from 18 to 32. The original (pre-SLEP) aircraft lifetime was 7,200 hours. Under this *normal* operating procedure, the aircraft lasted just beyond the

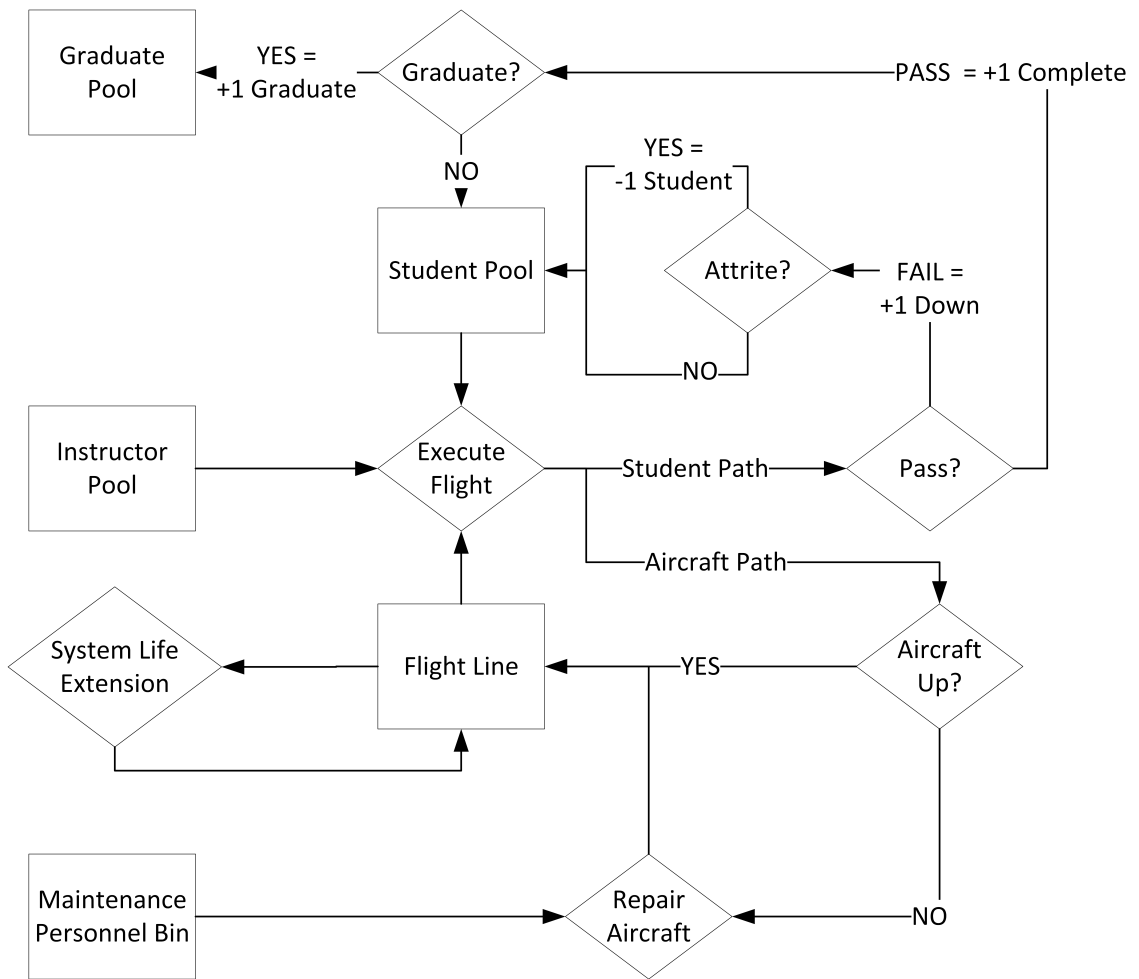


Figure 6.4: Squadron fleet operation flow of events

planned end of life, or fifteen years (Table 6.1).

The motivating problem was a change in sundown date due to a delay in the procurement of a follow-on training aircraft. To solve this problem the program manager initiated a SLEP for the airframe. As each aircraft approached its life limit, it entered the SLEP queue to receive modifications to enhance the lifetime. The study looked at extending operational use of the fleet in five year increments from 15 years (original lifetime) to 35 years. The study completed 1,660 runs of each

combination of SLEP scenarios, student surge scenarios, and stakeholder preference profile. Each combination of functional output, SLEP course of action, and student surge status met a stopping criterion of less than 1% standard error on the mean [Sandborn, 2013].

The following sections define the simulation entities in more detail.

Table 6.1: Simulation Paramager Starting Values

Parameter	Value
Aircraft	50
Students	50
Instructors	40
Aircraft Lifetime	7,200 Hours
Aircraft SLEP trigger	7,000 Hours
Minimum Class Size	18
Maximum Class Size	32

6.3.1 Aircraft Model

An aircraft comprised three parts: an airframe, avionics, and propulsion. A part had a lifetime, a repair time, a failure rate. Part failure rates depended upon flight hours only. An exponential distribution with λ set as depicted in Table 6.2 represented the parts' time to failure. Repair quality was to good-as-new using a log-normal distribution to model the time to repair.

Each part subclass, airframe, avionics, and propulsion, could have its own failure and repair distribution parameters, SLEP trigger time, lifetime, and lifetime added through SLEP. For this study, the airframe is the part of primary significance and was the only part to limit the aircraft lifetime and receive SLEP.

Table 6.2: Aircraft Simulation Values

Part	Characteristic	Value (Hours)
Airframe	Average Time to Failure	100
	Average Time to Repair	720
	Fatigue Life to Trigger SLEP	7000
Propulsion	Average Time to Failure	40
	Average Time to Repair	240
Avionics	Average Time to Failure	30
	Average Time to Repair	240

6.3.2 Aircrew

The aircrew class included students and instructors. Both students and instructors recorded hours flown for the aircrew. Instructors could fly up to three flights a day. A student graduated from the curriculum with 61 complete flights and less than 4 failed flights [Chief of Naval Air Training, 2009]. The student entered the “graduated students” pool when the curriculum is complete. The student entered the “attrited students” pool after failing four flights. Each flight had a 3.5% chance to result in a failure. Over the course of 61 graded flights, a student had an 84 % chance to graduate the syllabus. If a part on the aircraft failed during the flight, the flight grad was incomplete, and must be re-flown. The student had no limits to incomplete flights. A student could fly up to two flights per day. The simulation began with a set amount of students. Every 30 days, a new class of students matriculated into the flight program. A uniform distribution for 70-130% of the average class size provided variation in the class size per month. Table 6.3 summarizes the students parameters. The class size changed to reflect the fluctuating demand of

the squadron commander stakeholder.

Table 6.3: Model Parameter Values for Students and Instructors

Parameter	Student Value	Instructor Value
Events per Day	2	3
Events in Curriculum	61	NA
Event Failure Rate	3.5%	NA
Failed Events Allowed	3	NA

6.3.3 SLEP Simulation

The program manager faced three different SLEP strategies: “No SLEP”, “Small SLEP,” and “Large SLEP.” “No SLEP” did not add any life to the aircraft, but it also avoided taking aircraft out of the flight schedule for the extended time required to conduct SLEP. “Small SLEP” increased the lifetime of the aircraft to 14,400 flight hours but removed aircraft from the flightline for 9 months. “Large SLEP” increased the lifetime of the aircraft to 18,000 flight hours but removed aircraft from the flightline for 12 months.

An aircraft entered the SLEP queue when it reaches its SLEP flight hour limit. The SLEP line had a limited number of slots available in the hangar, so the program manager gradually introduced aircraft to the SLEP line. The simulation assigns each aircraft a SLEP flight limit ranging from 3,500 to 7,000 flight hours to reduce wait times.

6.3.4 Flight Scheduling

The scheduler defined flight days, flight events, and matched instructors, students and aircraft for the flight. The scheduler used a simplified calendar with a five-day flying week and two day weekend with maintenance but no flying. Each flying day had 4 flight events with start times spaced by 3 hours. The scheduler used a uniform distribution to select a flight time between 0.5 and 2.0 hours for a single event. For each event, the scheduler made student-instructor-aircraft matches for each event until one of the pools is exhausted. The potential results of a flight were:

- Student outcomes:
 - Flight incomplete due to aircraft failure
 - Passing flight for the student
 - Failure of curriculum hop for the student

- Aircraft outcomes:
 - Down status
 - Up status
 - Send to SLEP line
 - End of life

The scheduler updated all the objects involved in the flight: adds flight hours added to the aircraft and parts; updates student syllabus completion data; assesses

student status (graduate, attrite, continue); adds a new class of students monthly; assesses aircraft repair status (up or down); assesses aircraft flightline status (flightline, SLEP line, end of life); and assesses status of aircraft in the SLEP line (waiting, in-SLEP, complete).

6.4 Stakeholder Preference Profiles: Intertemporal Substitutability

The value of χ could be constant for the entire time horizon, or it could be dependent upon time and/or events. Two special values of χ are the *ephemeral* ($\chi = 0$) case and *permanent* ($\chi = 1$) case. The *ephemeral* case allows no substitution across time. When the system had a shortage at time t_j , surplus from time t_i had no value. In the *permanent* case, a surplus retained its full value or utility throughout the time horizon. Any surplus at time t_i had full value at time t_j . Earlier studies addressed these cases as well as fractions of the *permanent* case which remained constant throughout the time horizon.

The *adjacent* case of intertemporal substitutability enabled time- and event-dependent surplus “transfer” from time steps adjacent to a time step with a shortfall. A coefficient moderates the “transfer” value, decreasing the value of substitution as t_n moves further away from the shortfall time. Intertemporal substitutability (χ) became a scalar two-column matrix of an arbitrary length (Table 6.4). The first column was an index (j) defining the amount of steps from the shortfall that is transferable. The second column was the fraction of transferable surplus. Using Table 6.4 as an example, 75% of surplus occurring one time step after shortfall was

available to transfer while 100% of surplus one time step before the shortfall was available to transfer.

Table 6.4: Example of the χ matrix

\mathbf{j}	χ_j
3	0
2	0.25
1	0.75
-1	1
-2	0.5
-3	0.25
-4	0.1
-5	0

The following proposed algorithm applied a surplus to shortfall substitution for an arbitrary number of steps away from the performance shortfall. The algorithm assumed the surpluses closest in time to the shortfalls were first to transfer. Table 6.5 defines the key terminology in the algorithm and figures 6.5 through 6.10 demonstrate the algorithm for surpluses occurring before the shortfall.

1. Define the indices (j) and the fraction of substitutability (χ_j) for the intertemporal substitutability matrix.
2. Find a performance shortfall, $\varphi_t < Q_t$. This defines the time (t) of the shortfall
3. Calculate the transferable surplus from the closest index (j) before the shortfall, $\psi_{t,j} = \chi_j(\varphi_{t-j} - Q_{t-j})$
4. If $\varphi_t + \psi_{t,j} < Q_t$,
 - (a) set $\varphi_t : \varphi_t + \psi_{t,j}$ and $\varphi_{t-j} : Q_{t-j}$.
 - (b) Return to Step 2.
5. If $\varphi_t + \psi_{t,j} \geq Q_t$,
 - (a) Set $\varphi_t : Q_t$
 - (b) Remove the transferred surplus from $\varphi_{t-1} : Q_t + \frac{\psi_{t,j} - (Q_t - \varphi_t)}{\chi_j}$.

- (c) Return to Step 3 with j one step further from the current replacement step.
- 6. If $\varphi_t < q_t$ and no surplus remains, return to Step 3 and apply surplus occurring after the shortfall.
- 7. When all *available* surpluses are exhausted, set φ for all remaining surpluses to Q_t . This step ensures that the resilience analytic model does not incorporate inaccessible surpluses. The result is $\tilde{\varphi}_t$

The *adjacent* intertemporal substitutability algorithm allowed a stakeholder to account for the value of surplus before and after a disturbance causing a shortfall in desired functional output of the system. The fleet resilience case study demonstrated the algorithm.

Table 6.5: Intertemporal Substitutability Terminology

Symbol	Definition
φ_t	Performance at time t
Q_t	Endogenous preference at time t
χ_j	Intertemporal substitution coefficient j time steps from time t
$\psi_{t,j}$	Transferable surplus at j time steps from time t
$\tilde{\varphi}_t$	Modified performance at time t

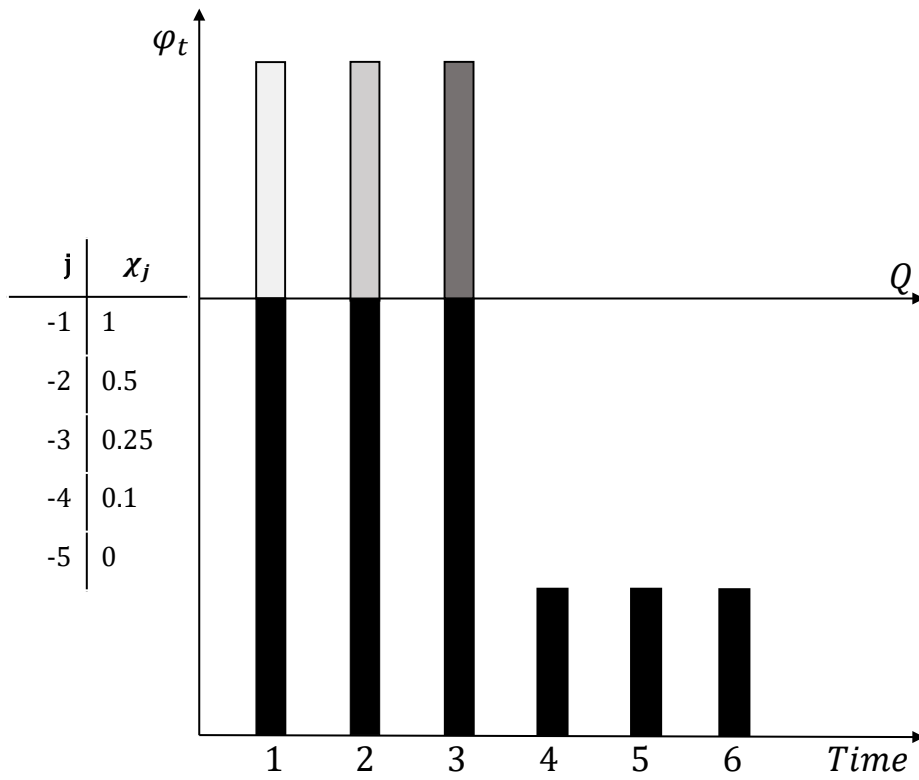


Figure 6.5: Intertemporal substitutability algorithm example: The left portion of the figure defines the χ matrix (Step 1). The first shortfall occurs at $t = 4$ (Step 2).

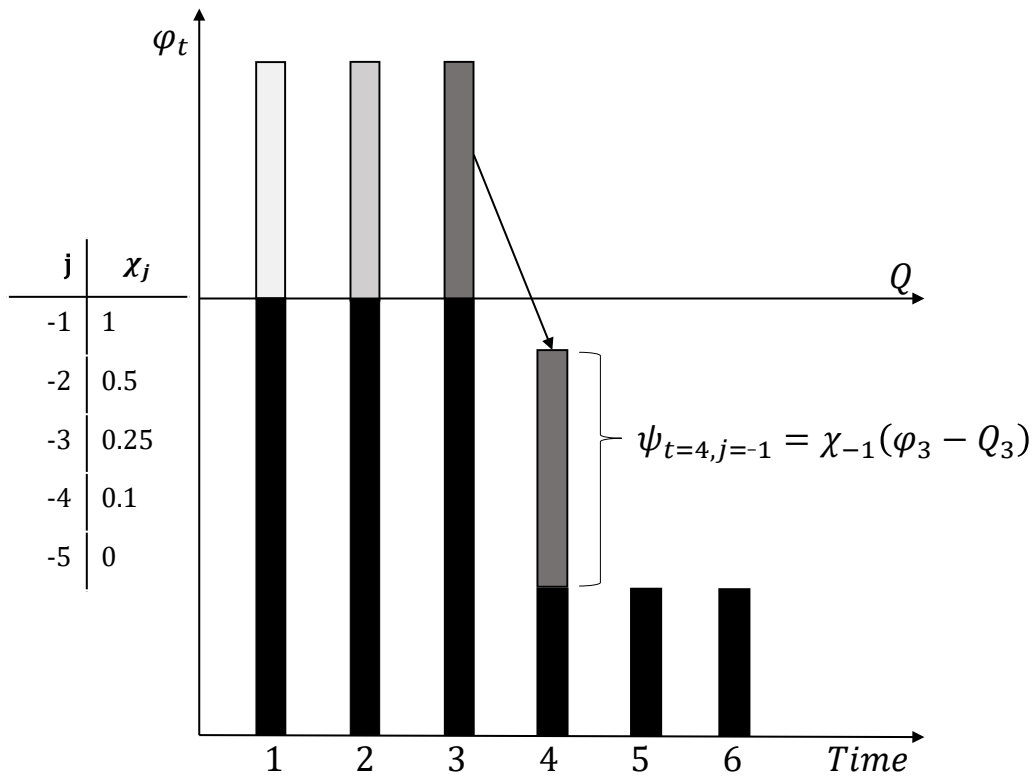


Figure 6.6: Intertemporal substitutability algorithm example: the available surplus ψ applied to $t = 4$ using $j = -1$ (Step 3).

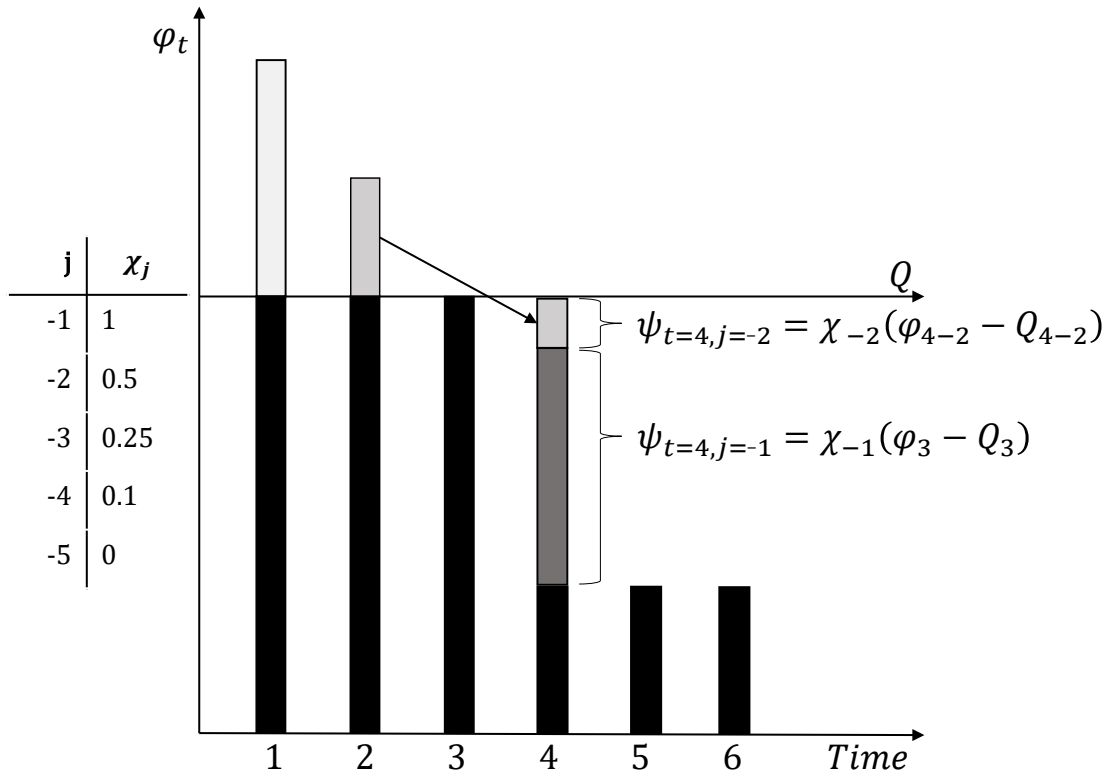


Figure 6.7: Intertemporal substitutability algorithm example: the surplus from $t = 3$ cannot overcome the shortfall (Step 4). This transfer expended all surplus from $t = 3$ (Step 4a), and the algorithm transferred surplus from one step further, $t = 4$ (Step 3).

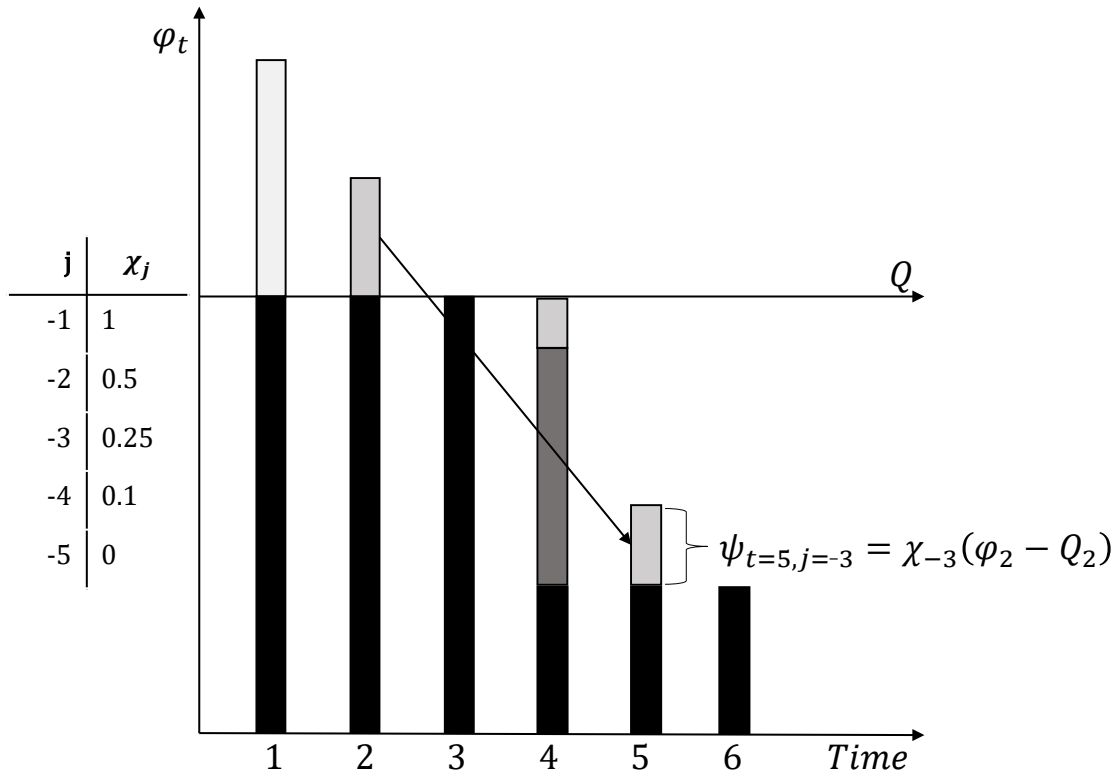


Figure 6.8: Intertemporal substitutability algorithm example: transfer satisfied the shortfall with surplus remaining at $t = 2$ (Step5). With $t = 4$ satisfied, the algorithm found the next shortfall at $t = 5$. The first two time steps, $t = 4$ & 3 are exhausted, so the algorithm transferred surplus from $t = 2$, three steps before $t = 5$. This transfer exhausted the surplus from $t = 2$ ($\psi_{5,3}$).

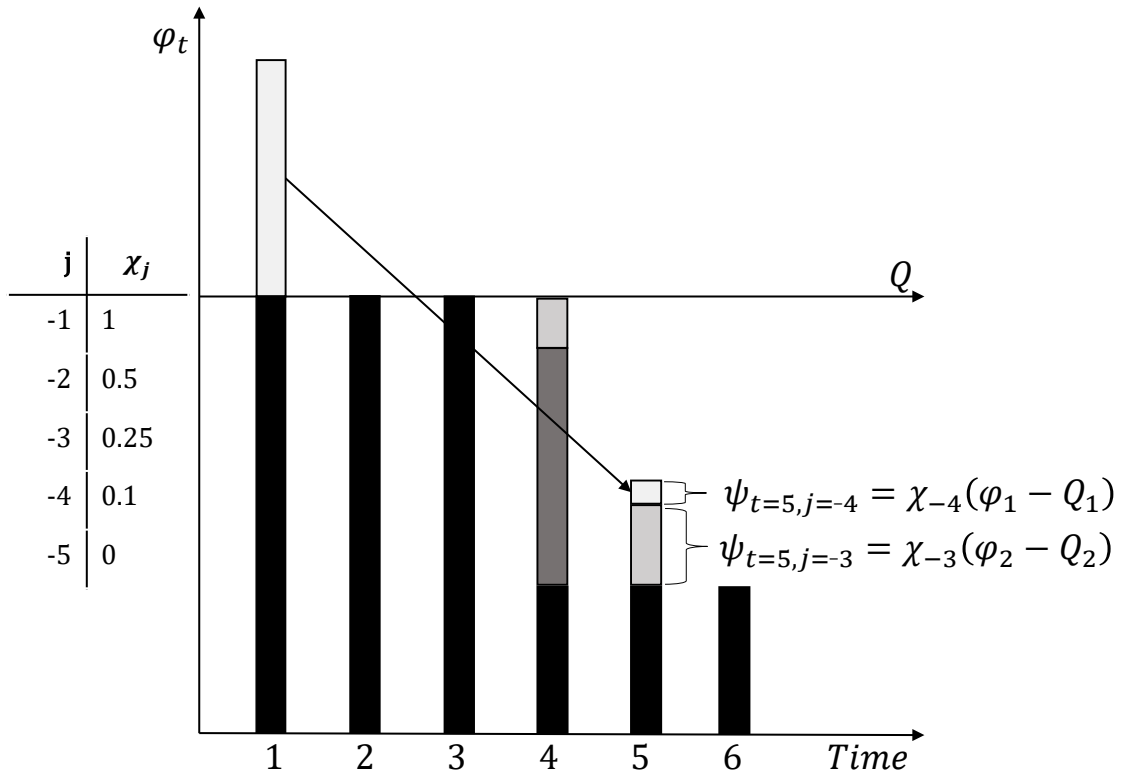


Figure 6.9: Intertemporal substitutability algorithm example: the entire surplus from $t = 1$ transferred to $t = 5$

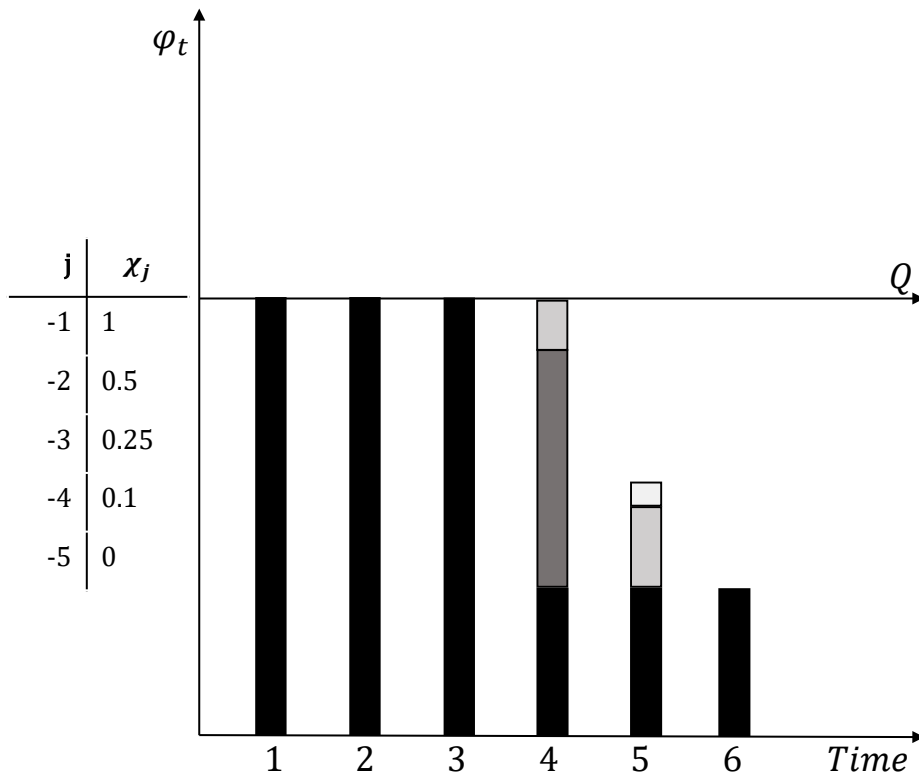


Figure 6.10: Intertemporal substitutability algorithm example: the total available surplus from Figure 6.5 cannot satisfy the shortfall during the distribution. The algorithm is completed and produced the modified functional output $\tilde{\varphi}_t$.

6.5 Resilience Analytical Model

The extended Integral Resilience model was:

$$R_{EIR} = \frac{M_\chi \Delta T_i + F_\chi \Delta T_f + R_\chi \Delta T_r + H_\chi \Delta T_h}{\Delta T_i + \Delta T_f + \Delta T_r + \Delta T_h} \quad (6.1)$$

where the factors M_χ , F_χ , etc., for continuous system are:

$$F_\chi(t) = \begin{cases} \frac{\int_{t_i}^{t_f} \varphi(t) dt}{\int_{t_i}^{t_f} Q(t) dt} & \text{for } \varphi(t) \leq Q(t) \\ 1 + \chi(t) \frac{\int_{t_i}^{t_f} \varphi(t) - Q(t) dt}{\int_{t_i}^{t_f} Q(t) dt} & \text{for } \varphi(t) > Q(t) \end{cases} \quad (6.2)$$

This formulation was inappropriate for the functional outputs of the discrete event simulation. The study developed a discrete representation of the extended Integral Resilience. The overall equation for resilience, R , remains unchanged, but the equations for each profile must be modified incorporating Equation 6.1.

$$F_{\chi,t} = \left\{ \begin{array}{l} \frac{\sum_{\tau=t_i}^{t_f} \varphi_{\tau}}{t_f} \quad \text{for } \varphi_t \leq Q_t \\ \sum_{\tau=t_i}^{t_f} Q_{\tau} \\ 1 + \chi_t \frac{\sum_{\tau=t_i}^{t_f} \varphi_{\tau} - Q_{\tau}}{t_f} \quad \text{for } \varphi_t > Q_t \ \& \ \chi_t = \text{constant} \\ \sum_{\tau=t_i}^{t_f} Q_{\tau} \\ \frac{\sum_{\tau=t_i}^{t_f} \tilde{\varphi}_{\tau}}{t_f} \quad \text{for } \chi_t = \text{adjacent} \\ \sum_{\tau=t_i}^{t_f} Q_{\tau} \end{array} \right. \quad (6.3)$$

6.6 Hybrid Resilience Framework Demonstration

The study had two main thrusts of inquiry. One effort demonstrated the hybrid resilience framework in the domain of a fleet of systems satisfying multiple stakeholders with multiple preference profiles. The other effort demonstrated the *adjacent* intertemporal substitutability algorithm and how it affected resilience outcomes.

6.6.1 Stakeholder Profiles

The study defined two stakeholder profiles: squadron commanders and the program manager. Table 6.8 shows the functional outputs of interest and the associated

values for time horizon, endogenous preference, and intertemporal substitutability for each stakeholder.

The program manager was responsible for maintaining the viability of the fleet of aircraft until a replacement system was operational. The program manager desired a certain fraction of aircraft ready to provide training events at the beginning of each fly day. The program manager ensured the flight system produces the desired graduates per quarter over its lifetime and that student satisfaction rate (fraction of students graduating under a certain time threshold) was reasonable. The program manager's time horizon was uncertain. The study investigated time horizon values of 15, 20, 25, 30, and 35 years of aircraft operations.

The commanding officer had two functional outputs of interest: graduates per quarter and satisfaction rate. Squadron Commanders had tenures lasting three-years. This tenure defined their time horizon t_h . Although, in reality, Squadron Commanders are conscientious individuals, the simulation treated them as individuals singularly focused upon their period of command with no concern of health of the fleet before or after them. From the squadron commanders' perspectives, a graduate surplus during one quarter could have value transferable to the previous or following quarter. The study investigated different types of intertemporal substitutability including *ephemeral*, *permanent*, and *adjacent* values. Graduate satisfaction rates were *ephemeral* ($\chi = 0$).

6.6.2 Study Scenarios

The program manager had three courses of action for supporting the aircraft (Table 6.6): do nothing (“No SLEP”), increase the operational life to 14,400 flight hours (“Small SLEP”), or increase the operational life to 18,000 flight hours (“Large SLEP”). The program manager also considered a change in demand for graduates. This study investigated the impact of a two year “surge” of desired graduates manifested by larger incoming classes and an increase in endogenous need. During a surge period, the average class size increased to 35 per month from a normal size of 25. The demand for students increased from 65 students per quarter to 90 students per quarter.

Table 6.6: SLEP Courses of Action

Course of Action	post-SLEP Lifetime	Time To SLEP (months)
No SLEP	NA (7,200)	NA
Small SLEP	14,400	6
Large SLEP	18,000	9

Table 6.7: Student Class Sizes

Operations	Minimum Class (month)	Maximum Class (month)	Desired Graduates (quarter)
Normal	18	32	65
Surge	25	41	90

Table 6.8: Stakeholder Preference Profile

Stakeholder	Critical Output	Time Horizon	Endogenous Preference	Intertemporal Substitutability
Commanding Officer	Quarterly Graduates Student Satisfaction	Three Years	Normal (65) / Surge (90) 85%	Ephemeral, Permanent, Adjacent Ephemeral
Program Manager	Daily Availability Quarterly Graduates Student Satisfaction	15-35 Years	85% Normal (65) / Surge (90) 85%	Ephemeral Ephemeral, Permanent, Adjacent Ephemeral

6.6.3 Intertemporal Substitutability Investigation

The study conducted an exploration of intertemporal substitutability values applied to the algorithm described above. The *adjacent* intertemporal substitutability applied to the graduates per quarter functional output. Simulation data post-processing applied 12 different values for χ to graduates per quarter. The values for χ adjusted the amount of time steps that had value, the coefficient of the value, and whether surplus before and after had an impact. Table 6.9 shows the values used. Negative time steps are time steps before the shortfall while positive time steps are after the shortfall.

Table 6.9: Values for χ Matrices

Case	Index (j)							
	-4	-3	-2	-1	1	2	3	4
Substitute only <i>after</i> shortfall								
A1	0	0	0	0	0.5	0	0	0
A2	0	0	0	0	0.5	0.25	0	0
A3	0	0	0	0	1	0.5	0	0
A4	0	0	0	0	1	1	1	1...
Substitute only <i>before</i> shortfall								
B1	0	0	0	0.5	0	0	0	0
B2	0	0	0.25	0.5	0	0	0	0
B3	0	0	0.5	1	0	0	0	0
B4	...1	1	1	1	0	0	0	0
Substitute <i>before & after</i> shortfall								
C1	0	0	0	0.5	0.5	0	0	0
C2	0	0	0.5	1	1	0.5	0	0
C3	0	0	0.25	0.5	0.5	0.25	0	0
C4	0.25	0.5	0.75	1	1	0.75	0.5	0.25
Ephemeral	0	0	0	0	0	0	0	0
Permanent	...1	1	1	1	1	1	1	1...

6.7 Simulation Outputs

The discrete event simulation produced time-series data for aircraft disposition and status status; graduates, attrited students, and matriculated students; and time to graduate for each student. Figures 6.11 shows an example run for the “No surge” scenarios for each course of action. The solid line is the number of aircraft on the flightline, the dashed line is the desired number of graduates per quarter, and the points are the actual number of graduates in a quarter. Figure 6.12 shows the same information for the “Surge” scenario. The shaded area from 12-14 years highlights the two year surge in required graduates.

6.7.1 Resilience Results

The configuration of the boxplots show the maximum, minimum and quartiles of the resilience values. The ends of the vertical lines are the maximum and minimum resilience; the top and bottom edges of the box are the 75th and 25th percentiles; and the dark hash is the median resilience.

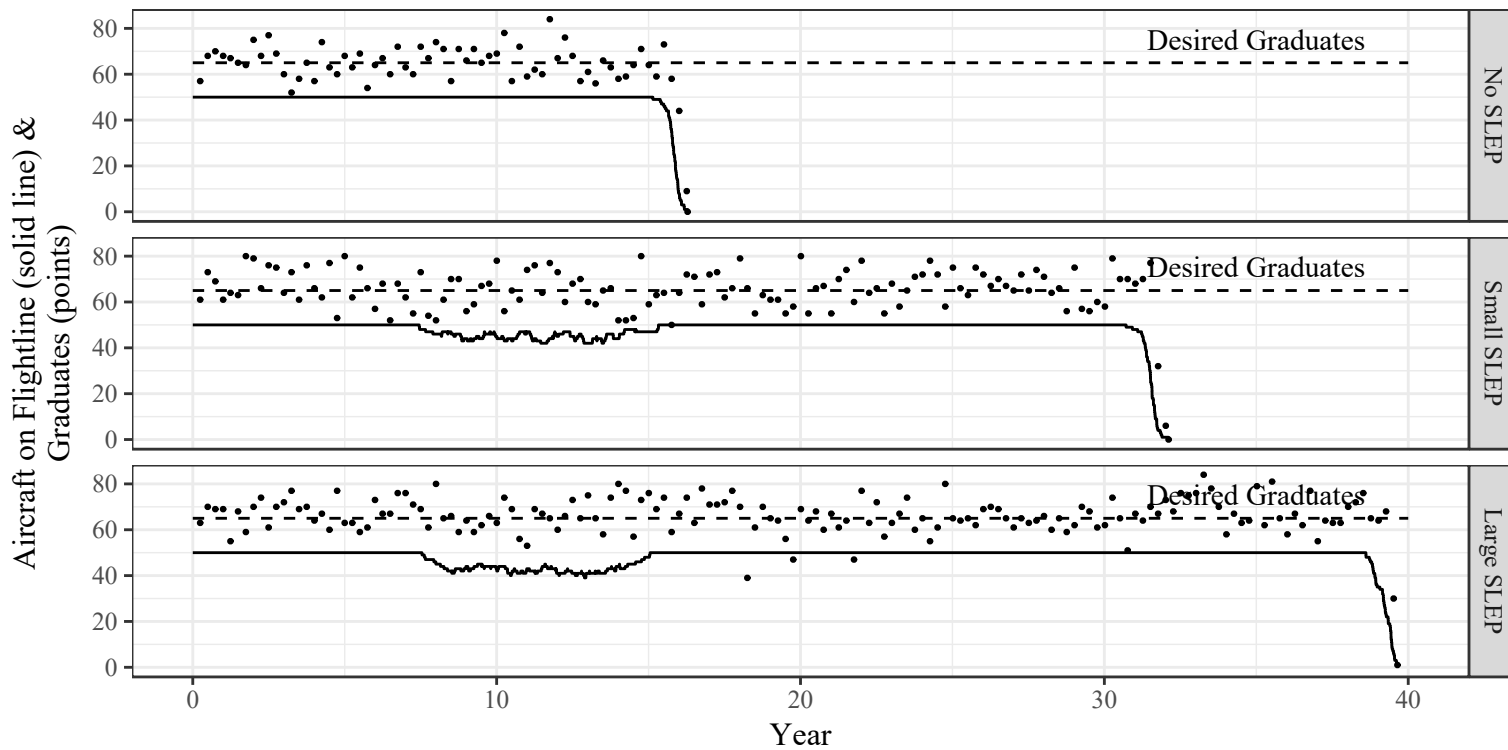


Figure 6.11: Flightline size and quarterly graduates for a single run: no surge

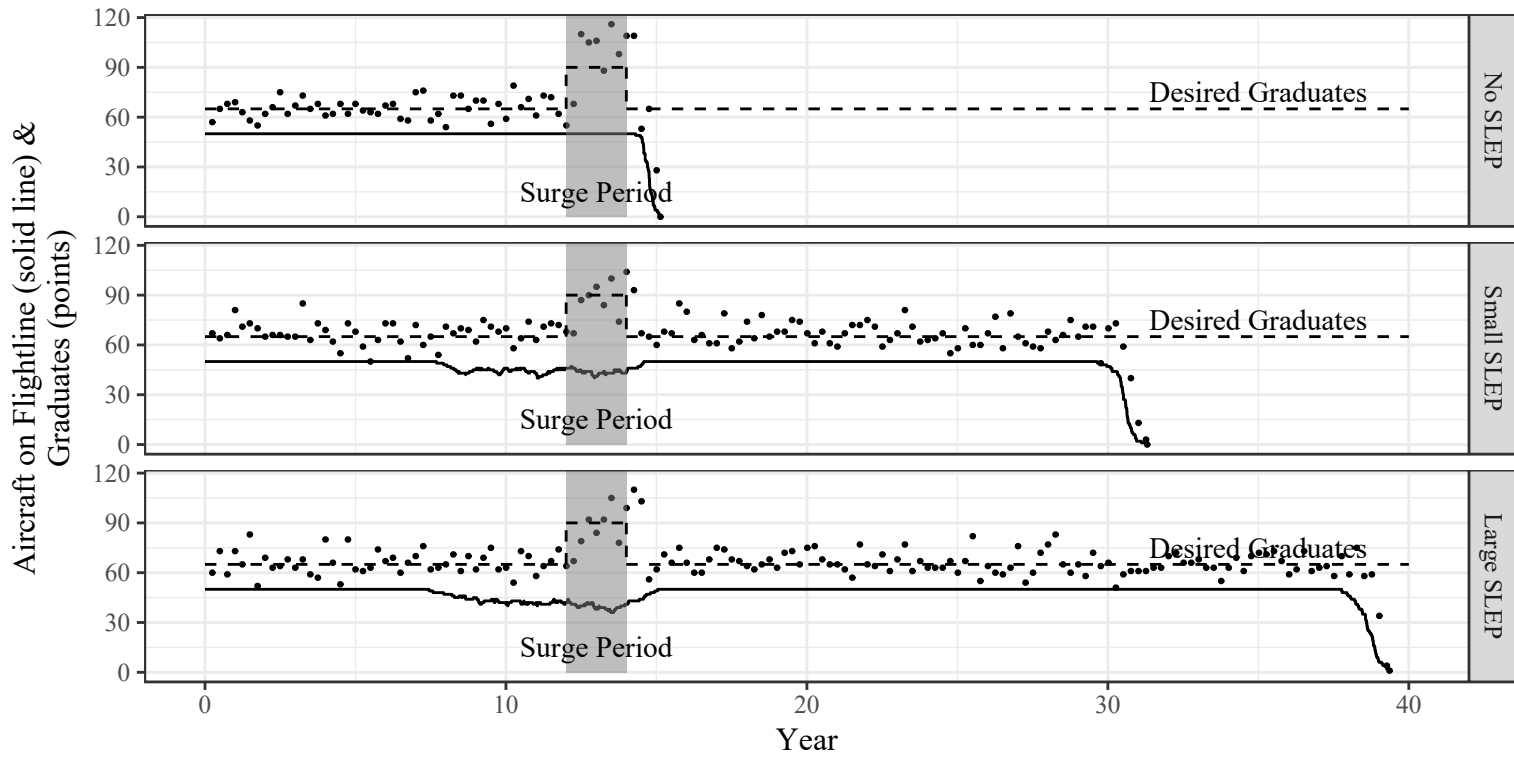


Figure 6.12: Flightline size and quarterly graduates for a single run: surge

6.8 Program Manager Perspective

The hybrid resilience framework applied the program manager’s preference (Table 6.8) profiles to the desired functional outputs using the discrete extended Integral Resilience analytical model. Each functional output has its own figure depicting the the program manager resilience results. This presentation enables visual inspection of the preferred course of action. Figure 6.13 shows results for the daily aircraft ready to fly functional output. Figure 6.14 shows surge and non-surge results for the graduates per quarter output over all time horizons of interest and for the *ephemeral* and *permanent* values of χ . Figure 6.15 shows results for the student satisfaction functional output. Table 6.10 shows the program manager’s preferred course of action for each functional outputs’ resilience at each time horizon. In the table, “Adjacent” refers to case C4.

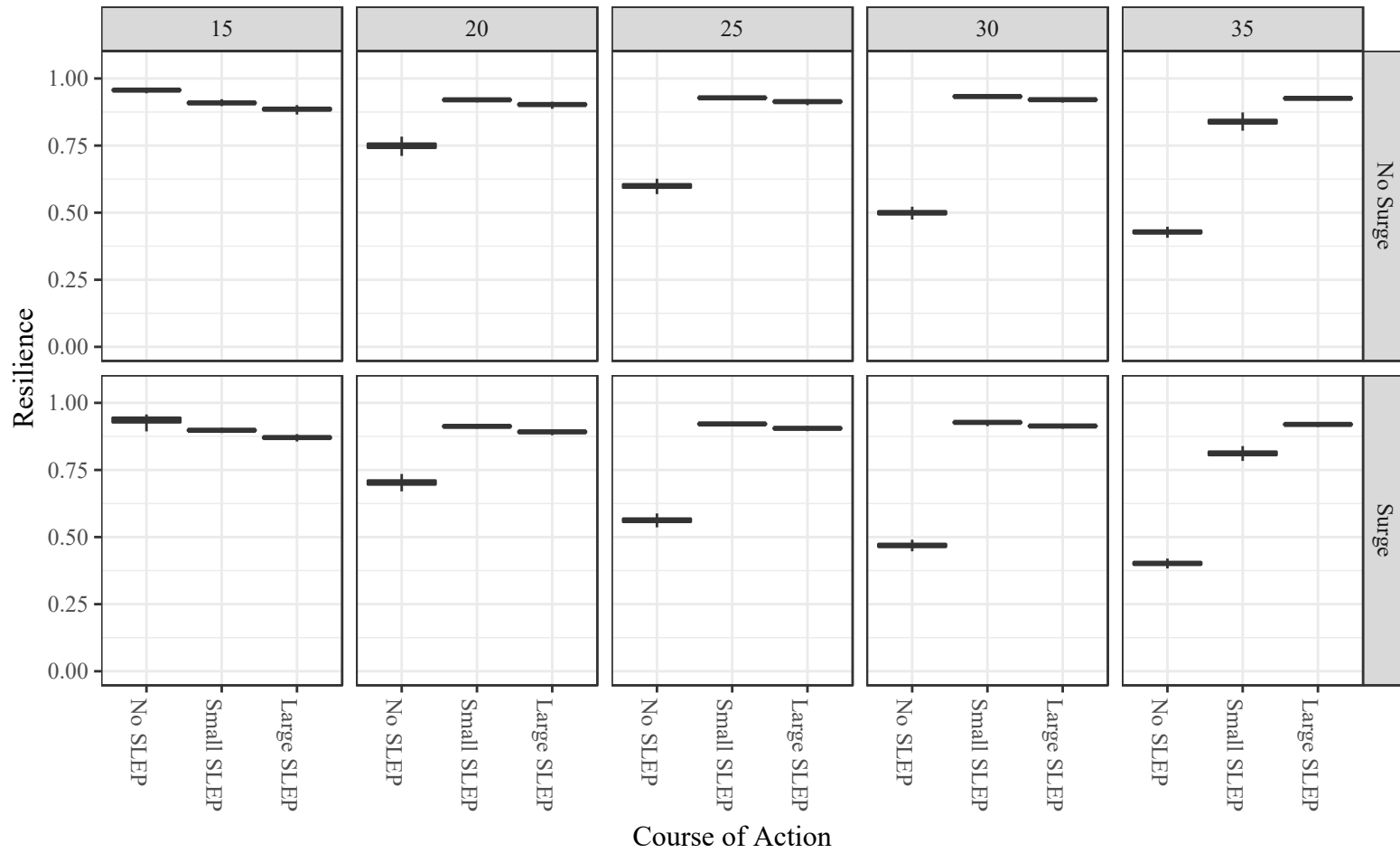


Figure 6.13: Program manager daily ready aircraft resilience results for 15, 20, 25, 30, and 35 year time horizons with and without a surge in student matriculation

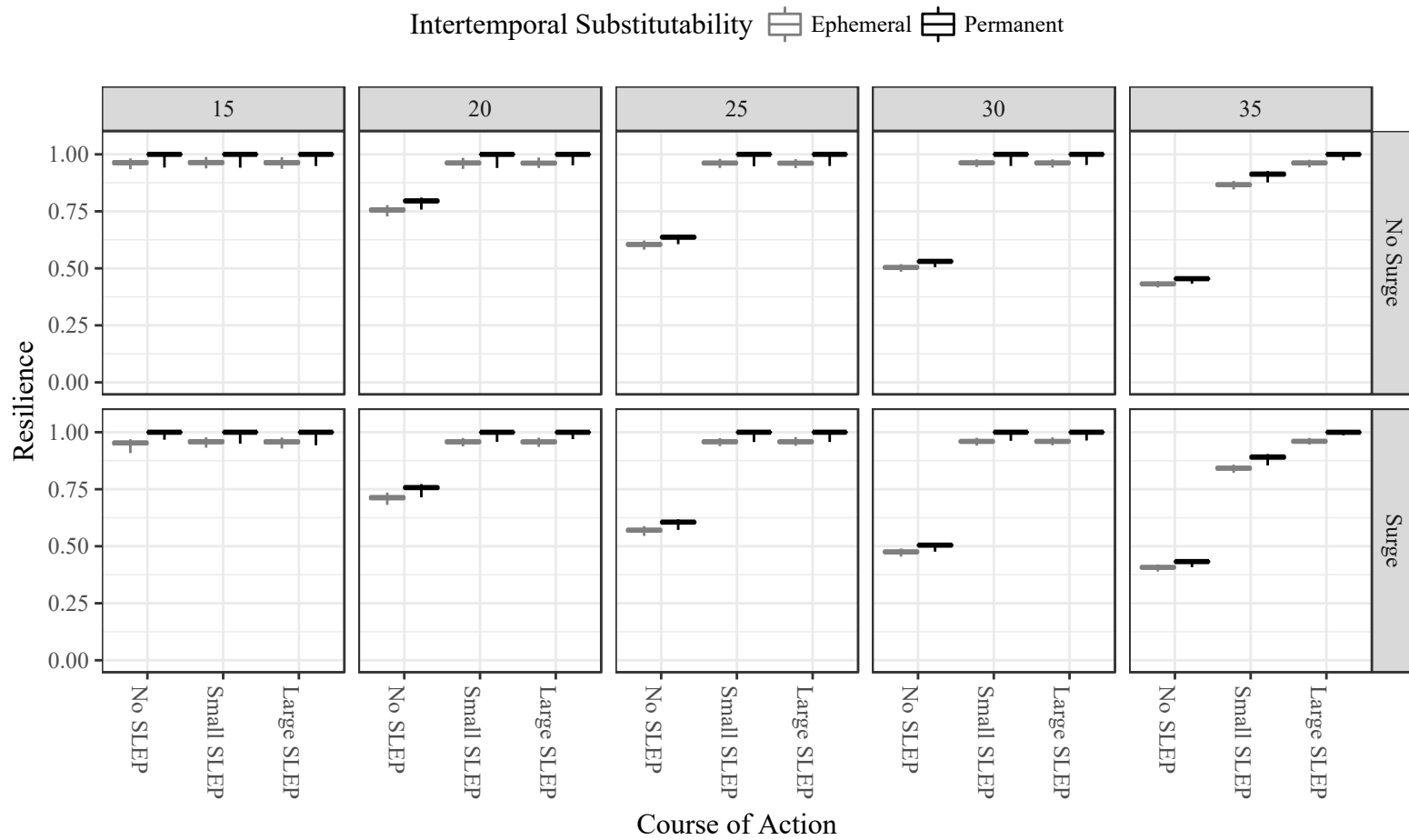


Figure 6.14: Program manager graduate resilience results for 15, 20, 25, 30, and 35 year time horizons with and without a surge in student matriculation *ephemeral* and *permanent* intertemporal substitutability profiles

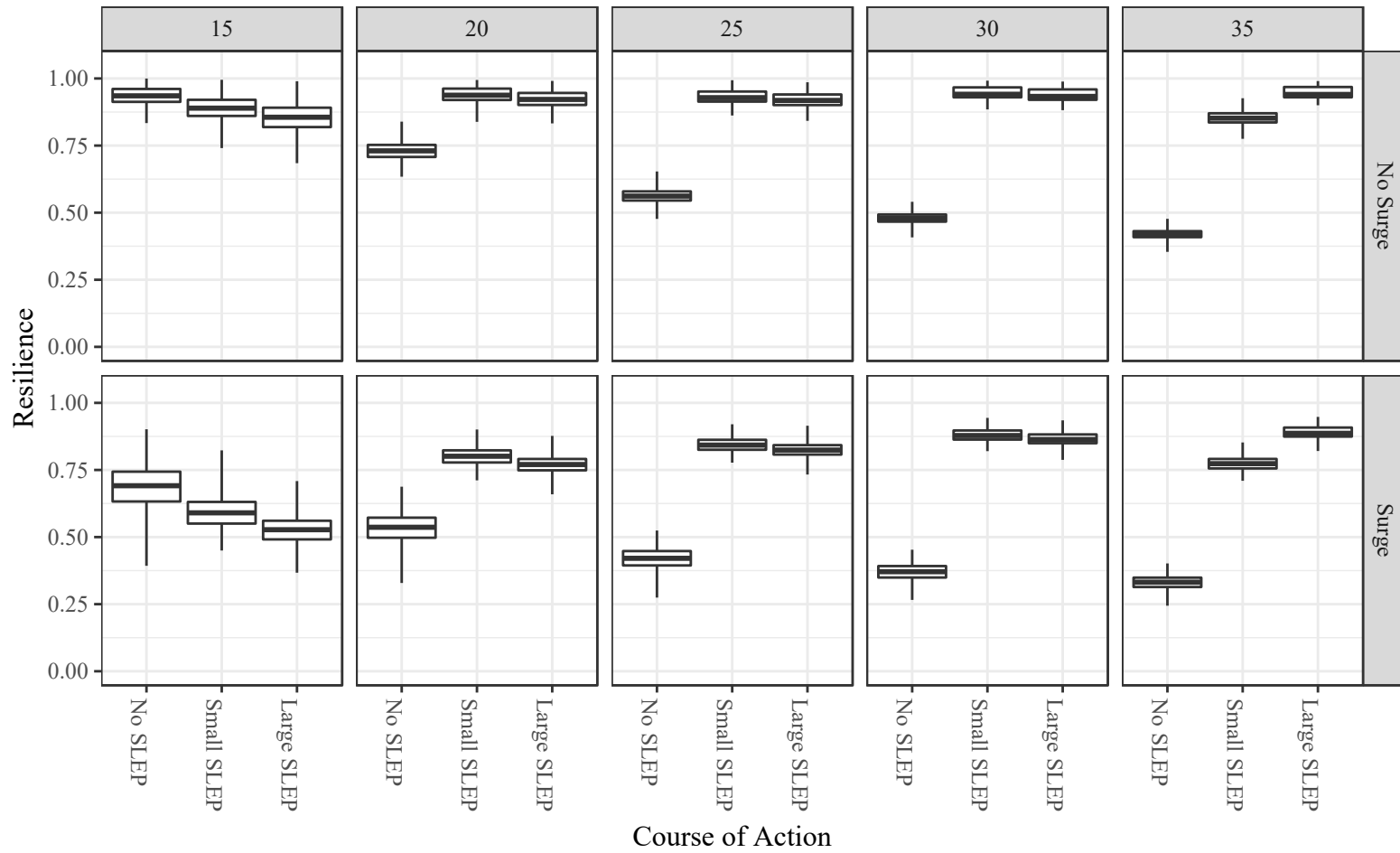


Figure 6.15: Program manager satisfaction resilience results for 15, 20, 25, 30, and 35 year time horizons with and without a surge in student matriculation.

Table 6.10: Program Manager Preferred Course of Action

Surge Status	Time Horizon	Availability	Student Satisfaction	Graduates	
				Ephemeral	Permanent
No Surge	15	No SLEP	No SLEP	Small	All
	20	Small	Small	Small	Large & Small
	25	Small	Small	Small	Large & Small
	30	Small	Small	Small	Large & Small
	35	Large	Large	Large	Large
Surge	15	No SLEP	No SLEP	Small	Large & Small
	20	Small	Small	Small	Large & Small
	25	Small	Small	Small	Large & Small
	30	Small	Small	Large	Large & Small
	35	Large	Large	Large	Large

6.9 Squadron Commander Perspective

The Squadron Commander applied the preference profiles and functional outputs defined in Table 6.8. Every Squadron Commander had a three year time horizon. The squadron commanders each have an alphabetical identifier. Time periods with all aircraft life expended had no commanding officers. The first commanding officer was Commander Alpha (A). The “No SLEP” course of action typically ended with Commander Foxtrot (F); the “Large SLEP” course of action ended with Commander November (N); and the “Small SLEP” course of action usually ended with Commander Kilo (K), but occasionally reached Commander Lima. When a simulation exhausts all aircraft flight hours, the Commander receives no resilience value.

Figure 6.17 shows the resilience results for graduates per quarter for three

intertemporal substitutability values: the *ephemeral* case, the *permanent* case and *adjacent* case C3 (Table 6.9). Figure 6.16 shows the results for resilience of satisfied graduates (less than 60 days in the squadron) for each course of action and surge status.

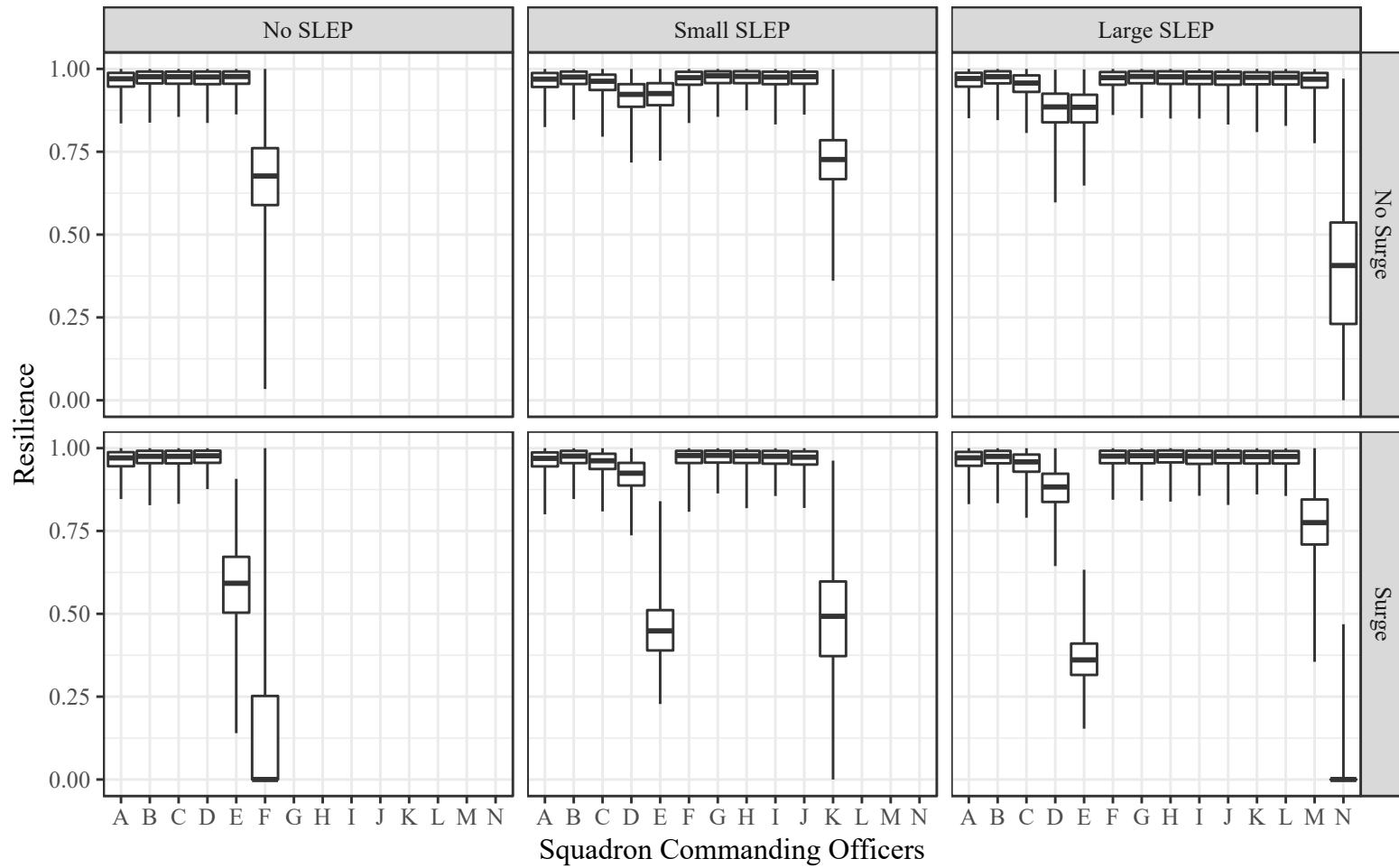


Figure 6.16: Squadron commander student satisfaction resilience results

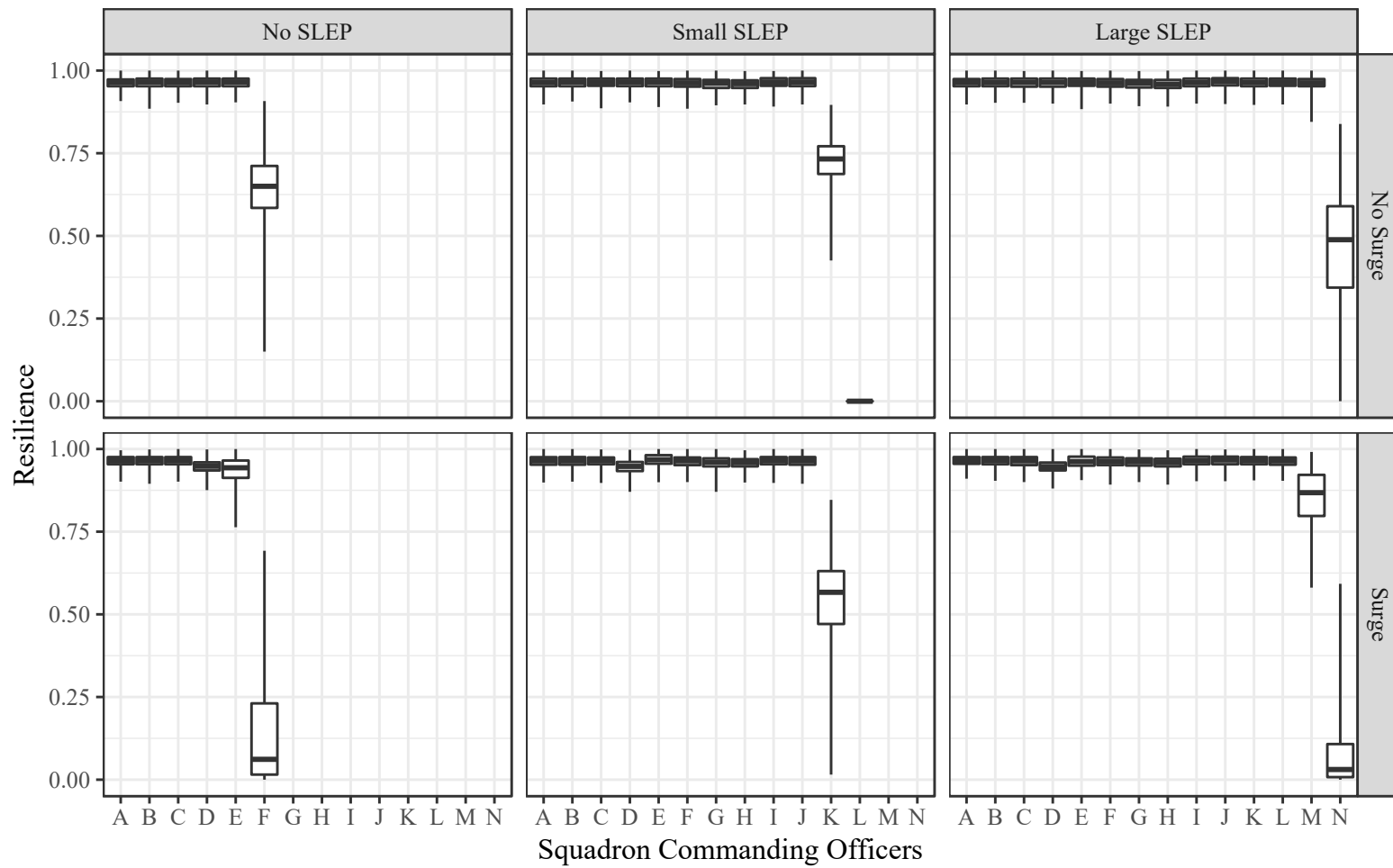


Figure 6.17: Squadron commander graduates resilience results ($\chi = 0$)

6.10 Intertemporal Substitutability Investigation

The second part of this study focused on implementing the Intertemporal Substitutability algorithm. The study applied 12 *adjacent* algorithms and the pre-existing *permanent* and *ephemeral* cases. Intertemporal substitutability applied to the graduates per quarter functional output of the simulation. Figures 6.18, 6.19, 6.20, 6.21, and 6.22 show the change in resilience as the intertemporal substitutability changes for the program manager.

Figures 6.23 and 6.24 show the resilience values for all intertemporal substitutability preferences from the perspective of Commanders Delta and Echo. The SLEP process and surge occur during these two commanders' tenure.

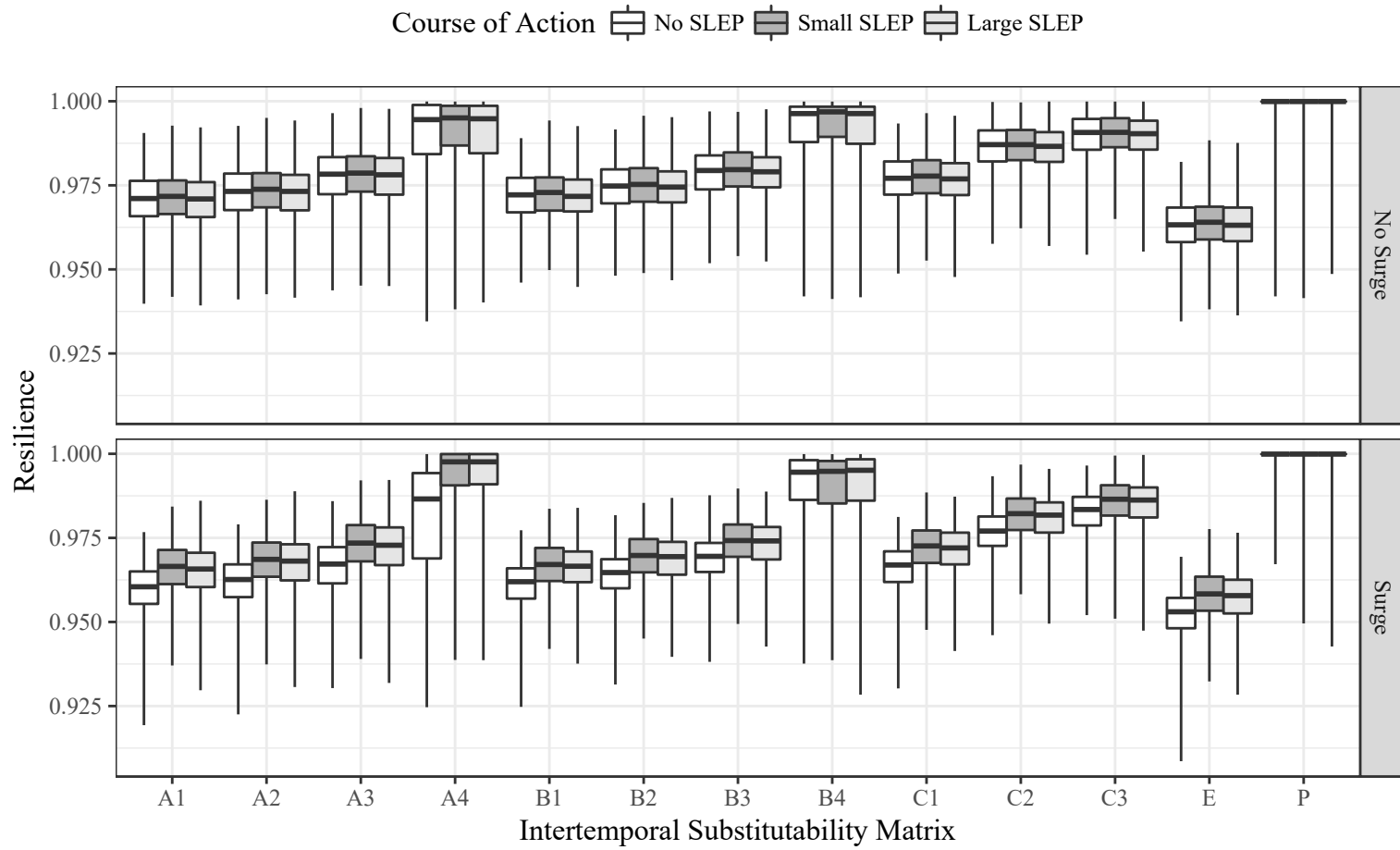


Figure 6.18: Program manager intertemporal substitutability, 15 year time horizon

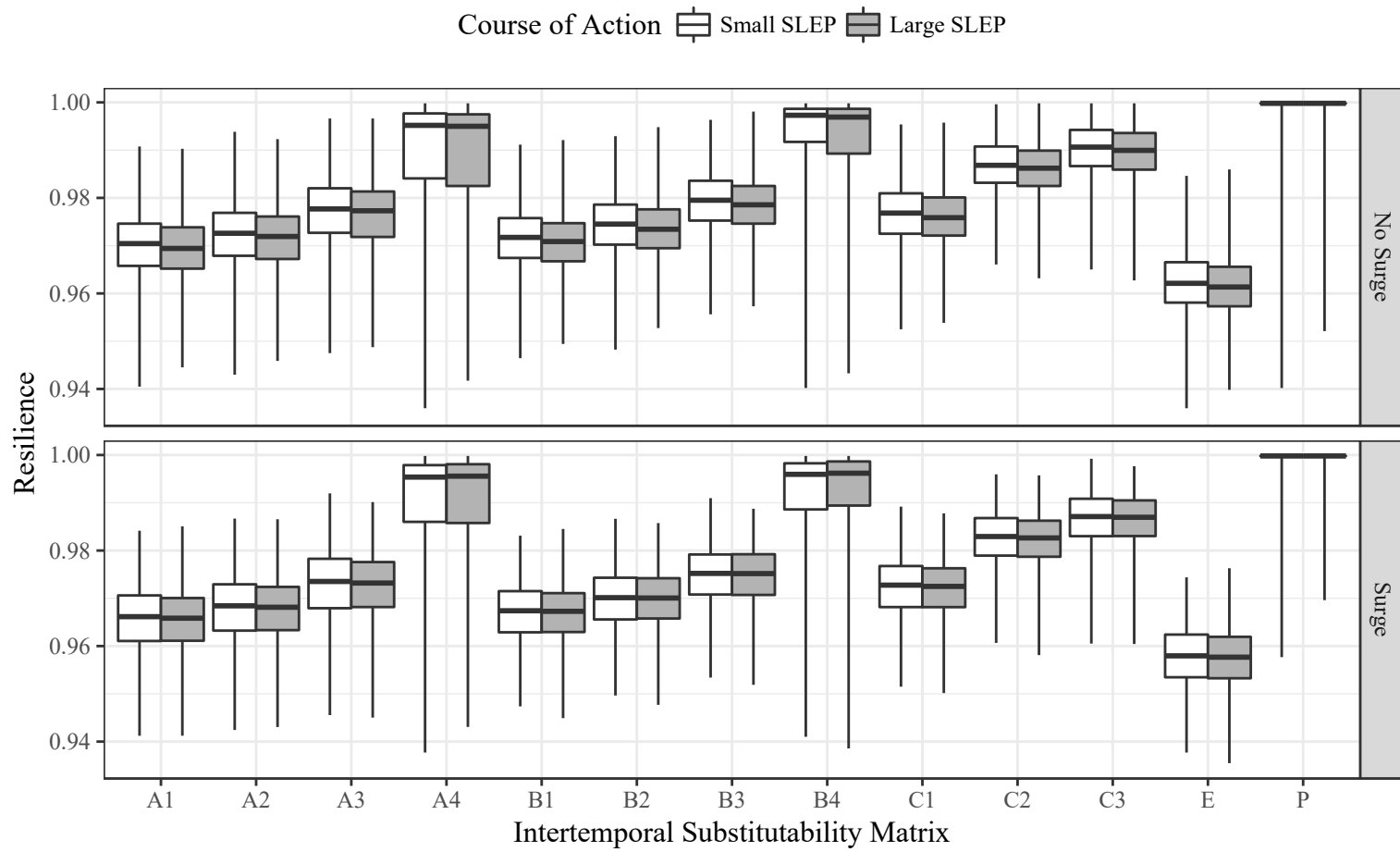


Figure 6.19: Program manager intertemporal substitutability, 20 year time horizon. “No SLEP” course of action removed to allow smaller scale on resilience axis.

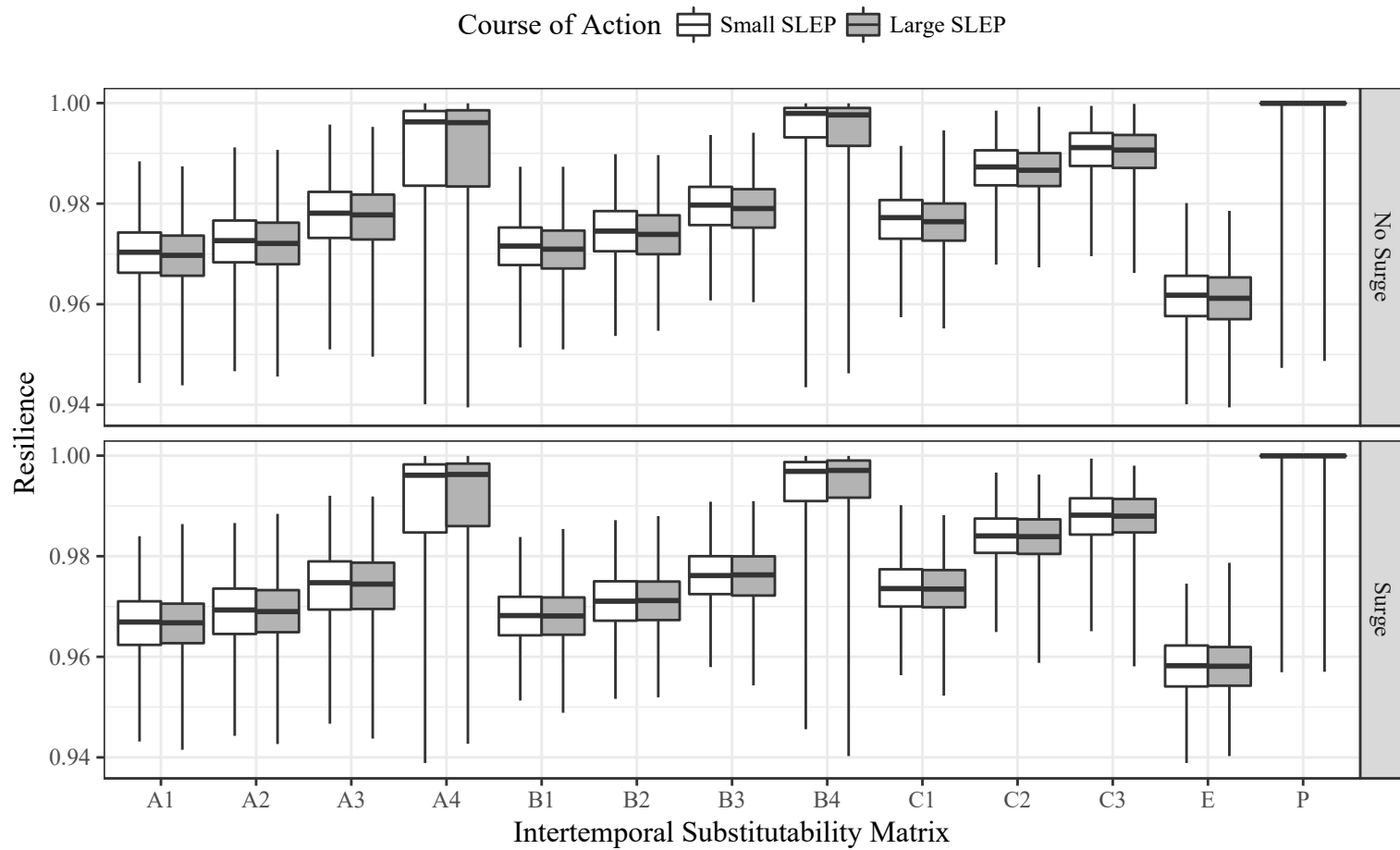


Figure 6.20: Program manager intertemporal substitutability, 25 year time horizon. “No SLEP” course of action removed to allow smaller scale on resilience axis

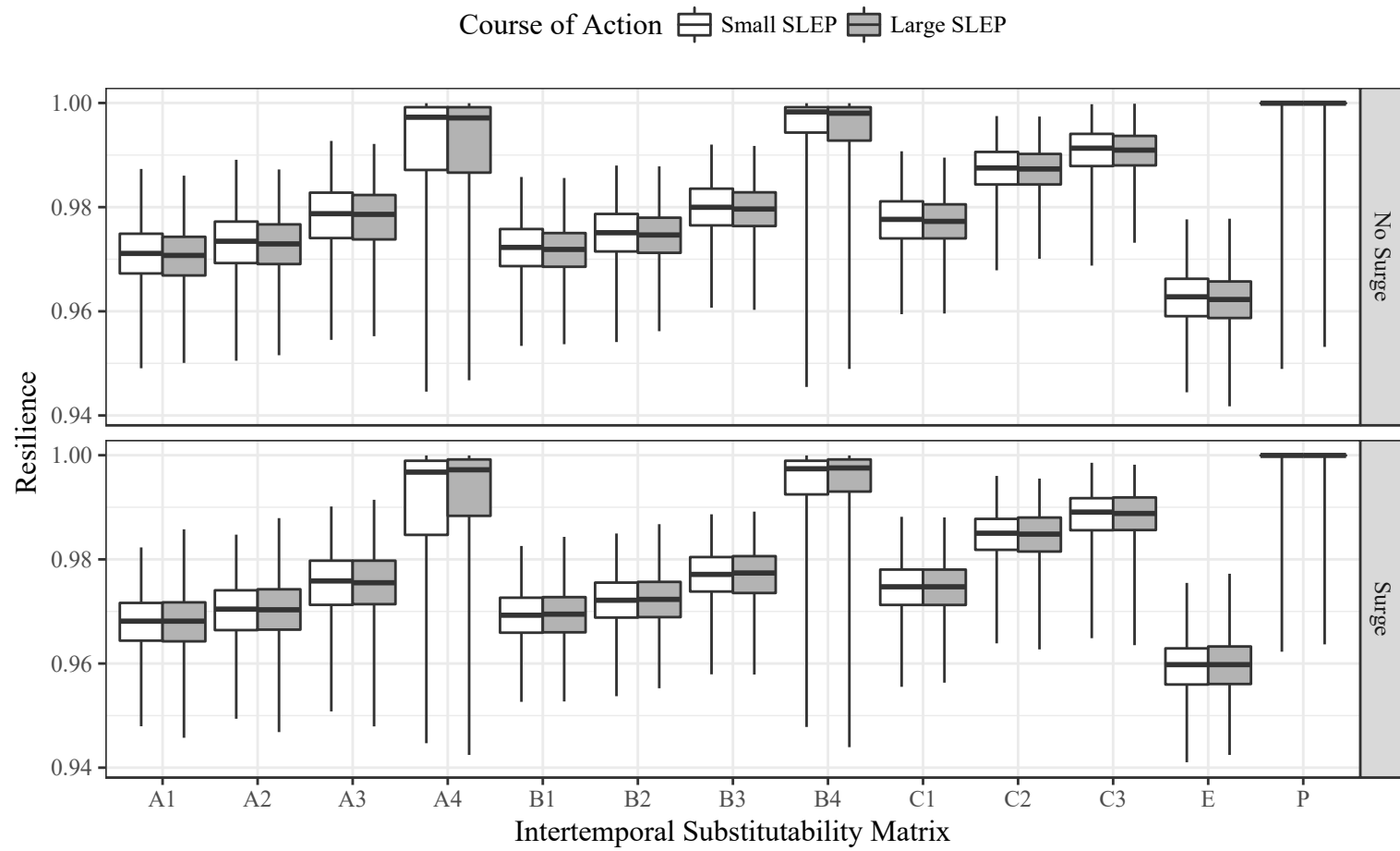


Figure 6.21: Program manager intertemporal substitutability, 30 year time horizon. “No SLEP” course of action removed to allow smaller scale on resilience axis

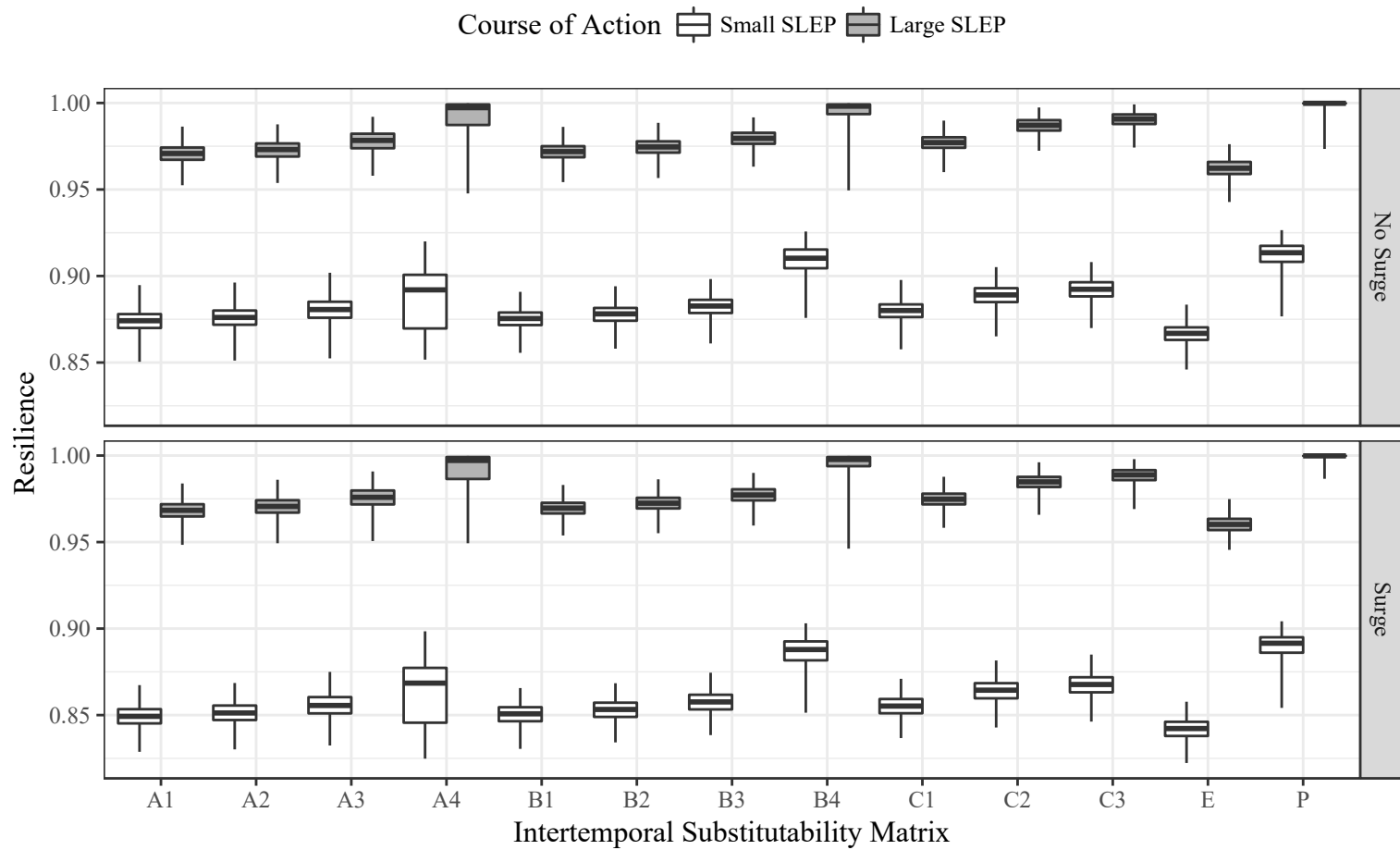


Figure 6.22: Program manager intertemporal substitutability, 35 year time horizon. “No SLEP” course of action removed to allow smaller scale on resilience axis

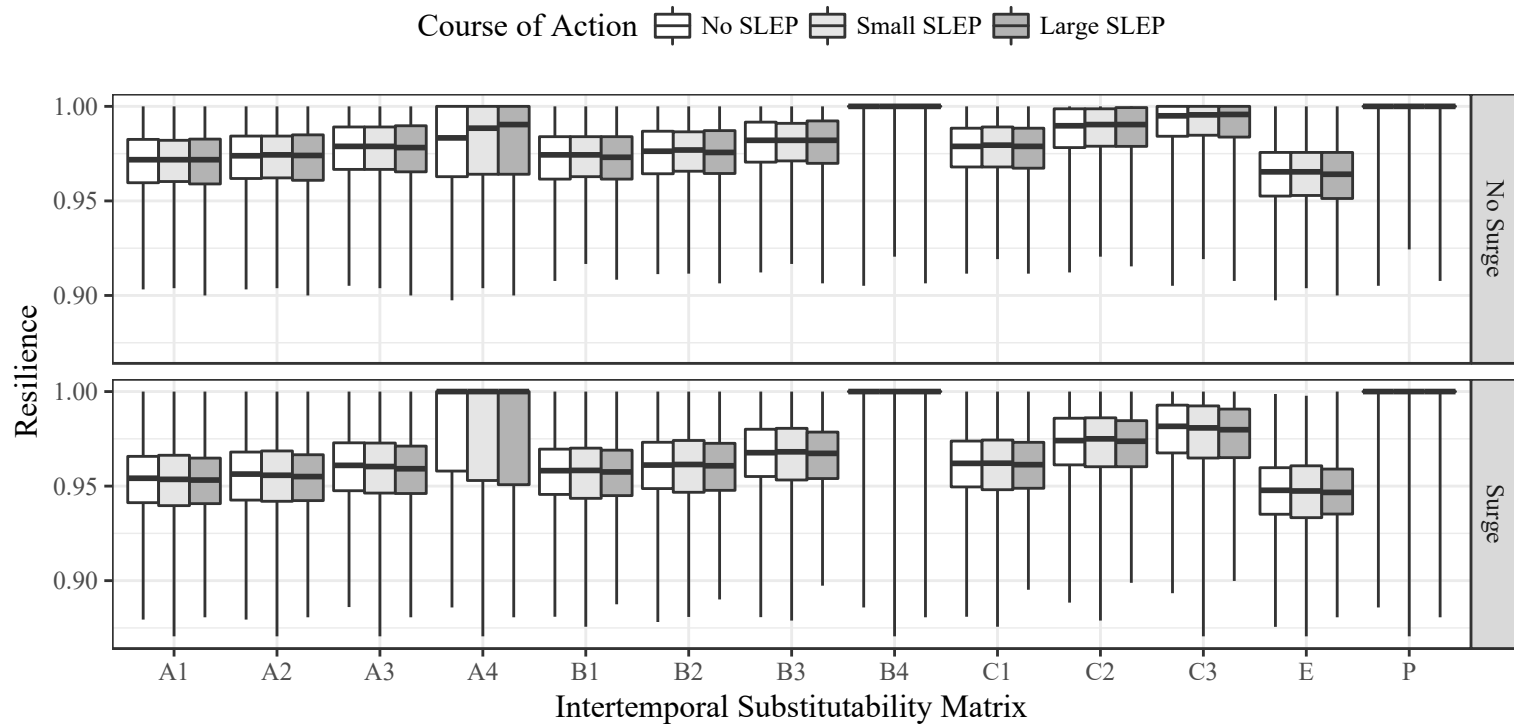


Figure 6.23: Commander Delta intertemporal substitutability

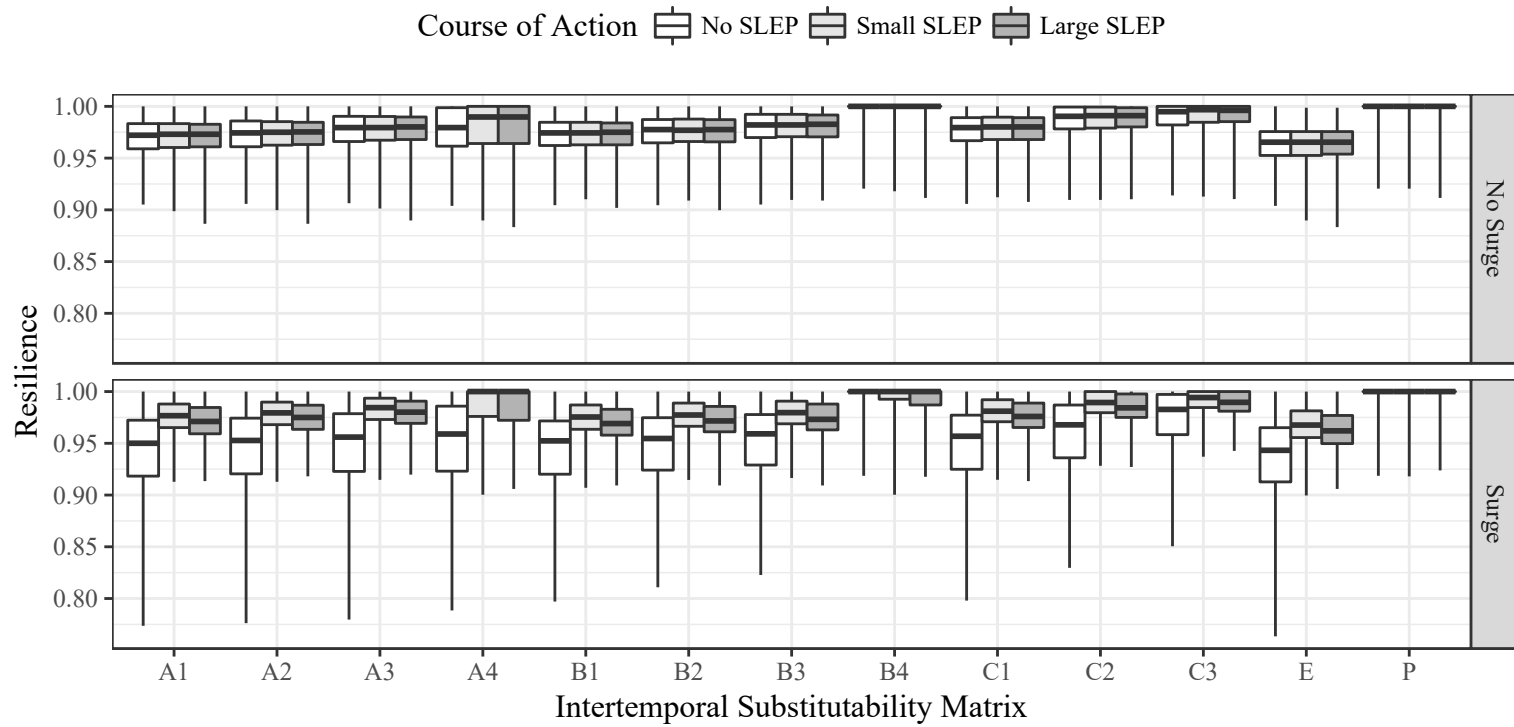


Figure 6.24: Commander Echo intertemporal substitutability

6.11 Hybrid Resilience Framework Demonstration Discussion

The study applied a hybrid resilience framework to a flight training squadron. The framework produced nuanced results to inf. The preferred most-resilient solution varied from stakeholder to stakeholder and within stakeholders from output to output.

The results show resilience to be dependent upon time horizon for the program manager. With no delay in fielding a replacement system, the “No SLEP” course of action has the highest resilience in ready aircraft and student satisfaction. From 20-30 years, “No SLEP” becomes untenable, and the “Small SLEP” course of action has a slight advantage over the “Large SLEP” course of action. The “Large SLEP” is the only tenable course of action at 35 years. The program manager would also look at resilience from the Commanding Officers’ perspective. The program manager should avoid courses of action that makes it impossible for a Commanding Officer to meet their quotas. Figure 6.16 shows the sacrifice the Commanding Officers would make. The “No SLEP” course of action almost guarantees meeting the student satisfaction goals with “Small SLEP” and “Large SLEP” becoming worse.

6.12 Algorithm Demonstration Discussion

The study demonstrated a novel intertemporal substitutability algorithm. The algorithm enabled time and event dependent surplus substitutability. The algorithm prepped the graduates per quarter time-series data for the resilience analytical

model. Figures 6.14, 6.18-6.22, and 6.23-6.24 show these results. The algorithm differentiates between surplus before and after a shortfall. The *permanent* case showed little decision support when a course of action was viable (Figures 6.18, 6.19, 6.20, 6.21, and 6.22) as the bulk of the resilience values went to one. The intertemporal substitutability demonstrated case-to-case resilience changes. The trend fits with intuition with an increasing trend when more time steps surplus percentage are available to transfer.

Chapter 7: Conclusion, Contributions, and Future Work

This chapter summarizes this dissertation’s accomplishments, the contribution to the state of the art, and direction for future work in the area of resilience.

7.1 Summary

Chapter 1 reviewed the historical usage of resilience and the current state of the art of resilience modeling. Chapter 2 identified three gaps in the literature and laid out research objectives intended to fill the gaps. Chapter 3 described the methodology for the studies. The chapter defined the analysis steps that make up the hybrid resilience framework; defined and applied the criteria for choosing the resilience models included in the study; and extended the resilience models to include stakeholder preferences. Chapter 4 conducted the resilience model comparison using fundamental models of performance and stakeholder preference. Chapter 5 performed additional resilience model comparisons using a system dynamics model of the critical infrastructure systems of the city of Austin, TX. The infrastructure case study applied the hybrid resilience framework, using extended Integral Resilience as the analytical resilience model, to DOE field data collected from Puerto Rico during the recovery from Hurricane Maria damage and to a Monte Carlo model

of a city under the threat of hurricane landfall. Chapter 6 applied the hybrid resilience framework to a fleet of aircraft with program manager and commanding officer stakeholders. The study developed a discrete version extended Integral Resilience model and demonstrated an algorithm to apply time- and event-dependent intertemporal substitutability.

7.2 Contributions

The first gap in the resilience state-of-the-art was a lack of stakeholder input. The first research objective filled this gap. The following comparison of models resulted in selection of the extended Integral Resilience model for use in the hybrid resilience model. This is the first work to explicitly define key stakeholder preferences and incorporate them into resilience models in such a way as to be system agnostic.

The second gap in the resilience state-of-the-art was a lack of model-to-model comparisons. While earlier studies had considered time horizon [Ayyub, 2015] and endogenous preference [Ouyang et al., 2012], this course of study was first to assess resilience model performance when changing these parameters. The study found extended Integral Resilience sensitive to the most parameters in the fundamental models of performance and preference.

The third gap was lack of a portable resilience methodology to apply to systems and systems of systems in a uniform way. The hybrid resilience framework fills this gap. The class III hybrid model defined by Shanthikumar and Sargent [1983] served as the foundation for the development of the hybrid resilience model. The

case studies demonstrated the framework’s portability to different domains and its ability to differentiate different courses of action depending upon the stakeholders’ preference profiles. The infrastructure resilience case study demonstrated the framework using deterministic, stochastic, and real-life data sources and applied them to multiple stakeholders developed a time and event dependent algorithm for applying a stakeholder’s intertemporal substitutability.

The course of study achieved the identified research objectives. Chapter 3 developed the hybrid resilience framework based upon the class III hybrid simulation/analytic model (Research objective 1). Chapters 4 and 5 conceptually validated the resilience models in the context of the hybrid resilience framework. The conceptual validation activity applied fundamental models and the infrastructure case study to the eight analytic resilience models developed in the study (Research objective 2). The critical infrastructure and training fleet case studies demonstrated the hybrid resilience framework and the extended integral resilience model using data generated from operating systems and two different types of simulations (Research Objective 3).

7.3 Future Work

Future research opportunities exist within the resilience model, the application of the hybrid resilience framework, and extending beyond the hybrid resilience framework.

7.3.1 Stakeholder Preferences

The dissertation investigated a single intertemporal substitutability algorithm; an algorithm that selected filled shortfalls with the most recent surplus. Other algorithms, such as using the oldest surplus first, may yield different results. The method for filling a shortfall may itself be a preference defined by the stakeholder. A course of study could investigate developing optimal intertemporal substitutability algorithms to suggest strategies for surplus storage and usage by the stakeholder.

Future work could investigate and assess the value of incorporating additional stakeholder preferences into the hybrid resilience framework. The study identified three different stakeholder preferences. These serve as a foundation as time horizon and endogenous preference were implicit in many studies. Intertemporal substitutability became available after defining these two preferences. Other preferences may be available in the fields of economics, operations research, human factors, and psychology.

7.3.2 Case Studies

The training squadron discrete event simulation held many parameters constant for this study. The study could investigate the impact of: different reliability profiles for the systems; SLEP applied to the propulsion and avionics systems; instructor pilots and the maintenance personnel as stakeholders with their own preference sets; and simulating additional disturbances to the squadron such as inclement weather, total aircraft loss due to accidents, and variable student surge events.

Many opportunities exist to apply the hybrid resilience framework. This course of study applied the hybrid model to two systems. The portability and flexibility of the framework enables resilience analysis to a spectrum of systems and systems of systems.

7.3.3 Benefit-Cost Analysis

A potentially powerful course of research is integrating the hybrid resilience framework with a benefit-cost analysis as described by [Ayyub \[2014a\]](#). The dissertation does not address monetary costs, which is a shortcoming from stakeholders' perspective. The hybrid resilience framework could become a key component of a larger analysis methodology incorporating cost.

7.4 Conclusion

In summary, the dissertation made significant contributions to both the practical application of resilience and the theory of resilience. Incorporating stakeholder preferences in the resilience models improved the quality of decision support from the models. The hybrid resilience framework is extensible to other systems, additional stakeholder preferences, and novel resilience analytical models.

Bibliography

- David L. Alderson, Gerald G. Brown, W. Matthew Carlyle, and R. Kevin Wood. Solving Defender-Attacker-Defender models for infrastructure defense. *12th INFORMS Computing Society Conference*, pages 28–49, 2011. doi: 10.1287/ics.2011.0047. URL <http://www.informs.org/Community/Conferences/ICS2011>.
- David L Alderson, Gerald G Brown, and W Matthew Carlyle. Assessing and improving operational resilience of critical infrastructures and other systems. In *TutORials in Operations Research INFORMS*, pages 180–215, 2014. ISBN 9780984337859.
- David L. Alderson, Gerald G. Brown, and W. Matthew Carlyle. Operational models of infrastructure resilience. *Risk Analysis*, 35(4):562–586, 2015. ISSN 15396924. doi: 10.1111/risa.12333.
- D. E. Alexander. Resilience and disaster risk reduction: An etymological journey. *Natural Hazards and Earth System Sciences*, 13(11):2707–2716, 2013. ISSN 15618633. doi: 10.5194/nhess-13-2707-2013.
- American Society of Civil Engineers. Infrastructure Resilience Division, 2017. URL <http://www.asce.org/infrastructure-resilience/infrastructure-resilience-division/>.
- Anaconda Inc. Anaconda Software Distribution, 2016. URL <https://anaconda.com/>.
- Austin Energy. City of Austin service area map, 2013. URL <https://austinenergy.com/ae/about/company-profile/electric-system/service-area-map>.
- Terje Aven. *Foundations of Risk Analysis*. John Wiley & Sons Ltd, West Sussex, 2003. ISBN 0-471-49548-4.
- Bilal M Ayyub. Systems resilience for multihazard environments: definition, metrics, and valuation for decision making. *Risk Analysis*, 34(2):340–55, 2 2014a. ISSN 1539-6924. doi: 10.1111/risa.12093. URL <http://www.ncbi.nlm.nih.gov/pubmed/23875704>.

- Bilal M. Ayyub. Systems resilience for multihazard environments: Definition, metrics, and valuation for decision making. *Risk Analysis*, 34(2):340–355, 2014b. ISSN 02724332. doi: 10.1111/risa.12093.
- Bilal M. Ayyub. *Risk Analysis in Engineering and Economics*. Francis & Taylor, Boca Raton, FL, second edition, 2014c. ISBN 9781466518254.
- Bilal M Ayyub. Practical Resilience Metrics for Planning, Design, and Decision Making. *ASCE-ASME Journal of Risk and Uncertainty in Engineering Systems*, pages 1–11, 2015. doi: 10.1061/AJRUA6.0000826.
- Bilal M Ayyub and George J Klir. *Uncertainty Modeling and Analysis in Engineering and the Sciences*. 2006. ISBN 1584886447. doi: 10.1201/9781420011456.
- Kash Barker, Jose E. Ramirez-Marquez, and Claudio M. Rocco. Resilience-based network component importance measures. *Reliability Engineering & System Safety*, 117:89–97, 9 2013. ISSN 09518320. doi: 10.1016/j.res.2013.03.012. URL <http://linkinghub.elsevier.com/retrieve/pii/S0951832013000823>.
- Kash Barker, Charles D Nicholson, and Jose E Ramirez-Marquez. Vulnerability importance measures toward resilience-based network design. In *12th International Conference on Applications of Statistics and Probability in Civil Engineering*, Vancouver, 2015. ICASP12.
- Hiba Baroud, Kash Barker, Jose E. Ramirez-Marquez, and Claudio M. Rocco. Importance measures for inland waterway network resilience. *Transportation Research Part E: Logistics and Transportation Review*, 62:55–67, 2014. ISSN 13665545. doi: 10.1016/j.tre.2013.11.010. URL <http://dx.doi.org/10.1016/j.tre.2013.11.010>.
- Bill Bartkus. Naval Air Depot North Island Begins SLEP on Greyhounds, 2002. URL http://www.navy.mil/submit/display.asp?story_id=1161.
- John Black, Nigar Hashimzade, and Gareth Myles. *A Dictionary of Economics*. Oxford University Press, fifth edition, 2017. ISBN 9780191819940. doi: 10.1093/acref/9780198759430.001.0001. URL <http://www.oxfordreference.com/view/10.1093/acref/9780198759430.001.0001/acref-9780198759430>.
- Dan Broadstreet. Navy Modernizes Amphibious Ships and Hovercraft, 2007. URL http://www.navy.mil/submit/display.asp?story_id=34023.
- Michel Bruneau, Stephanie E. Chang, Ronald T. Eguchi, George C. Lee, Thomas D. O’Rourke, Andrei M. Reinhorn, Masanobu Shinozuka, Kathleen Tierney, William A. Wallace, and Detlof von Winterfeldt. A Framework to Quantitatively Assess and Enhance the Seismic Resilience of Communities. *Earthquake Spectra*, 19(4):733–752, 2003. ISSN 87552930. doi: 10.1193/1.1623497.

- Richard R. Burgess. Navy to Modify T-45 Training Jets for Improved Performance, 2015. URL <http://hrana.org/news/2015/07/navy-to-modify-t-45-training-jets-for-improved-performance/>.
- Steve Carpenter, Brian Walker, J. Marty Anderies, and Nick Abel. From Metaphor to Measurement: Resilience of What to What? *Ecosystems*, 4(8):765–781, 2001. ISSN 14329840. doi: 10.1007/s10021-001-0045-9.
- Binchao Chen, Aaron Phillips, and Timothy I. Matis. Two-terminal reliability of a mobile ad hoc network under the asymptotic spatial distribution of the random waypoint model. *Reliability Engineering & System Safety*, 106:72–79, 10 2012. ISSN 09518320. doi: 10.1016/j.res.2012.05.005. URL <http://linkinghub.elsevier.com/retrieve/pii/S0951832012000889>.
- L. Chen and E. Miller-Hooks. Resilience: An Indicator of Recovery Capability in Intermodal Freight Transport. *Transportation Science*, 46(1):109–123, 2012. ISSN 0041-1655. doi: 10.1287/trsc.1110.0376.
- Chief of Naval Air Training. CNATRAININST 1542.160: T-45 Combined Strike Flight Instructor Training Curriculum. Technical Report May, Naval Air Training Command, 2009.
- C. A. Davis, T. D. O’Rourke, M. L. Adams, and M. A. Rho. Case Study: Los Angeles Water Services Restoration Following the 1994 Northridge Earthquake. In *Proceedings of the 15th World Conference Earthquake Engineering*, Lisbon, 2012.
- Craig A. Davis. Water system service categories, postearthquake interaction, and restoration strategies. *Earthquake Spectra*, 30(4):1487–1509, 2014. ISSN 87552930. doi: 10.1193/022912EQS058M.
- Harold Demsetz. The core disagreement between Pigou, the profession, and Coase in the analyses of the externality question. *European Journal of Political Economy*, 12(4):565–579, 1996. ISSN 01762680. doi: 10.1016/S0176-2680(96)00025-0.
- Department of Defense. Mission Assurance (DoD Directive 3020.40). Technical report, Washington, DC, 2016.
- Thomas Donaldson and Lee E Preston. Stakeholder Theory: Concepts, Evidence, Corporations and its Implications. *Management*, 20(1):65–91, 1995. ISSN 03637425. doi: 10.2307/258887.
- Megan Eckstein. Navy Will Extend All DDGs to a 45-Year Service Life ; “No Destroyer Left Behind” Officials Say, 2018. URL <https://news.usni.org/2018/04/12/navy-will-extend-ddgs-45-year-service-life-no-destroyer-left-behind-officials-say>.

- Jane Edwards. Report: Army Sees 4-Year Delay in Anti-Missile C2 System IOC Based on FY 2018 Budget Request, 2017. URL <http://www.executivegov.com/2017/05/report-army-sees-4-year-delay-in-anti-missile-c2-system-ioc-based-on-fy-2018-budget-request/>.
- Dane Egli, David Flanigan, Brian Donohue, Steven Taylor, Michael Newkirk, and Richard Waddell. Critical Infrastructure Security & Resilience: Resilience Implementation Proof of Concept Guidebook, 2015.
- Roy N. Emanuel. Resilience and Stakeholder Need. In *Reliability and Maintainability Symposium*. IEEE, 2017. ISBN 0814472605.
- Roy N. Emanuel and Bilal M. Ayyub. Assessing Resilience Model Responsiveness in the Context of Stakeholder Preferences in Decision Support Systems. *ASCE-ASME Journal of Risk and Uncertainty in Engineering Systems*, in press.
- Royce A. Francis and Behailu Bekera. A metric and frameworks for resilience analysis of engineered and infrastructure systems. *Reliability Engineering & System Safety*, 121:90–103, 1 2014. ISSN 09518320. doi: 10.1016/j.res.2013.07.004. URL <http://linkinghub.elsevier.com/retrieve/pii/S0951832013002147>.
- R. Edward Freeman. *Strategic Management: A Stakeholder Approach*. Pitman Publishing Inc., Marshfield, MA, 1984. ISBN 0-273-01913-9.
- Dante Gama Dessavre, Jose E. Ramirez-Marquez, and Kash Barker. Multidimensional approach to complex system resilience analysis. *Reliability Engineering & System Safety*, 149:34–43, 2016. ISSN 09518320. doi: 10.1016/j.res.2015.12.009. URL <http://linkinghub.elsevier.com/retrieve/pii/S0951832015003610>.
- Mica Garbarino. F-16 Service Life Extension Program a great deal for DoD, taxpayers, 2018. URL <https://www.af.mil/News/Article-Display/Article/1516090/f-16-service-life-extension-program-a-great-deal-for-dod-taxpayers/>.
- Ahjon S. Garmestani, Craig R. Allen, and Heriberto Cabezas. Panarchy , Adaptive Management and Governance: Policy Options for Building Resilience Panarchy , Adaptive Management and Governance: Policy Options for Building Resilience. *Nebraska Law Review*, 87(4), 2008. URL <http://digitalcommons.unl.edu/nlr/vol87/iss4/5>.
- Simon R. Goerger, Azad M. Madni, and Owen J. Eslinger. Engineered resilient systems: A DoD perspective. *Procedia Computer Science*, 28(Cser):865–872, 2014. ISSN 18770509. doi: 10.1016/j.procs.2014.03.103. URL <http://dx.doi.org/10.1016/j.procs.2014.03.103>.
- Sam Goldstein and Robert B. Brooks, editors. *Handbook of Resilience in Children*. Springer Science & Business Media, 2012.

- Devanandham Henry and Jose E. Ramirez-Marquez. Generic metrics and quantitative approaches for system resilience as a function of time. *Reliability Engineering & System Safety*, 99:114–122, 3 2012. ISSN 09518320. doi: 10.1016/j.ress.2011.09.002. URL <http://linkinghub.elsevier.com/retrieve/pii/S0951832011001748>.
- Devanandham Henry and Jose Emmanuel Ramirez-Marquez. On the Impacts of Power Outages during Hurricane Sandy-A Resilience-Based Analysis. *Systems Engineering*, 19(1):59–75, 1 2016. ISSN 10981241. doi: 10.1002/sys.21338. URL http://ezproxy.lib.ucf.edu/login?url=http://search.proquest.com/docview/926281441?accountid=10003%5Cnhttp://sfx.fcla.edu/ucf?url_ver=Z39.88-2004&rft_val_fmt=info:ofi/fmt:kev:mtx:journal&genre=article&sid=ProQ:ProQ:civilengineering&atitle=Model+Based+Syste.
- Arelis R. Hernández, Whitney Leaming, and Zoeann Murphy. How Puerto Rico power outage affects citizens after Hurricane Maria - Washington Post, 2017. URL https://www.washingtonpost.com/graphics/2017/national/puerto-rico-life-without-power/?utm_term=.503469a1f0a1.
- Jeffery P Holland. Engineered Resilient Systems. In *NDIA Systems Engineering Conference*, Springfield, VA, 2014.
- C. S. Holling. Engineering Resilience versus Ecological Resilience. In Lance H. Gunderson, Craig R. Allen, and C. S. Holling, editors, *Foundations of Ecological Resilience*, chapter Article 2, pages 51–66. Island Press, Washington D.C., 2010. ISBN 978-1-59726-511-9.
- C.S. Holling. Resilience and the Stability of Ecological Systems. *Annual Review of Ecology and Systematics*, 4(1973):1–23, 1973. URL <http://www.jstor.org/stable/2096802>.
- Seyedmohsen Hosseini, Kash Barker, and Jose E. Ramirez-Marquez. A Review of Definitions and Measures of System Resilience. *Reliability Engineering & System Safety*, 2015. ISSN 09518320. doi: 10.1016/j.ress.2015.08.006. URL <http://linkinghub.elsevier.com/retrieve/pii/S0951832015002483>.
- Idaho National Laboratories. Resilience Week, 2017. URL <http://resilienceweek.com>.
- INCOSE. What is Systems Engineering?, 2017. URL <http://www.incose.org/AboutSE/WhatIsSE>.
- Thomas Jagger, James B. Elsner, and Xufeng Niu. A Dynamic Probability Model of Hurricane Winds in Coastal Counties of the United States. *Journal of Applied Meteorology*, 40(5):853–863, 2001. ISSN 0894-8763. doi: 10.1175/1520-0450(2001)040<0853:ADPMOH>2.0.CO;2.

- Mo Jamshidi. Introduction to System of Systems. In Mo Jamshidi, editor, *System OF Systems Engineering: Innovations for the 21st Century*, chapter 1, pages 1–20. John Wiley & Sons Ltd, Hoboken, New Jersey, 2009. ISBN 9780470195901.
- Gareth Jennings. Boeing continues T-45 SLEP effort with Phase 2 contract, 2018. URL <http://www.janes.com/article/77447/boeing-continues-t-45-slep-effort-with-phase-2-contract>.
- Justin Katz. Zumwalt (DDG-1000) sees delays in path to IOC, 2018. URL <https://insidedefense.com/insider/zumwalt-ddg-1000-sees-delays-path-ioc>.
- Xiangyong Kong, Liqun Gao, Haibin Ouyang, and Steven Li. Solving the redundancy allocation problem with multiple strategy choices using a new simplified particle swarm optimization. *Reliability Engineering & System Safety*, 144:147–158, 12 2015. ISSN 09518320. doi: 10.1016/j.res.2015.07.019. URL <http://www.sciencedirect.com/science/article/pii/S0951832015002240>.
- Sam LaGrone. Navy Lays Bare F/A-18 Hornet, Super Hornet Readiness Gaps, 2016. URL <https://news.usni.org/2016/05/26/navy-lays-bare-fa-18-readiness-gaps-take-year-surge-air-wing>.
- Averill M. Law. *Simulation Modeling and Analysis*. McGraw-Hill, New York, NY, fifth edition, 2015. ISBN 978-0-07-340132-4.
- Lockheed Martin Public Relations. U.S. Air Force Authorizes Extended Service Life for F-16, 2017. URL <https://news.lockheedmartin.com/2017-04-12-U-S-Air-Force-Authorizes-Extended-Service-Life-for-F-16>.
- Denise Lu and Chris Alcantara. After Maria, Puerto Ricos electricity grid is still recovering - Washington Post, 2018. URL https://www.washingtonpost.com/graphics/2017/national/puerto-rico-hurricane-recovery/?utm_term=.3daf5c2a2589.
- Ontje Lünsdorf and Stefan Scherfke. SimPy, 2018. URL <https://simpy.readthedocs.io/en/latest/index.html>.
- J W McPherson. Reliability physics and engineering. 2010.
- Aaron Mehta. Budget constraints delay new trainer. *Air Force Times*, page 19, 5 2013. ISSN 0002-2403. URL https://infoweb-newsbank-com.proxy1.library.jhu.edu/apps/news/openurl?ctx_ver=z39.88-2004&rft_id=info%3Aid/infoweb.newsbank.com&svc_dat=AWNB&req_dat=0DOCB535F3149F6A&rft_val_format=info%3Aofi/fmt%3Akev%3Amtx%3Actx&rft_dat=document_id%3Anews%252F146C733F5.
- Aaron Mehta. Welsh Confident in F-35, Disappointed in KC-46 Delay, 2016. URL <https://www.defensenews.com/2016/06/14/welsh-confident-in-f-35-disappointed-in-kc-46-delay/>.

- Ian I. Mitroff. *Stakeholders of the Organizational Mind*. Jossey-Bass Inc., San Francisco, CA, 1983. ISBN 0-87589-580-8.
- Mohammad Modarres, Mark Kaminskiy, and Vasilii Krivtsov. *Reliability Engineering and Risk Analysis A Practical Guide*. CRC Press, Boca Raton, second edition, 2010. ISBN 978-0-8493-9247-4.
- National Institute of Standards and Technology (NIST). Community Resilience Panel for Buildings and Infrastructure Systems, 2016. URL <https://crpanel.nist.gov/>.
- Naval Sea Systems Command. LCAC Program Summary, 2018. URL <https://www.navsea.navy.mil/Home/Team-Ships/PEO-Ships/LCAC-SLEP/>.
- Robert Neches. Engineered Resilient Systems (ERS) S & T Priority Description and Roadmap Engineered Resilient Systems Spans the Systems Life cycle Resilience : Effective in a wide range of situations ,. In *NDIA 8th Annual Disruptive Technologies Conference*, number November, Washington D.C., 2011.
- Robert Neches. Engineered Resilient Systems (ERS): Insights and Achievements within the ERS Secretary of Defense Science and Technology (S & T) Priority Director , Advanced Engineering Initiatives for Systems Engineering Coming Attractions. *Proceedings NDIA 15th Annual SE Conference*, (October):1–21, 2012.
- Min Ouyang and Leonardo Dueñas-Osorio. Time-dependent resilience assessment and improvement of urban infrastructure systems. *Chaos: An Interdisciplinary Journal of Nonlinear Science*, 22(3):033122, 2012. ISSN 10541500. doi: 10.1063/1.4737204. URL <http://scitation.aip.org/content/aip/journal/chaos/22/3/10.1063/1.4737204>.
- Min Ouyang and Zhenghua Wang. Resilience assessment of interdependent infrastructure systems: With a focus on joint restoration modeling and analysis. *Reliability Engineering & System Safety*, 141:74–82, 2015. ISSN 09518320. doi: 10.1016/j.res.2015.03.011. URL <http://www.sciencedirect.com/science/article/pii/S0951832015000691>.
- Min Ouyang, Leonardo Dueñas-Osorio, and Xing Min. A three-stage resilience analysis framework for urban infrastructure systems. *Structural Safety*, 36-37: 23–31, 2012. ISSN 01674730. doi: 10.1016/j.strusafe.2011.12.004. URL <http://www.sciencedirect.com/science/article/pii/S0167473011000956>.
- Raghav Pant, Kash Barker, Jose Emmanuel Ramirez-Marquez, and Claudio M. Rocco. Stochastic measures of resilience and their application to container terminals. *Computers and Industrial Engineering*, 70(1):183–194, 2014. ISSN 03608352. doi: 10.1016/j.cie.2014.01.017. URL <http://dx.doi.org/10.1016/j.cie.2014.01.017>.

- PPD (Presidential Policy Directive). National Preparedness, 2011. URL <https://www.dhs.gov/presidential-policy-directive-8-national-preparedness>.
- PPD (Presidential Policy Directive). Critical Infrastructure Security and Resilience, 2013. URL <https://obamawhitehouse.archives.gov/the-press-office/2013/02/12/presidential-policy-directive-critical-infrastructure-security-and-resil>.
- Radar Operations Center. Service Life Extension Program (SLEP), 2018. URL <https://www.roc.noaa.gov/WSR88D/SLEP/SLEP.aspx>.
- Jos Emmanuel Ramirez-Marquez and Claudio M. Rocco S. Stochastic network interdiction optimization via capacitated network reliability modeling and probabilistic solution discovery. *Reliability Engineering and System Safety*, 94(5):913–921, 2009. ISSN 09518320. doi: 10.1016/j.res.2008.10.006.
- Marvin Rausand and Arnljoy Høyland. *System Reliability Theory*. John Wiley & Sons, Inc, Hoboken, second edition, 2004. ISBN 0-471-47133-X.
- Redacted. Repair or Rebuild: Options for Electric Power in Puerto Rico. Technical report, Congressional Research Service, Washington D.C., 2017. URL https://www.everycrsreport.com/files/20171116_R45023_25e92b53bcc47c3c961932a935791373e8e3af1d.pdf.
- Dorothy A. Reed, Kailash C. Kapur, and Richad D. Christie. Methodology for assessing the resilience of networked infrastructure. *IEEE Systems Journal*, 3(2): 174–180, 2009. ISSN 19328184. doi: 10.1109/JSYST.2009.2017396.
- David W Roberts. T-38 completes 50 years of service, 2011. URL <https://www.af.mil/News/Article-Display/Article/113899/t-38-completes-50-years-of-service/>.
- Peter A Sandborn. *Cost Analysis of Electronic Systems*. World Scientific Publishing Co. Pte. Ltd., Singapore, 2013. ISBN 978-981-4383-34-9.
- Samantha Schmidt, Joel Achenbach, and Sandhya Somashekhar. Puerto Rico entirely without power as Hurricane Maria hammers island with devastating force, 2017. URL https://www.washingtonpost.com/news/post-nation/wp/2017/09/20/hurricane-maria-takes-aim-at-puerto-rico-with-force-not-seen-in-modern-history/?utm_term=.5661b62d4858.
- Timothy Schott, Chris Landsea, Gene Hafele, Jeffrey Lorens, Arthur Taylor, Harvey Thurm, Bill Ward, Mark Willis, and Walt Zaleski. The Saffir-Simpson Hurricane Wind Scale. Technical Report February, 2012. URL <https://www.nhc.noaa.gov/pdf/sshws.pdf>.
- Sgt. Dengrier M. Baez. T-45s train aboard Fightertown, 2015. URL <https://www.beaufort.marines.mil/Photos/igphoto/2001291166/>.

- J. G. Shanthikumar and R. G. Sargent. A Unifying View of Hybrid Simulation/Analytic Models and Modeling. *Operations Research*, 31(6):1030–1052, 1983. ISSN 0030-364X. doi: 10.1287/opre.31.6.1030.
- Society for Risk Analysis. Risk and Resilience: Viva la Revolución!, 2016. URL <http://www.sra.org/events/sra-2016-annual-meeting>.
- Staff Sgt. Gabriela Garcia. FA-18 maintenance repair depot, 2016. URL <https://www.hqmc.marines.mil/cmc/Photos/igphoto/2001455967/>.
- The Office of the Director of Operational Test and Evaluation. FY17 ARMY PROGRAMS. Technical report, 2017. URL <http://www.dote.osd.mil/pub/reports/FY2017/pdf/army/2017atacms.pdf>.
- Kathleen Tierney and Michel Bruneau. Conceptualizing and measuring resilience: a key to disaster loss reduction. *TR News*, (250):14–17, 2007.
- John Tirpak. Air Force Collectin F-16 SLEP Info, 2016. URL <http://www.airforcemag.com/DRArchive/Pages/2016/January2016/January252016/Air-Force-Collecting-F-16-SLEP-Info.aspx>.
- John A. Tirpak. F-15 SLEP Coming, 2015. URL <http://www.airforcemag.com/DRArchive/Pages/2015/September2015/September162015/F-15-SLEP-Coming.aspx>.
- Walter Tomczykowski. DMSMS Acquisition Guidelines Implementing Parts Obsolescence Management Contractual Requirements. Technical report, ARINC prepared for Defence MicroElectronics Activity (DMEA), Annapolis, 2001.
- Andrew Toussaint and James Collery. Service Life Extension Program Breathes New Life into an Aging Warrior with an Upgrade to the AN/TSC, 2012. URL https://www.army.mil/article/79084/Service_Life_Extension_Program_Breathes_New_Life_into_an_Aging_Warrior_with_an_Upgrade_to_the_AN_TSC/.
- Huy T Tran. *A Complex Networks Approach To Designing Resilient System-of-Systems a Complex Networks Approach To Designing Resilient System-of-Systems*. PhD thesis, Georgia Institute of Technology, 2015.
- Huy T. Tran, Michael Balchanos, Jean Charles Domercant, and Dimitri N. Mavris. A framework for the quantitative assessment of performance-based system resilience. *Reliability Engineering and System Safety*, 158:73–84, 2017. ISSN 09518320. doi: 10.1016/j.res.2016.10.014. URL <http://dx.doi.org/10.1016/j.res.2016.10.014>.
- Donald J. Trump. The National Security Strategy United States of America. Technical report, EXECUTIVY OFFICE OF THE PRESIDENT, WASHINGTON DC, United States, 2017. URL <https://www.whitehouse.gov/wp-content/uploads/2017/12/NSS-Final-12-18-2017-0905.pdf>.

- UNISDR. Chart of the Sendai Framework for Disaster Risk Reduction, 2015. URL <https://www.preventionweb.net/publications/view/44983>.
- United Nations Office for Disaster Risk Reduction. The Making Cities Resilient Campaign: Resilience of Cities to Disasters in Central Asia and South Caucasus. Technical report, United Nations Office for Disaster Risk Reduction, 2015.
- U.S. Department of Energy. Hurricane Maria and Irma Event Reports, 2018. URL <https://www.energy.gov/oe/downloads/hurricanes-nate-maria-irma-and-harvey-situation-reports>.
- Eric D. Vugrin, Drake E. Warren, Mark A. Ehlen, and R. Chris Camphouse. A framework for assessing the resilience of infrastructure and economic systems. In Kasthurirangan Gopalakrishnan and Srinivas Peeta, editors, *Sustainable and Resilient Critical Infrastructure Systems: Simulation, Modeling, and Intelligent Engineering*, chapter 3, pages 77–116. Springer, Berlin, Heidelberg, 2010. ISBN 9783642114045. doi: 10.1007/978-3-642-11405-2{_}3.
- Weather Forecast Office. Major Hurricane Maria - September 20, 2017, 2017. URL <https://www.weather.gov/sju/maria2017>.
- Ben Werner. Schedule at Risk for Navy F-35C Fighters to be Combat Ready by End of Year - USNI News, 2018. URL <https://news.usni.org/2018/03/29/current-schedule-risk-navy-f-35c-fighters-combat-ready-end-year>.
- W.J. Hennigan. Upgrades aim to extend B-52 bombers' already long lives - latimes, 2013. URL <http://articles.latimes.com/2013/aug/19/business/la-fi-ageless-b52-bomber-20130819>.
- Zacks Equity Research. Lockheed Martin to Upgrade U.S. Army's ATACMS for \$78M, 2015. URL <https://www.nasdaq.com/article/lockheed-martin-to-upgrade-us-armys-atacms-for-78m-analyst-blog-cm430902>.
- Christopher W. Zobel. Representing perceived tradeoffs in defining disaster resilience. *Decision Support Systems*, 50(2):394–403, 2011. ISSN 01679236. doi: 10.1016/j.dss.2010.10.001. URL <http://dx.doi.org/10.1016/j.dss.2010.10.001>.